MICROSTRUCTURAL EVALUATION OF Sn3.0Ag0.5Cu SOLDER ALLOY FABRICATED VIA POWDER METALLURGY METHOD

NADHRAH BINTI MURAD

MASTER OF SCIENCE

UNIVERSITI MALAYSIA PAHANG

UNIVERSITI MALAYSIA PAHANG

DECLARATION OF THESIS AND COPYRIGHT

Author's Full Name : NADHRAH BINTI MURAD

Date of Birth : 23 JULY 1991

Title : MICROSTRUCTURAL EVALUATION OF

Sn3.0Ag0.5Cu SOLDER ALLOY FABRICATED

VIA POWDER METALLURGY METHOD

Academic Session : SEMESTER 2 2020/2021

I declare that this thesis is classified as:

☐ CONFIDENTIAL (Contains confidential information under the Official Secret Act 1997)*

☐ RESTRICTED (Contains restricted information as specified by the organization where research was done)*

☒ OPEN ACCESS I agree that my thesis to be published as online open access (Full Text)

I acknowledge that Universiti Malaysia Pahang reserves the following rights:

1. The Thesis is the Property of Universiti Malaysia Pahang
2. The Library of Universiti Malaysia Pahang has the right to make copies of the thesis for the purpose of research only.
3. The Library has the right to make copies of the thesis for academic exchange.
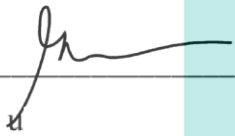
Certified by:

_____
(Student's Signature)

910723-06-5100
NEW IC NUMBER
Date: 10 JUNE 2021

_____
(Supervisor's Signature)

TS DR SITI RABIATULL AISHA IDRIS
NAME OF SUPERISOR
Date: 10 JUNE 2021

SUPERVISOR'S DECLARATION

We hereby declare that We have checked this thesis and, in our opinion, this thesis is adequate in terms of scope and quality for the award of the degree of Master of Science.

_____

(Supervisor's Signature)

Full Name   : TS DR SITI RABIATULL AISHA BINTI IDRIS
Position   : SENIOR LECTURER
Date   : 10 JUNE 2021

_____

(Co-supervisor's Signature)

Full Name   : DR MAHADZIR BIN MUHAMMAD@ISHAK
Position   : PROFESSOR
Date   : 10 JUNE 2021

MICROSTRUCTURAL EVALUATION OF Sn3.0Ag0.5Cu SOLDER ALLOY FABRICATED VIA POWDER METALLURGY METHOD

NADHRAH BINTI MURAD
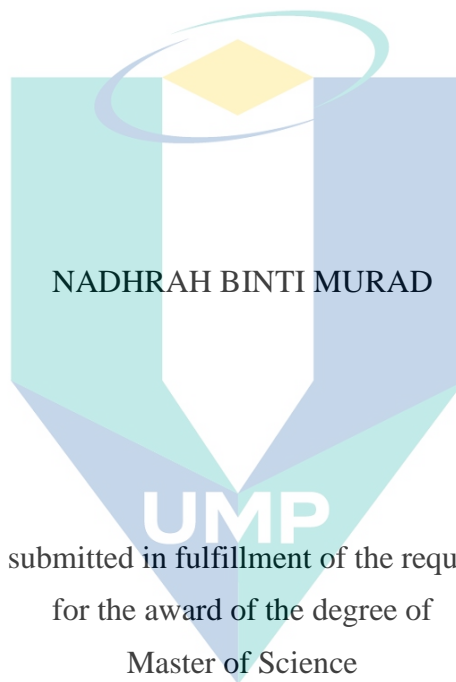
Thesis submitted in fulfillment of the requirements

for the award of the degree of

Master of Science

Faculty of Mechanical and Automotive Engineering Technology

UNIVERSITI MALAYSIA PAHANG

JUNE 2021

ACKNOWLEDGEMENTS

ABSTRAK

Selama beberapa dekad, proses pembuatan industri adalah kaedah yang sering digunakan dalam pembuatan aloi pateri dan memperkasakan sifat aloi pateri. Walau bagaimanapun, teknik pengadukan atau mengacau cecair logam yang biasa digunakan dalam kaedah Casting perlu diberi perhatian untuk perbincangan lebih lanjut. Menurut kajian literatur, teknik Casting telah menunjukkan permasalahan dari segi kualiti sifat aloi pateri iaitu kesamarataan taburan unsur dalam aloi pateri. Oleh itu, suatu Teknologi Hijau yang dikenali sebagai kaedah Powder Metallurgy (PM) telah dipilih kerana fungsi pemprosesan bahannya yang dapat membantu mewujudkan tahap kesamarataan taburan unsur dalam aloi pateri. Ia mempunyai dua prosedur asas iaitu mengisar dan memadat. Ini berfungsi untuk pembuatan aloi pateri yang lebih baik di mana ia hanya menggunakan suhu bilik dalam menyatukan bahan yang berbeza sekaligus. Lebih-lebih lagi, persekitaran kerja yang bersih dan lebih selamat dalam praktiknya dan memerlukan satu cetakan untuk menghasilkan puluhan produk yang menjimatkan kos yang besar. Kajian ini dilakukan untuk mencari jurang yang terdapat dalam tinjauan literatur mengenai isu kesamarataan taburan unsur aloi pateri. Oleh itu, penyelidikan ini dijalankan untuk mengkaji sifat-sifat aloi pateri Sn3.0Ag0.5Cu yang disediakan dengan kaedah PM. Pemilihan bahan yang melibatkan ukuran dan bentuk bahan mentah adalah faktor penting semasa mempraktikkan kaedah PM kerana akan mempengaruhi hasil akhir. Oleh itu, empat jangka masa pengisaran yang berbeza iaitu 2, 4, 6 dan 8 jam dijadikan pemboleh ubah untuk mencapai campuran homogen di dalam aloi. Campuran ini kemudian dipadatkan dengan mesin pemadatan hidraulik untuk 1, 3, 5, 7 dan 9 tan. Langkah ini adalah untuk memastikan campuran akan dapat digunakan untuk meneruskan prosedur ujian *reflow* (kecairan) dan juga ujian *microhardness*. Melalui ujian *reflow*, terdapat empat topik utama yang akan dibincangkan termasuk hasil ujian *reflow*, ujian *wettability*, pembentukan IMC dan ketebalan IMC. Semua sampel disejukkan melalui proses penyejukan perlahan. Hasil kajian menunjukkan bahawa ada kaedah PM boleh dijadikan kaedah alternatif yang lebih baik dari kaedah Casting dalam pembuatan paduan pateri. Ini disebabkan oleh taburan unsur yang berbeza dilihat lebih baik selepas proses mengisar telah disahkan oleh analisis SEM dan EDX, manakala tahap *wettability* juga tinggi bagi semua sampel yang mana berada di bawah 90 °. SEM dan EDX juga memperlihatkan bentuk IMC Cu_6Sn_5 yang wujud pada perantaraan aloi pateri dan matriks pateri. Ketebalan IMC menggambarkan nilai yang cukup tinggi kerana masa penyejukan yang lebih lama. Kesimpulannya, kaedah PM adalah pilihan pembuatan aloi pateri yang lebih baik untuk mempraktikkan Teknologi Hijau dan sesuai dengan pengeluaran kos rendah serta persekitaran yang lebih selamat. Campuran aloi pateri yang dihasilkan dengan kaedah ini juga sesuai dalam menghasilkan sifat aloi pateri yang sangat baik.

ABSTRACT

For decades, casting has been the most influential industrial manufacturing process to fabricate and promote higher properties of solder alloy. However, stirring technique which is commonly applies in casting method has brought some attentions for further discussions. According to literatures, the stir casting technique has showed quality issue towards solder alloy property of elementary particles distribution. Thus, concerning the issue, a green technology known as Powder Metallurgy(PM) method is selected due to its material processing function which can also offer particle distribution deals. It is basically having two basic procedures which are milling and compacting. These works for better solder alloy production where it only uses room temperature to consolidate different materials at once. Moreover, a clean and safer working environment is in practice and it takes one mould to produce dozens of products which is a big cost saving. This study is conducted to seek out the gap found in the literature reviews on the homogeneity issue of the solder alloy's elemental distributions. Thus, this research is carried out to study the properties of Sn3.0Ag0.5Cu solder alloy prepared by PM method. The selection of materials involving size and shape of the raw materials are important factors whilst practising PM method due to the end up result of milling. Therefore, four different milling durations listing 2, 4, 6 and 8 hours which became the variables to reach off a homogenize granulated mixture inside the alloy. These mixtures were then compacted with a hydraulic press machine for 1, 3, 5, 7 and 9 ton of compaction loads. This step is to ensure the mixture will be in handable form to move on into reflow test procedure as well as the microhardness test. Through the reflow test, there are four major topics to be discussed on including the behaviour of solder pallet by reflow test, wettability test, formation of IMC and the thickness of IMC. All samples are cooled down by the slow cooling process. Results showed that there is high possibility to utilize PM method in solder alloy fabrication due to high distribution of different elements after milling process as being confirmed by the SEM and EDX analyses, high degree of wettability by all samples which lined below 90°. The SEM and EDX also displayed scallop IMC of Cu_6Sn_5 existed at the solder joint and matrix. The IMC thickness depicted quite high values due to longer cooling time. In conclusion, PM method is a better option of solder alloy fabrication to practice Green Technology plus fits the low-cost production and safer environment. The produced solder alloy by this method also fits the excellent solder alloy properties.

TABLE OF CONTENT

LIST OF TABLES

LIST OF FIGURES

UMP

اونيـۆرسيتي مليـسيا قهڠ

UNIVERSITI MALAYSIA PAHANG

xi

LIST OF SYMBOLS

Cu_3Sn	Copper$_3$ Tin
Cu_6Sn_5	Copper$_6$ Tin$_5$
°	degree
℃	Degree Celcius
℃/s	Degree celcius per second
g	gram
Hv	Hardness value
kg	kilogram
μm	micrometer
%	percent
s	second
wt	weight
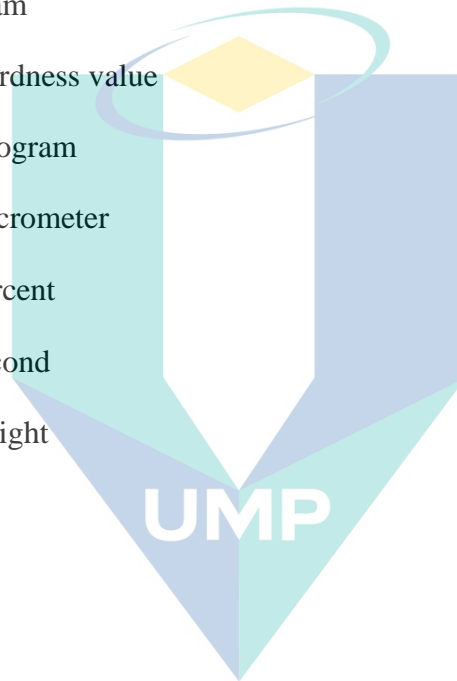
LIST OF ABBREVIATIONS

ASTM	American Standard
Cu	Copper
HAp	hydroxyapatite
IMC	Intermetallic Compound
Pb	Lead
Mg	Magnesium
PRT	Peak-Reflow-Temperature
PM	Powder Metallurgy
PCB	Printed Circuit Board
rpm	Rotation per minute
Ag	Silver
SMT	surface mount technology
THT	through-hole technology
Sn	Tin
XRD	X-Ray Diffraction
Zn	Zinc
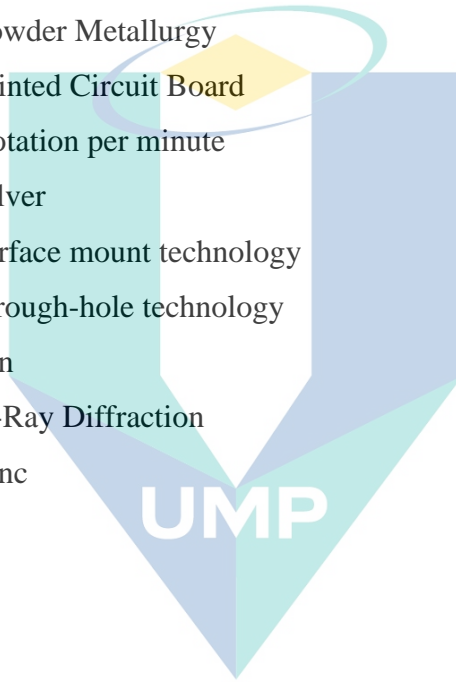
CHAPTER 1

INTRODUCTION

1.1   Homogeneity of Alloy

Solder alloy industries have grown and prospered alongside the fabrication of conventional casting method for decades. The quality of manufacturing solder alloy determines how the solder alloy will deliver its performance which governs the standard of electronic and electrical devices. Alloy is made up of one to more different elements with various fabrication techniques. The combination of alloy requires the elements to well-mix in order to preserve important properties and to deliver significant properties for distinctive purposes. Thus, an understanding on homogeneity of mixture need to be clarified. Figure 1.1 below displays the differences of heterogeneous and homogeneous structures of a material which becomes the major discussions in this research.
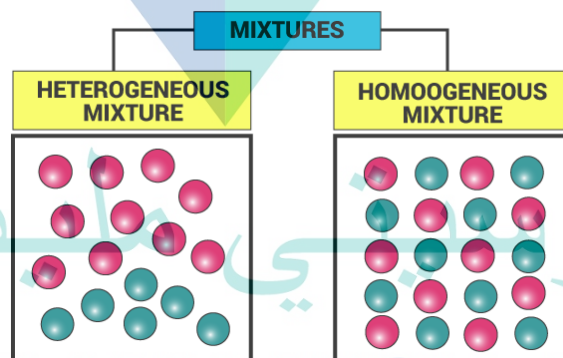
Figure 1.1   The differences of heterogeneous and homogeneous structures of a material

Conventionally, casting method is the most popular method among electronics manufacturer to produce a homogeneous solder alloy. It is by the help of stir casting technique that commonly applied in conventional casting method is barely noticeable technique in solder alloy fabrication. Nevertheless, this method also has limitations both to alloy properties and nature(Soltani, 2017).

Therefore, a new approach of solder alloy fabrication needs to interframe nowadays to be an alternative. Hence, it is an interesting and significant study to highlight Powder Metallurgy(PM) technology in the manufacture of solder alloys in this research. PM method is not currently a new technology in metal forming industries but it might be the new one to solder alloy fabrication. It is a sustainable Green Manufacturing Technology for mass production from simple to complex net shape engineering components. This powder technology is practical, cost-effective and much safer than the conventional casting method. It is also approved to be recognized as Green Technology(Salleh, 2013).

PM method is basically having three basic procedures which are milling, compacting and sintering. The principle of milling process in PM method is to blend which is to shrink the size and mix up materials This process is to ensure all the different materials are physically mix to each other and homogenous at its maximum (Kumar, 2017). Compacting process offers various shapes and designs to be invented by the milled materials while sintering process is a heat treatment to enhance the joining of structural integrity of compacted-milled materials. However, this research had not using sintering process due to maintaining the mechanical mixing procedures and preserving the Green Technology concept. It is also considered as unnecessary to do so as the solder alloy will melt and get sintered to create bond and strength between particles during reflow process.

Application of solder alloy fabricated by PM method is nowadays utilize into the Surface Mount and Through-Hole Soldering Technology where the solder alloy can help solder paste deficiency issue. A tiny compacted solder alloy can increase the solder volume at the joining through reflow soldering technology. Thus, this can improve the reliability and performance of solder alloy as well as the electronic and electrical devices to be well-functioned.

For these reasons, this research is exclusively conducted to study the elementary preparation and properties of Sn3.0Ag0.5Cu solder alloy prepared by PM method based on several scopes as to discover what it has to offer to the solder and soldering industries.

2

1.2   Problem Statement

A review of the literature revealed that most studies have only been attempts to fabricate new alloy compositions of lead-free alloys with the hope of obtaining a better replacement for joining alloys. These researches have introduced many fabrication techniques, specifically lead-free development. These techniques can be grouped into two common methods: Powder Metallurgy (PM) methods and casting method. PM is increasingly popular on the development of lead-free composite solders. There is a bright future for this powder technique with the introduction of advanced sintering methods which uses microwave-assistance for rapid sintering.

It was known that the grain size of casted solder alloy is controlled by the cooling rate of the solder after melting, whereas in PM the grain size is controlled by the heating rate during sintering. Besides, it is easier to control the grain growth of pre-solder in PM fabrication. Furthermore, PM solder has denser grain and therefore higher values of UTS and yield strength. Apart from that, PM solder shows about twice the wettability of cast solder. As overall, the PM method can improve lead-free solder's mechanical and solderability properties. Even though PM was found to be promising method to produce solder alloy, the basic explanation on how does solder alloy produced through PM method affecting IMC formation and growth is still unclear, especially when the solder alloy itself consist of Ag and Cu which is difficult to melt during soldering due to its high melting temperature.

Therefore, the primary focus of this research is to understand the effect of Sn3.0Ag0.5Cu lead-free solder fabricated through PM, on IMC formation and growth. The milling duration and compaction load was varied in order to study the solder alloy distribution as well as hardness which might affect IMC formation at the interface of the solder joint.   In this research, the basic properties used for comparison were microstructure, mechanical properties and also wettability of solder. This study is an introduction of PM as an upcoming method for lead-free solder fabrication in the future.

1.3 Objectives of Research

The objectives of the current study are listed as follows:

i.   To investigate the effects of different PM method parameters such as milling and compaction load onto intermetallic compound formation and growth at solder joint interface.

ii. To examine the solder joint performance through wettability study.

iii. To characterise the intermetallic compound formation at the solder joint interface in terms of type and thickness.

1.4 Scopes of Research

The scopes for current study are listed as follows:

i.   Material used in this research were: 96.5% of Sn, 3.0% of Ag and 0.5% of Cu.

ii. PM parameters varied were: (a) Milling durations with the duration of 2, 4, 6 and 8 hours with fixed 1400 rpm of rotational speed under normal environment, and (b) Compaction load used were 1,3,5,7 and 9 ton to form solder alloy in circular pellet shape with the size of 13mm. Solder joint formation was made through reflow soldering at the temperature of 250 ℃ for 25 minutes under normal environment.

iii. Characterisation in terms of IMC type, thickness, grain size as well as wettability of the solder alloy, were carried out using Scanning Electron Microscopy (SEM), Energy Dispersive X-Ray (EDX), optical microscope and ImageJ Software.

1.5   Overview of Thesis

This thesis was divided into 5 chapters. In Chapter 1, fabrication chronology of solders in electronic packaging industries was discussed. This includes the exchange method of solder fabrication and how it is implemented in today's electronic board assembly. The problem statement, objectives, and scope of research were also elucidated.

Meanwhile in Chapter 2, summary of solder material, soldering method, types of solder, and fabrication method of solder have been presented. Flux system and interfacial reaction between solder and copper board also have been discussed and cited from previous research works with different sources.

Not only that, the flow of works, research methodology and sample preparation were described in Chapter 3. The details calculation on weight percentage of solder alloy used in this research had also shown.

Besides, Chapter 4 in this thesis presented the experimental results from several analyses. Critical discussion of what had been happened during milling, compacting as well as reflow condition in the furnace also discussed in here in terms of illustrations based on what previous researchers have found. But there might be some independent opinions on several issues should be expected as well.

Finally, Chapter 5 presented the conclusions and recommendations that would suggest the better extension research works in the future.

CHAPTER 2

LITERATURE REVIEW

2.1   Introduction

This chapter presents a review on the electronic packaging system and the SnAgCu solder family. Besides, a review on the solder fabrication including casting and PM were presented. The formation and thickness of IMC derived from PM method from previous studies were also presented in this chapter as well. From this literature review, it is more convenient to tackle the research gap and the work of research scopes both from past or current works would be easily study and investigated.

2.2   Electronic Packaging

Electronic packaging is considered as a major discipline in the field of electronic engineering. The package refers to a microsystem that build up with dozen features of microchips and electronic components onto a solid, flat substrate called the printed circuit board(PCB). For that reasons, different electronic components needs different microsystem of electronic packaging (Kahar, 2017). For instance, the cellphones, televisions, radios and other electrical and electronic devices demand their own packaging technologies. This is due to dissimilar functionalities and components to deliver the function of devices. The packaging is crucial in electronic assembly as to ensure the interconnection of chips and wires to disseminate signals and power as well as a protection from mechanical damage, heat and cooling exposure, heat dissipation and cost.

2.3   Material Selection

There are huge numbers of metals combination to form the alloy. Some of the alloys are the brass and steel which composed of copper and zinc as well as iron and carbon respectively. To that, solder is being classified as metal alloy too because it is

6

made up of two or more metals. Solder comes in variety of metal combinations to form the alloy. Besides, not just any metal that can be merged up into solder alloy but there are few factors that need to be considered when alloying metals to become one.

Because of solder alloy is designed to make interconnection between two pieces of metallic items such as electrical connection, households plumbing and joining jewellery, solder alloy must have relatively low melting point than that of two pieces of metals. Such solder is called as eutectic solder alloy. Thus, this obviously includes thermal properties other than the mechanical properties which commonly seek for an alloy. Besides, other significant function of making solder alloy in terms of electronic assembly, it must be able to wet and spread out well onto the printed circuit board(PCB) during the soldering to create metallurgical bonding as to deliver electrical connection between electronic devices and the PCB. Hence, the soldered joint is the part where one should check up when reliability and solderability issues come out. These are the two factors to ensure the credibility of solder alloy and the continuity of its performances for a long time which likely to known as warranty.

As a matter of fact, any good manufacturing fields will thoroughly look in details into real costs which divide into cost of raw material, cost of production and the final cost of finished packaging. Moreover, material selection for solder alloy should be taking environment sustainability as one of the factors in order to preserve the nature and conveying legal products to the customers. Material selection on making the solder alloy will consider a lot of factors based on these aspects; such as manufacturing-relevant and reliability-relevant. Table 2.1 summarized the crucial properties of solder alloy.

Table 2.1   Important Properties of Solder Alloy

Manufacturing-Relevant	Reliability-Relevant
Melting temperature	Electrical conductivity
Wettability	Thermal conductivity
Real costs	Coefficient of thermal expansion
Environment suitability	Shear and tensile properties
Availability and numbers of supplies	Fatigue and creep properties
Manufacturability using current process	Corrosion and oxidation resistance
Recyclability	Intermetallic compound formation

Source : Akhtar & Malek (2017)

2.3.1 Lead Solder

Composition of solder alloy had going through several changes in order to fulfil the requirement of the electrical applications and legislations. Lead-based solder alloy such as SnPb, SnPbZn, SnPbCu and many more used to be very popular in the first usage of solder due to their magnificent operational features including low melting point among solder alloy, commonly 183℃ for eutectic Sn67-Pb33 alloy and high wettability (Razak et al., 2018). These features have contributed to high performance and reliability of electrical applications long time ago. Nonetheless, those days have been replaced by the first premiere requirements of product policy, European legislators who claimed that lead(Pb) must be banned due to environment issues and human health in the earlier year of 2006 (Pal, Gergely, Horváth, & Gácsi, 2018).

2.3.2 Lead Free Solder

By the implementation of Pb-free solder alloy legislation was introduced by European Union, other governments have begun to initiate the same effort all over the world. This had somehow brought challenges to the development of lead-free solder where companies, industries and research universities had to cope with. The research groups designated set of lead-free solder alloy criteria which eventually agreed that there was no replacement for Sn-Pb eutectic alloy but the SnAgCu system. In fact, the research stated that SAC solder alloy is being identified as a primary replacement candidates of SnPb solder Kotadia, Howes, & Mannan, (2014). Alloy in this system have melting points ranges from 217℃ to 222℃, closed enough to the eutectic Sn-Pb alloy and almost no reliability issues compared to other lead-free system such as SnZnBi, SnAgBi, Sn3.5Ag and Sn0.7Cu alloy (Reeve, Anderson, & Handwerker, 2015; M. Xiong & Zhang, 2019; Zhang, Long, Yu, Pei, & Qiao, 2015).

In addition, there are lots of economic analyses research organisations that studying about lead-free solder alloy such as Transparency Market Research, Decision Database and Market Research Store. To note, there is a summarized reports mentioned that the market size of lead-free solder alloy would be expanded fast due to increasing demand in automation, standard living and population growth especially in Asia Pacific

sector (Transparency Market Research, 2018). This shows a positive respond from global manufacturers on the effort to implement lead free solder alloy.

2.3.2.1 SnAgCu Solder

Mechanical properties of a solder alloy can be influenced by the composition of the based materials used in it. Tin (Sn) is a material readily available on earth, and it was chosen to be the most widely composition in solder. This is due to its soft, pliable and low melting point (232℃). Meanwhile, silver (Ag) is added into the solder due to its high conductivity in electrical flows but it is high in cost hence the applications is limited. Besides, according to Zeng, Xue, Zhang, & Gao (2011), adding Ag to SnCu solder alloy may increase mechanical properties and wettability of the alloy. Copper (Cu) also is an extremely good conductor due to its free valence electron in the outer most layer of its shell. Thus, considering the reliability and melting point of a solder alloy, Sn-Ag-Cu system has been adjudged to be one of the most promising solder alloys for electrical and electronic purposes.

Figure 2.1 shows the phase diagram of ternary composition of SnAgCu solder alloy system. It is crucial to highlight this phase diagram onto this research in order to provide a primary base criteria of material selection. It is also helps to provide insights on the properties of wetting and spreading resulted by the molten solder alloy(Kattnet, 2002). Phase diagrams for lead-free solder alloys. According to the phase diagram, primary microstructures that develop from SnAgCu system are mainly Cu_6Sn_5 and Ag_3Sn which formed after solidification.

There was plenty composition range of SnAgCu system that have melting temperatures near to eutectic temperature of Sn-Pb alloy by according to several research groups. Q. Wang (2005) has ranged out 3.0-4.0wt.% of Ag content whereby 0.25-1.5wt.% of Cu content in Sn-Ag-Cu system. For instance, European Union believed on Sn3.8Ag0.7Cu composition, The International Electronics Manufacturing Initiative (INEMI from America) used Sn3.9Ag0.6Cu and by disciplinarily concern on the patent issue of lead-free solder alloy, Japan industry via Japan Electronics and Information Technology Industries Association (JEITA) has recommended the Sn3.0Ag0.5Cu solder

alloy. Thus, due to the fact of lower Ag content among these three valid compositions, Sn3.0Ag0.5Cu solder alloy is the composition of choice to be study in this research.
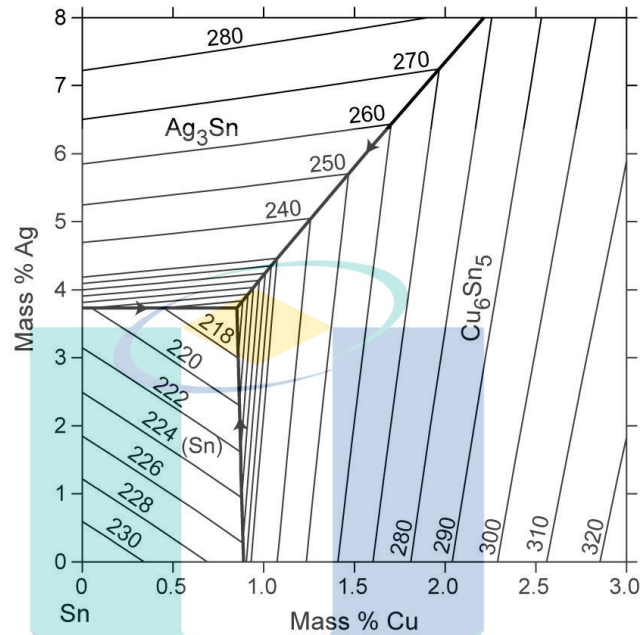
Figure 2.1   The phase diagram of ternary SnAgCu

Source: Melting behaviour and phase diagram prediction in the Sn-rich corner of the ternary system

2.4   Fabrication Process of Solder Alloy

After identifying the suitable material for solder alloy, there is a method to combine these elements into incorporated mixture. The conventional method to produce solder alloys are casting which being conducted by melting the elements together. Then they were formed in various shapes according to the applications. Nonetheless, for composite solder, researchers have move towards mechanical mixing and powder metallurgy method due to its benefits such as permits a wide variety of alloy systems, provides materials which may be heat treated for increased strength, minimizes scrap losses, provides controlled porosity and good surface finish. Mechanical mixing is used to produce cast solder ingot or solder paste. Whereas powder metallurgy method is used to produce solder ingots and solder wire. This research will focus on powder metallurgy since it is the suitable method to produce composite solder.

2.4.1   Powder Metallurgy (PM) Method

PM method allows solid state reduction of elements and processing them into desired shapes as well as sizes especially when energy was not available for melting and processing. In PM method, the energy required for processing and shaping is less and it is possible to introduce desired properties at various sections of the same part to meet performance requirements. There are four main stages in making PM products which includes making of powder, compaction, sintering and secondary or other finishing operations. Nowadays, PM method has become the top methods in manufacturing since it can produce near net shape components with properties that are comparable with those parts produced from conventional method.

It also has become one of the most flexible and versatile metal forming technologies with its ability to process a wide spectrum of materials including conventional alloys, ceramic as well as composites which are difficult to process through conventional methods. For example, PM can process materials with high melting point for instance nickel, copper and hard as well as brittle materials like beryllium. All type of materials can be processed by PM including ceramics and polymers. Besides, PM also helps to achieve high production rates, precision forming with high tolerance level and near net shape products requiring minimum machining. PM can form simple and also complex shapes economically. The importance of PM in manufacturing can be seen from the increasing number of PM parts used in computers, television, automobiles, office equipment and many more from industrial until aerospace sectors.

2.4.1.1   Steps in Powder Metallurgy

The main steps in PM component production are:

i.   Milling (Powder production)

Powder milling is a process performs with a machine in which breaks solid materials into smaller pieces by grinding, crushing, or cutting. Ball-milling is used mainly as a physical method to modify physical properties of materials such as morphology, crystallinity, solubility, and swelling behaviour. After milling, the morphology changes due to the mechanical energy delivered by the hits and the friction of balls. The milling

11

process by PM method involves the theory of particle collision-agglomeration. Thus, it is important to have a touch on this theory in order to particularly understand the principle.

2.4.1.2 Particle Collision-Agglomerates Principle

Particle collision can occur in two conditions; particle-particle and particle-wall collision(Sgrott & Sommerfeld, 2019). While travelling in the free space, the particle carries together kinetic energy that loses during collisions. The kinetic energy was then transformed into heat energy and dissipated through the collided particles. Here, heat inside the milling jar starts to generate and increasing which causes colliding particles experiencing stickiness effect(Ducros, 2012).

Collisions among coarser particles are less frequent and efficient to form agglomerates than smaller particles(Njobuenwu & Fairweather, 2017). Thus, smaller particle has higher tendency to rapidly grown to a greater size and agglomeration will form. Inter-particles collision causes particle size reduction during milling. Large particle has high-rate fracture. A continuous milling duration causes the particles to becomes smaller and reduces its fracture resistance(Rajkhowa & Wang, 2014). This situation will continue to occur until no further size reduction takes place and particles reaches the fineness limit. Collision of particles is generally categories as permanent deformation as it is an elastic or inelastic collision. While colliding, the particles momentum changes and conserves the total momentum. The conservation of momentum leads to different particles velocity during collision(Wang & Fan, 2013). Therefore, this situation induces the particle to agglomerate and increases in size.

To ease the understanding of particle agglomeration theory, researchers have introduced three distinct agglomeration steps namely the transport step, the collision steps and the adhesion step. The transport step is where the particle initiates kinetic movement, the collision is whenever the inter-particle and particle-wall occurs and shrinking in size and the adhesion is the governed by the physiochemical interactions between two bodies. This has resulted the colliding particles to stick together and becomes larger and form the sphere shapes(Njobuenwu & Fairweather, 2017).

There were few other sizes and shapes of agglomerated particles resulted by the collision. The aggregates were found as elongated and tubular rather than symmetrical

12

sphere just the same with what the research found(Inci, Arnold, Kronenburg, & Weeber, 2014). This aggregates forms happened due to particles that loosen up their rotational symmetry while mixing inside the milling jar. This has happened because of weak binding agglomeration particles(Inci, 2014). Figure 2.2 shows the aggregates of elongated and tubular found in this study. Further discussion needs to be investigated to enhance the understanding of this Brownian motion creation. Spherical form of agglomerated particles is the most compacted particle and this shape has high resistance to movement and probability with another particle. In addition, heat dissipation through compacted solder is flowing smoother(Ducros, 2012).

While planetary plate was rotating, the situation inside the ceramic jar was definitely hectic. The different raw materials inside were hitting, impacting, crushing, shaking, and smashing with each other in the empty area. This has made every piece of different raw materials mixed and combined around yet homogenous new material has been created in a new size, form, and colour. Figure 2.3(c) illustrates the situation inside the ceramic jar during the rotational ball-milling process.
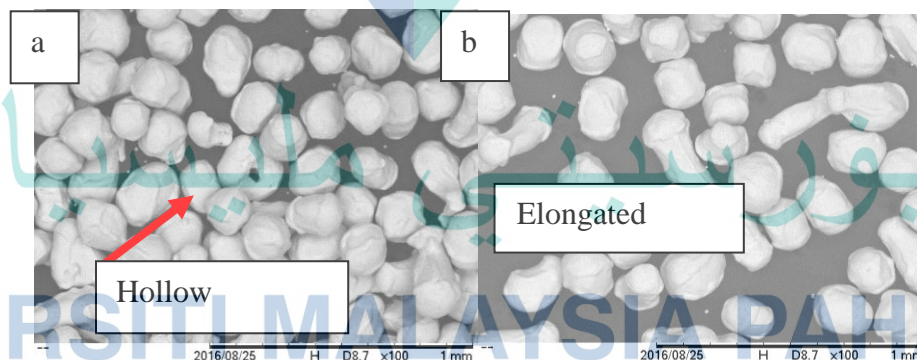
Figure 2.2   The aggregates of (a)hollow and (b)elongated found in this study

(a)   (b)

Smaller piece of raw
material creates massive
mixing in the empty
area and combining
with other pieces with
heat help thus
introducing new form
and size

Rotating

Wall
of the
cerami

Raw materials
crushing into
smaller piece

(c)
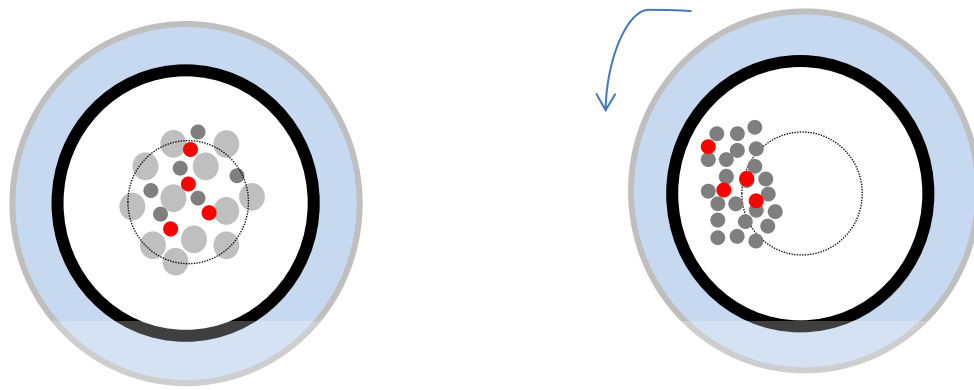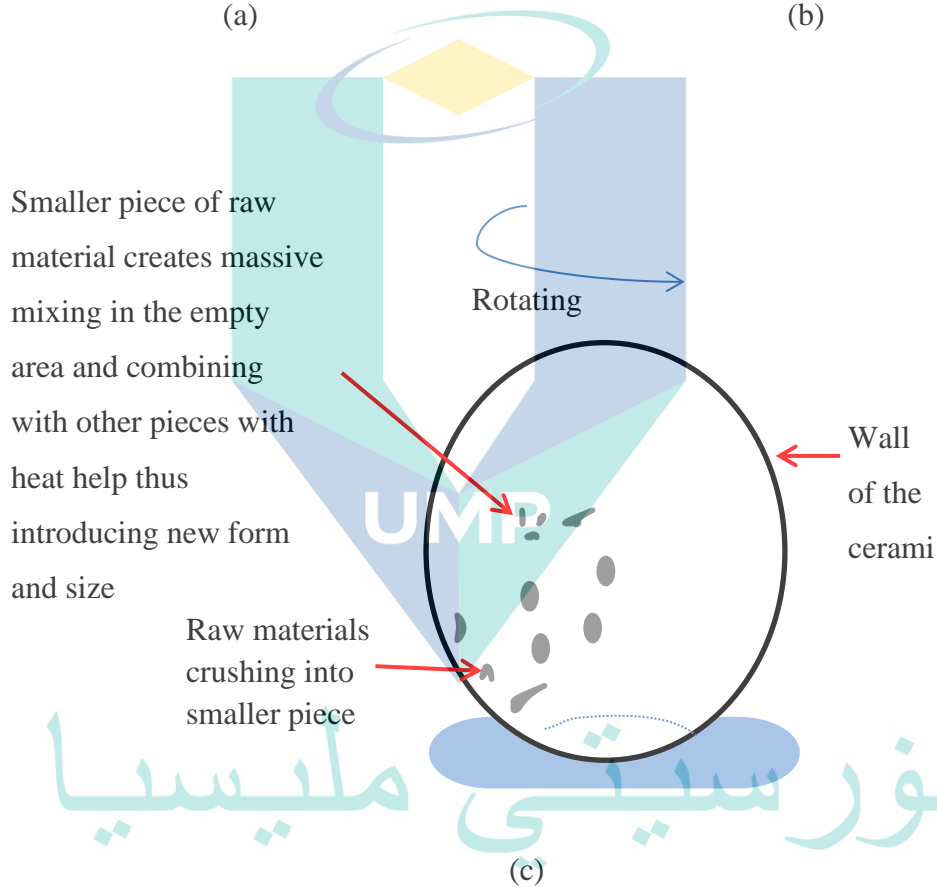
Figure 2.3   Situation of raw materials inside the ceramic jar:(a) at rest, (b) while it
was planetary rotating by counter-clockwise and mixing (top view), (c) the raw
materials were hitting the wall and crushed into irregular size and shape while mixing
(side view)

2.4.1.3   After Milling

The milling process had many effects to do with the microstructures of mixed particles in which it has alternated the sizes, shapes, and colours of the original element of particular SnAgCu materials(Cabeza et al., 2017). To paraphrase, this phenomenon could possibly be known as the deformation of elements. Deformation commonly subjected to several factors that could change the originality of anything. During milling, an individual element combined physically with another two elements and produced a new compound with a new microstructure. Thus, in this research, it is expected that the distinctive particles had gone through the factor of deformation which took place in the milling jar while processing and resulted in the completely different microstructure.

The resulted microstructure of the exposed area of solder alloy granules depends on stress and strain orientation as the factors of deformation(Zeng, Lai, Gan, & Schuh, 2016). Consequent to the high milling speed rotation, the granules collided with each other and hit the wall of milling jar vigorously in a long-time duration thus triggered a force that is applied to the area of collided granules. Eventually, this experience had become stress coordinately to each particle and they started to deform by mixing with each other. Upon mixing and combining, their properties has had synthesized and yielded an eutectic body, which was SnAgCu solder alloy.

As the vectors of collided particles during milling were not the same for all directions, these have caused each particle to experience differential stress(Ju et al., 2019). The unequal stresses will result in non-identical shapes and sizes of SnAgCu granulated particles at the end of the milling process. Those changes in shape are known as a strain caused by differential stress(Cox & Landis, 2018).

2.4.1.4   Sphericity and Roundness

Studying the sphericity and roundness of metal granule is rarely done in metal manufacturing. But when it comes to metal that has been derived from the PM method, the study is a must. This will help the researcher to have a better understanding and acknowledge the behaviour of molten solder alloy on the Cu board as solder should be performed. As these factors are crucial and started to be highlighted in solder alloy prepared by PM method, it is recommended to introduce and use the terminology by a

sedimentary particle in Geology field. Thus, there will be similarities and references in studying this particular factor.

Figure 2.4 below shows the Krumbein-Sloss chart, which is a conventional method of determining the degree of sphericity and roundness of particle shape parameter. It is a famous technique commonly used in Geology, Food Technology, and even Petroleum Engineering field areas to help researchers specify the measurement of any shape of particle grain(Zheng & Hryciw, 2016). The study of sphericity and roundness is crucial to determine the size and shape of particular granules. Such study helps to understand the behaviours of the end results and identifying the fundamental of the products.

All of listed field areas were referencing their particle according to Krumbein-Sloss image analysis chart like Figure 2.4. Thus, metal manufacturing should also utilize the same method as to ease the terminology and concept. According to experts in image analysis industry, Horiba Scientific also mentioned that the analysis on image of the particle is a crucial step in determining the behaviour of product and powder flow(Goh, Heng, & Liew, 2018). They also said that air flow for curvy surfaces as sphere move easily due to higher aerodynamics shape. Thus, the heat will flow equally in all directions if all the particles are spheres. By according to Krumbein-Sloss chart in Figure 2.4, samples in this research have been analysed to be in the broad value of roundness and sphericity range from 0.1 to 0.9 and 0.3 to 0.9 units, respectively.

ii.   Compaction

A mechanical work that done by a machine or mechanism which compress the milled production to reduce the size of material or bring powdered into a form of shapes and sizes. The finishing product becomes a solid and smooth body. It is done by a compacting machine. Purposeful compaction is intended to improve the strength and stiffness of a material.

iii.   Sintering

Sintering is the process of compacting and forming a solid mass of material by heat or pressure without melting it to the point of liquefaction. In PM, sintering is a heat treatment applied to a powder compact in order to impart strength and integrity. The temperature used is below the melting point of the major constituent of PM material.
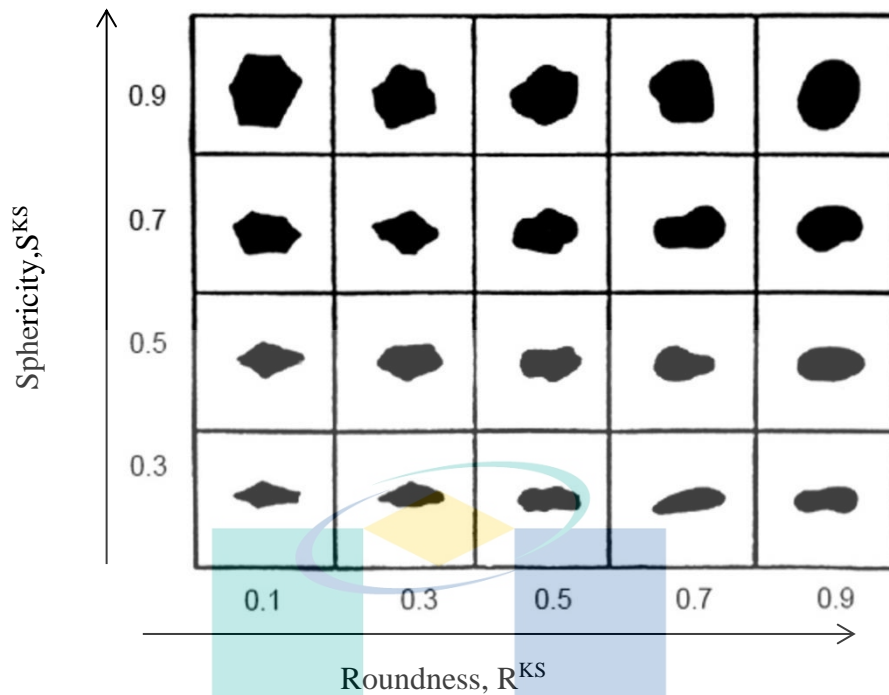
Figure 2.4   Krumbein-Sloss chart

Source: Kim, Suh, & Yun (2019)

2.4.1.5   Advantages of Powder Metallurgy Method

The main advantages of PM method include process, metallurgical and commercial advantages:

i.   Process advantages

PM offers the following important process advantages:

   a. Eliminates or minimizes machining (little or no scrap)

   b. Efficient materials utilization – above 95% material utilization.

   c. Enables close dimensional tolerance – near-nett shapes possible.

   d. Produces good surface finish.

   e. Provides option for heat-treatment, for increasing strength or enhanced wear resistance and plating for improving corrosion resistance.

   f. Facilities manufacture of complex shapes, which would be impractical with other metal working processes.

g. Suited to moderate to high-volume component production requirements.

h. Components can be produced at reduced cost as compared to many other processes, i.e. cost effective.

i. Components of hard materials which are difficult to machine can be readily manufactured, e.g. tungsten wires for incandescent lamps.

j. It is possible to produce components in pure form. Purity of the starting materials can be preserved throughout the process, a requirement for many critical applications.

k. Energy-efficient.

l. Environmental-friendly.

ii.   Metallurgical advantages

PM enables the production of the following items:

a. Powders with uniform chemical composition with the desired characteristics, resulting from the absence of segregation during solidification. These characteristics will be reflected in the finished part.

b. Elemental and pre-alloyed powders.

c. Unique compositions including non-equilibrium compositions and microstructures (crystalline, nanocrystalline and amorphous).

d. Wide variety of materials – metals and alloys of miscible and immiscible systems, refractory metals like tungsten and molybdenum, ceramics, polymers and composites.

e. Parts with controlled porosity.

f. Materials with improved magnetic property.

iii.   Commercial advantages/special characteristic of PM parts

Important commercial advantages of PM include:

a. Ferrous and non-ferrous powder metallurgy parts can be oil-impregnated to function as self-lubricating bearings. Similarly, parts can be resin-impregnated to seal-interconnected porosity to improve density or they can be infiltrated with a lower melting point metal for greater strength and shock resistance, and for making electrical contacts.

b. Parts can be heat-treated and plated if required. PM parts are also amenable to processing by conventional metal-forming processes like rolling and forging.

c. Cost-effective production of simple and complex parts, very close to final dimensions at production rates that can range from a few hundreds to several thousand parts per hour.

d. Offers long term performance reliability in critical applications.

Other than that, Nadia & Haseeb (2012) investigated on fabrication and properties of Sn3.5Ag-xCu solder was using ball milling by PM method. The researcher claimed that, a homogeneous milling had successfully achieved by using 120 hours of milling duration with 150rpm of rotation speed. It was also highlighted that a fine and well distribution of milled particles surrounded the Sn-rich regions as well as improvement of wetting angle in the range of 25° to 18° as a result of using milling technique. Meanwhile, it has conclusively shown that the value of microhardness of milled recycled aluminium beverage cans with Sn-0.7Cu base matrix solder material increased. This showed the combination of has been successfully done using milling by PM method (Salleh et al., 2013).

Milling process in PM method meets the managerial economic of solder alloy fabrication where it conserves energy by just using an amount of electricity to combine the raw materials to be the solder alloy. Thus, this will save a lot on fuel and heat consumption. It is also generating minimum scrap where less leftover from the solder alloy mixture is used, and therefore can allocate the amount of raw materials used. All of these benefits of PM method led to cost reduction, thereby attracting several industries particularly, lead-free solder alloy. The basic work of PM method requires all mechanical parts such as milling and compacting the metal powder using ball-mill and hydraulic press

19

machines, respectively. The final product is in a solid form as according to the mould which has the compaction pressures holding the structures.

In addition, PM method also has drawn interest in other non-solder alloy disciplines to utilize this method into their subjects of researches. For example, G. Xiong et al. (2016) in research on improving biomedical composite metal was using milling process to incorporate the Magnesium powder with hydroxyapatite (HAp) and bioactive glass by a ball milling for 4 hours. The results of this process reported that there was clearly confirmed by SEM and EDX analyses, a uniform distribution of HAp particles in the HAp/Mg composite. The same outcomes presented for El-Kady et al. (2017) which in different discipline ended up to be homogenously distributions by the usage of milling process. These has turned up the amplifier to use the PM method on solder alloy especially in this research.

Boostani et al. (2015) was not using any steel ball during the time of milling and rotation due to higher risks on particle agglomeration by the end of milling process. In fact, the steel ball test also been running out in pre-test where the agglomeration of particles did happen. Meanwhile, Azreen, Sutjipto, & Adesta (2011) in her metal composite research, have used binder to assist the pre-mixture to come out homogeneously spread but she reported that her green packed sample turned out cracked during the compacting process. Hence, this research has stand up to not using neither steel ball nor any binder to prepare the solder alloy mixtures.

Table 2.2   The summarized findings on the homogeneity of mixture prepared by mechanical mixing of PM method

Researcher	Materials	Parameters	Findings
Nadia & Haseeb (2012)	Sn0.7Cu alloy and Sn0.7Cu0.05Ni with TiO2 reinforcement	Machine : an airtight container using a tubular mixer Milling duration : 1 hour	A fine and homogeneous milling had successfully achieved by using a longer milling period.
Salleh (2013)	Recycled aluminium beverage cans with Sn-0.7Cu base matrix solder material	Machine : ball mill Milling duration : 4 hours	The combination of has been successfully done using milling.

20

Table 2.2 Continued

Researcher	Materials	Parameters	Findings
El-Kady, Yehia, & Nouh, (2018); Ghasali, Alizadeh, Niazmand, & Ebadzadeh (2017)	Magnesium powder with 5 wt% B4C in ethanol	Machine : high-energy ball mill without any protective atmosphere Milling duration : 10 minutes – 4 hours	Same compliment on their materials which end up to be excellent homogenous distributions absolutely by the usage of milling process.
Boostani (2015)	A mixture containing nano SiC and GNSs, aluminium powder, nano-b-SiC particles	Machine : planetary ball mill without interruption under high purity (99.999%) argon gas in a liquid nitrogen with steel ball Milling duration : 2 hours	A uniform distribution of SiC particles inside the aluminium matrix was achieved after the milling process Particle agglomeration by the end of milling process

2.5 Soldering

Soldering is a technique to join two or more pieces of component metals using metal filler known as solder alloy in which the alloy must indeed having lower melting point than those adjoining metals. Undoubtedly, it is a delicate operation process but yet complex at the same time. The successfulness of the operation highly rely on understanding and controlling skills upon thermodynamic processes such as intermetallic formation (IMC), surface free energy and surface oxidation (Bobal, 2018). This practice demands skilful operators to handle the soldering tools, machines and solder alloy itself which to be melted at the preferred mating surface of a joint. Notably, electrical application such as electronic assembly acquires suitable soldering techniques as per known so far, hand-soldering, reflow soldering, laser soldering and yet microwave soldering. Hand soldering was the first joining metals method introduced useful for basis regular do-it-yourself soldering, reflow soldering is popular among the surface mount technology (SMT), laser and microwave soldering are latest in soldering area but the applications are vast and promising.

2.5.1 Reflow Soldering Method

The general reflow thermal profile for Pb-free solder alloy is illustrated as in Figure 2.5. Normally, the standard reflow profile has four zones namely preheat, soak, reflow and cooling. The Peak-Reflow-Temperature (PRT) is evidently targeted to range from 245℃ to 260℃ for Pb-free solder alloy W. W. Lee, Nguyen, & Selvaduray(2000). As can be seen, the peak temperature recommended is always 250℃ but the time may vary according to solder alloy material, board level and size of package Kahar(2017); Microsemi Corporation(2008). As with Sn3.0Ag0.5Cu solder alloy, few researchers conceded to have 250℃ as the promising PRT.

In stage 1 known as preheating zone, this very stage is where the heat temperature is purposely raised for up to 3 to 6 ℃/s, which to heat up the assembly components, activate the flux and evaporating the solvents from flux. This low subsequent heat is to ensure no damage occur on the components. In addition, second zone is called as the soaking stage in which all components would be in thermal equilibrium level as they are all have different thermal inertia. Being in equal thermal condition makes they close up to the eutectic solder melting point. The zone where the solid solder started to turn into liquid form is known as reflow zone level. It is noticeable that the SAC solder alloy has melting point of 217℃, but all over researches increase the peak temperature to 250℃ like 33℃ beyond the temperature-above-liquidus (TAL). The reason of doing so is that SAC solder alloy is likely having better wetting on the solid substrate whenever at the hottest point it can be. Thus, solder alloy become genuinely coalesce with the Cu, wets boldly with the pads and components which creates strong metallurgical bonding at the solder joint. The final zone is the cooling stage which totally free-system control where depends on the research to let the body to be on slow, medium or fast cooling method. Figure 2.5 below shows the standard reflow profile.

Coincide with this research procedure in which a reflow soldering method is fully utilized, it is a must to list down several literature reviews on this method upon the application of Powder Metallurgy (PM) fabrication method. Researches on Pb-free solder alloy that practising PM fabrication method also using the similar reflow thermal profile for any soldering technique on Sn3.0Ag0.5Cu solder alloy. There were researchers that practising PM but the soldering method is differed. This statement can be clearly clarified

as numbers of research works were being tabulated in Table 2.3. Note that, all listed references in the table were the data from PM processed materials.
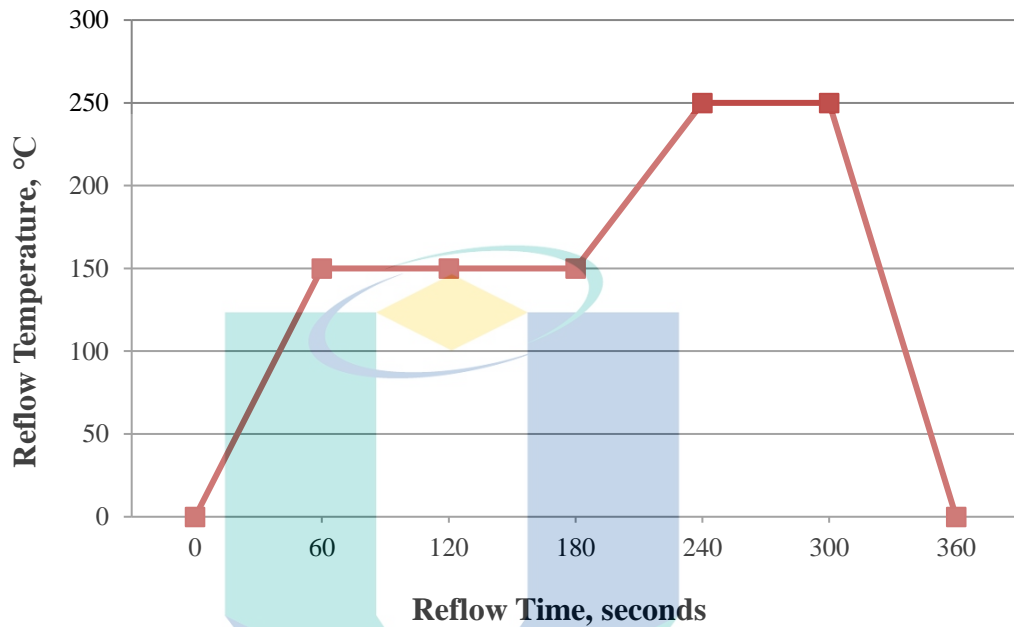
Figure 2.5   Reflow Profile Recommendation

Source: Thiadmer RiemersmaCompuPhase (2018)

Table 2.3   Thermal Reflow Soldering Profile for current works

Researchers	Material	Peak-Reflow-Temperature(PRT), °C	Reflow duration, s
M. A. A. M. Salleh, McDonald, & Nogita, (2017)	Sn0.7Cu and Sn0.7Cu0.05Ni solder powders	250	127
M. Salleh (2011)	SnAgCu powder and silicon nitride (Si3N4)	260	320

23

Table 2.3   Continued

Researchers	Material	Peak-Reflow-Temperature(PRT), °C	Reflow duration, s
Somidin, Salleh, Anuar, & Khairel, (2013)	Pb-free Sn-0.7Cu/re-Al composite solder materials	250	212
Yahya (2013)	Sn-3.5Ag-1.0Cu-xZn (x: 0, 0.1) powders	250	60
Najib, Salleh, Anuar, & Norainiza, (2013)	Sn-0.7Cu/1.0-Si3N4 composite	260	30

2.6   Wettability

Manko defines soldering as a metallurgical joining method using solder with a melting point of below 315 °C as a filler (Manko, 2001). To obtain this, wetting of the solder alloy on a base metal or substrate is important in order to create metallurgical bonding. Wetting refers to the capacity of molten solder to react with a substrate, at the interface of solder and substrate, to form a certain amount of IMC that acts as an adhesion layer to join the solder and the substrate. The reaction between the solder and substrate is essential as it will affect the microstructure and finally affecting the mechanical strength of the solder joint(Noor, 2010). The extent of wetting is measured by the spreading area and the contact angle that is formed at the juncture of a solid and a liquid in a particular environment(Vianco, 1999).

According to Mohd Salleh, Hazizi, Ahmad, Hussin, & Ahmad, 2011 which explained that wettability test is the most important test for solder alloy characterisations due to its role in ensuring the bonding between solder alloy and its substrate. In addition, Said et al., 2015 stated that wettability is the ability of the molten solder spreads or flows onto its substrate during the soldering. Thus, as the molten solder spreads out until it stops

24

due to temperature drop, it resulted with contact angle called wetting angle also known as wettability angle. Figure 2.6 displays the condition of solder alloy wettability.
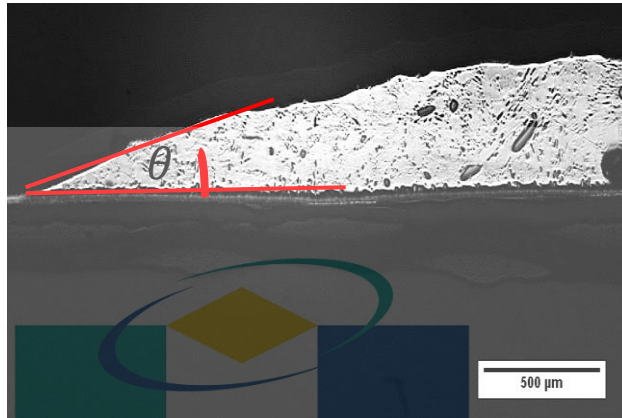
Figure 2.6   The spreading of molten solder alloy on Cu substrate

Sujan (2011) have categorised the wettability degree according to the contact angle as in Table 2.4 below. As Musa, Saud, Razak, & Hussin, 2015 stated that smaller degree of wetting angle is sought after due to strong interconnection of bonding. They also determined that their wetting angle on solder alloy which they described in their findings to be in the acceptable range of wettability in which below 45°.

Table 2.4   Wettability degree which indicated by wetting(contact) angle

Very good wetting	$0° < \theta < 30°$
Good wetting	$30° < \theta < 40°$
Acceptable wetting	$40° < \theta < 55°$
Poor wetting	$55° < \theta < 70°$
Very poor wetting	$\theta > 70°$

There was another melted solder characterization that crucial enough to be discussed. This is the shaping mechanism of molten solder droplet in which related to the spreadable of molten solder(B. Xu, Wu, Zhang, Chen, & Yuan, 2016). Figure 2.7 assists

the understanding of the melting mechanism of compacted solder particles. During reflow soldering, molten molecules that neighbouring the solid pre-alloy solder granulates experienced a surface tension and an internal pressure of gravity that caused them to pull inward. As pulled inwards, the molten molecules at the interconnection had a surface force of adhesion with the solid molecules of Cu board. The interaction has generated the spreadable of molten solder on Cu board. This situation continued until the heat temperature decreased and molten solder cooled down to be solid again. However, it should be noted that each sample had a different amount of melted solder where this could be the granule size and shape issues but still, they were successful to melt and further analyses are remained to proceed.
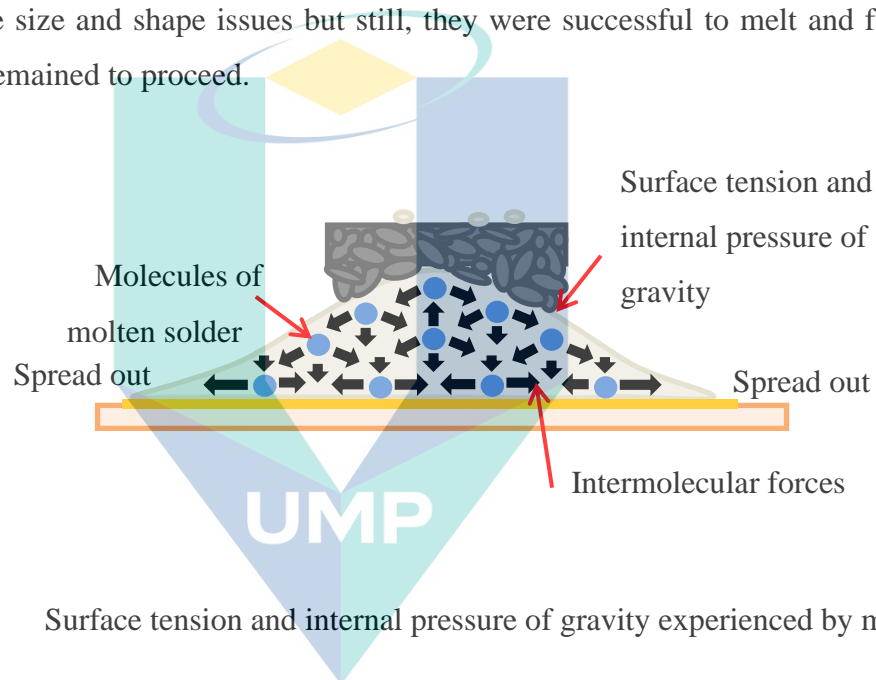
Figure 2.7   Surface tension and internal pressure of gravity experienced by molten molecules

2.7   Interfacial Reaction between Lead-Free Solder and Copper Substrate

This particular section would be discussed about what have been reviewed by the research community regarding interfacial reaction. By studying the topic, each concept by interfacial reaction was identified and categorised properly so that the flow of the concept would be more understandable by readers.

2.7.1   Formation of Intermetallic Compound (IMC)

This sub-chapter presents the findings from the compacted Sn3.0Ag0.5Cu milled powder solder and its substrate. Discussions on the cross-section morphology in terms of formation of the intermetallic compound at the solder joint and solder matrix

have been made purposely for this research. IMC is a form of a metallic alloy that resulted from two or more raw materials which undergoing chemical reaction by heat processing technique such as soldering(Abdelhadi & Ladani, 2012). The study of IMC with respects to its formation is a must to achieve an in-depth understanding of the structural integrity of interfaces along the solder joint. Meanwhile, the solder joint should consist with four major structures which include the substrate, the solder bulk, the IMC layer between the substrate and solder matrix bulk plus two interfaces namely as solder matrix bulk-IMC and IMC-solid substrate.

When it comes into raw materials like Sn, Ag, and Cu as the main pieces of solder alloy togetherness with the Cu substrate, there are few IMCs that could be found at the interfaces, for example, Cu_6Sn_5 and Cu_3Sn but this depends on the thermal factor(M. Park & Arróyave, 2012). IMCs will be formed when the molten solder is supersaturated by the Cu atoms from the Cu substrate. During the reflow process, the IMC form a scallop-like layer vertically to the solder matrix by the Cu substrate due to an effect of fast Cu diffusion into that solder. The phenomenon is called liquid grooving(Bokstein, Klinger, & Apikhtina, 1995).

2.7.2 Mechanism of IMC by the Powder Metallurgy method

Specifically, this section is going to expound the mechanism of IMC morphology in the point of Powder Metallurgy view. Starts off with the IMC along the solder joint, where it was obviously happened to have a non-uniform of shapes and sizes for all IMC. According to this research, these circumstances had a strong connection with reflow soldering process. The heating and liquefying the piece of compacted Sn3.0Ag0.5Cu milled powder solder occurred at the Cu substrate pad which heated upwards tangentially, as it was reaching the non-identical shapes and sizes of granulated and compacted solder alloy. A limited liquid-state reaction has left the unmelted pre-alloy granulates on top of the molten solder alloy.

The issue was coming from the different shapes and sizes of pre-alloy granules that have been placed on the Cu substrate for the reflow process. Figure 2.8 shows the cross-section image of compacted Sn3.0Ag0.5Cu milled powder solder. The yellow line was just to show difference of granules length. Longer line indicates longer time taken for heat distribution to melt a granule. When the environment temperature reached the

27

melting point of SnAgCu solder alloy which is 217℃, each of the compacted solder alloy granules tends to get into the molten state but with bothersome factors such as compression load, different sizes and shapes, made them so hard to melt all at once. Smaller granules succeeded to follow the liquid-state reaction in reflow time due to their low latent heat of fusion rather than the bigger one.
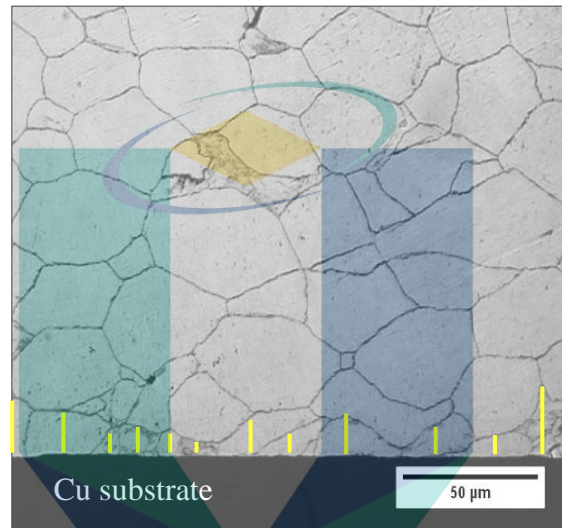
Figure 2.8   The cross-section image of compacted Sn3.0Ag0.5Cu pre-alloy granule; the yellow line is as an indicator

2.7.3   IMC Formation Mechanism

Topic on IMC growth is expounded more on this chapter because it means a lot to what makes those whole electronic and electrical packages favourable. This is also means that the IMC is responsible to the reliability and quality of those packages which lead to the up and down of company profitable record (Kotadia et al., 2014). IMC is defines as two or more metal atoms combined chemically under a relative heat as the results of liquid-solid reaction (O Y Liashenko, Lay, & Hodaj, 2016). This makes the IMC as the core subject of metal joining especially in soldering area. Not only that, the existence of IMC layer at the solder joint indicates a valid metallurgical bond between the solid substrate and the solder bulk and thus offering a high impact of any electronic systems (L. M. Lee & Mohamad, 2013; Pawełkiewicz, Danielewski, & Janczak-Rusch,

2015). Figure 2.9 displays the schematic illustrations of IMC formation during interdiffusion (Luu, Duan, Aasmundtveit, & Hoivik, 2013).
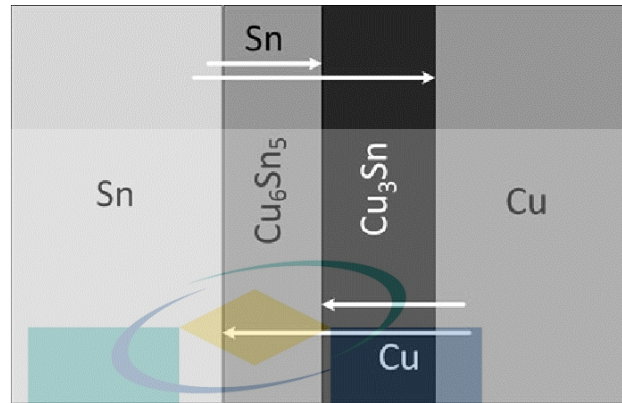
Figure 2.9   The schematic illustrations of IMC formation during interdiffusion

2.7.3.1   Atomic Migration

Whenever a solder alloy is attached directly to a solid substrate and allowed to be in a relatively thermal circumstance, that alloy would melt off on the piece of solid and tends to create a bond that chemically and physically contact to each other. Using SAC/Cu substrate, each atom in solder bulk should have to receive heat that makes them loosen up from their strong forces that holds between them and starts to move off. In this case, Cu atom which has been several times nominated as the dominant diffuse species in interfacial reaction initiates its migration upwards from the solid substrate and gets into the molten solder bulk right after it dissolves with Cu ions Kunwar et al., 2016; O Yu Liashenko & Hodaj, 2015; C. Wang, Li, Chiu, & Chang, 2018. In short, the Cu atom inside molten SAC is moving freely and as it is attaching with the Cu ion of Cu substrate, those atoms dissolve and diffuse. By means of diffuse, Cu atom from Cu substrate which certainly has lower concentration value than the molten solder diffuses vertically along the solder joint interface (Tian, Zhang, Hang, Niu, & Wang, 2014). This is where the IMC started to form and getting intense by the heat as long as the temperature is higher than the melting point of SAC solder alloy.

2.7.3.2   Atomic Reaction

The second mechanism of IMC ideology is the interfacial reaction amongst atoms whereby this would be a complex yet fundamental soldering basis to study on. Apparently, receiving heat of 220°C makes the Sn and Cu atoms to not only melts off but they do dissolve, coalesce and becoming the phase known as IMC precipitated at solder joint and solder matrix simultaneously. In a SnAgCu ternary alloy system, Sn and Cu atom would do the reaction at the first stage of solid-liquid interdiffusion (SLID) due to the degree of solubility that Sn has whenever with Cu. While Sn reaches the degree, this allows the molten Sn to dissolve with Cu in order to create a nucleation of Cu_6Sn_5 IMC(Tu & Liu, 2019). In short, the molten solder alloy being reacted with Cu substrate is following the effect of chemical reaction between Cu substrate and Sn atom(Hu, Xu, Keer, Li, & Jiang, 2017). This fact can be best described as a chemical equation below(Tang, Luo, Li, Hou, & Li, 2018):

$$6Cu + 5Sn \rightarrow Cu6Sn5 \qquad\qquad 2.1$$

Clearly, it acquires 6 atoms of Cu and 5 atoms of Sn to have Cu_6Sn_5 compound as the initial formation of interfacial IMC product. By the way, these atoms combination in Sn-rich environment also bring out the fact that the Sn diffusion into the Cu substrate is absolutely negligible (H. Li, An, Wang, & Jiang, 2015). However, there is no reaction of Ag with Cu to form any intermetallic since Ag has a very little effect on consumption rate of Cu substrate (Gong, Liu, Conway, & Silberschmidt, 2008; Sona & Prabhu, 2013).

2.7.3.3   Atomic Growth

The growth of IMC influences the reliability of soldering. When IMC is growing up by the full affection from heating surrounds each of individual of it, there must be something happened to the solid substrate, individual IMC itself and the solder matrix. Even to the layer of solid substrate-IMC interfacial and to the IMC-solder bulk. This section is exclusively brought to readers to fully achieving the understanding of IMC growth behaviours by reviewing the literatures over the years. The discussion would be

in general term of IMC growth, not affected by any means of practices, alloy fabrication and even soldering method. The atom would go through a phase called atomic reaction. The atoms would react to combine and precipitated along the solder joint and in the solder matrix. The thing is once they start to combine, there must be another same molecule that will do the same. This in-details process will perpetually occur which the below molecule will push the top molecule vertically and their height gets taller and taller eventually this becomes the growing thing. While the atoms are growing, there are few details that need to be bear off.

2.7.3.4   The kinetic growth of IMC

The IMC growth can be well explained by the classic kinetic theory where the growth is basically the common diffusion-controlled reaction which will about to answer the differences of any IMC morphologies (H. Li, 2015). According to the previous studies, H. Li (2015) reported that the growth of IMC is mainly from the supersaturated solder matrix when Cu atoms are consumed to the reaction combination of Cu_6Sn_5. The Cu-Sn IMC will grow in scallop shape with gap between the scallops. The gap would be a quick diffusion path for the Cu atoms from substrate to get into solder matrix (H. Li, 2015).

The growth mechanism governed by two principals which are diffusion-control and interfacial-control (H. Li, 2015; Tu & Liu, 2019; Yu & Shangguan, 2013). During reflow, the scallop grain formed by interfacial reaction and the effect of ripening mechanism (Ma, 2017). Due to continuous combination reaction of Cu atoms from substrate with the Sn from the molten solder, the height of Cu_6Sn_5 growing taller as long as heat is supplied (Tao, Benabou, Vivet, Le, & Ouezdou, 2016). However, Gong (2008) in his research reported that the Cu atoms precipitated on top of existence Cu_6Sn_5 interface which made the IMC layer become thicker. Likewise, during reflow due the SLID reaction, there were few researchers reported that this was the time when the Cu atoms migrate into solder matrix by diffusion-controlled mechanism through the interface of solder joint (Hu, 2017; Y. Li & Chan, 2015; Tao, 2016). Figure 2.10 depicts the changes of IMC growth due to increasing temperature.
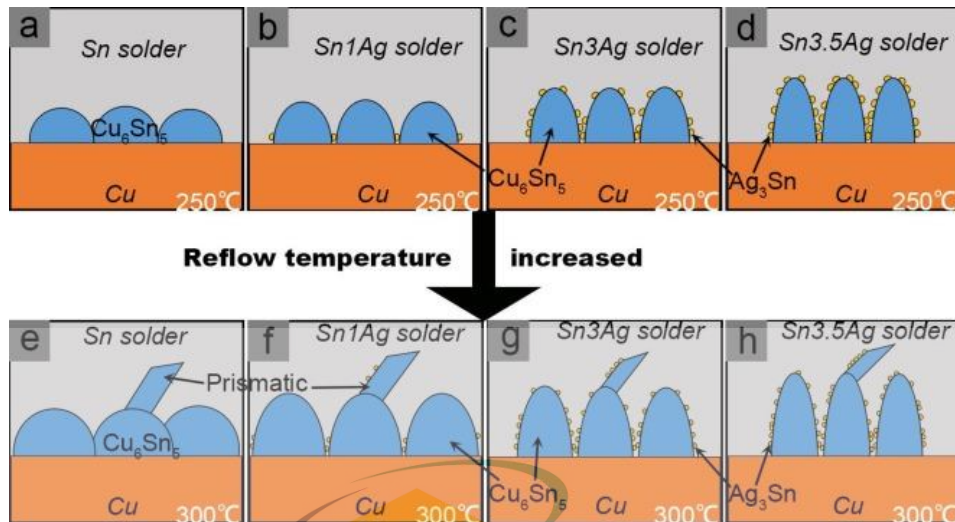
Figure 2.10   The changes of IMC growth due to increasing temperature

2.7.3.5   The scallop shape of Cu_6Sn_5

Increasing the heating temperature will cause the acceleration in elements diffusion across the interface to get into liquid solder(Sona & Prabhu, 2013). While dissolution of Cu atoms into solder matrix being called solid-liquid diffusion reaction, the rapid dissolution of Cu atoms into solder matrix would then be called as the heterogeneous solid-liquid diffusion reaction. This happens during the reflow process at 250°C heat temperature. As a consequence of this rapid reaction and differences in diffusion path, the combinations of Cu and Sn atom coalesced and emerged into spherical shape of scallops (Pawełkiewicz, 2015). Figure 2.11 below shows the scallop shape of IMC on top of the Cu substrate.
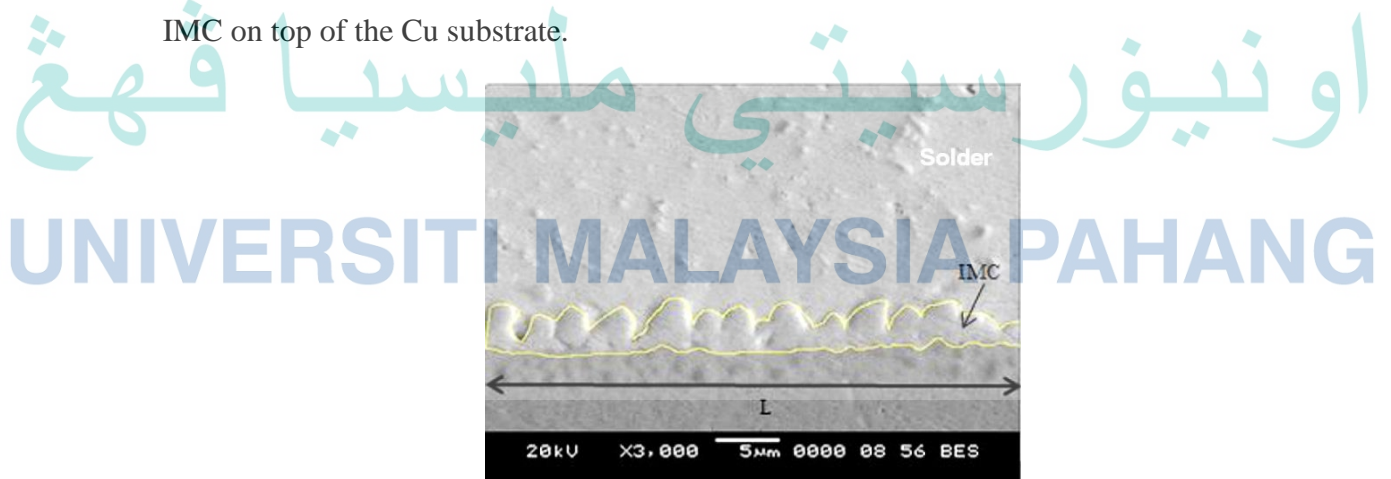

Figure 2.11   The scallop shape of IMC on top of the Cu substrate

2.8   Thickness of intermetallic compound(IMC)

One way to characterise the microstructure evolution of IMC layer is by identifying the average thickness of the IMC layer. Not only that, IMC thickness will perpetually grow under specific conditional such as during soldering and isothermal aging. According to An & Qin(2014), IMC at solder joint shall effecting few properties of solder alloy including tensile strength, shear strength and fracture toughness of solder joints. This is accordance to few reports that stated in scientific works saying that a thicker IMC layer is inherently brittle in nature mostly when concerning the issue to that of different thermal condition like thermal aging and thermal process (Shah, Mohamad, Yaakob, Razali, & Ishak, 2016; Tan, Tan, & Yusof, 2015).

The IMC of Cu_6Sn_5 is a form of solid compound that it can react as a barrier to that of diffusion reaction between Sn atom from solder bulk or Cu atoms from Cu substrate from migrating in or out of its original location if and only if the IMC layer is thick enough and inhibit the diffusion path (An & Qin, 2014). Thus, whenever the amount of Cu atom is insufficient in the solid-liquid reaction, it would resulted in lower IMC thickness and grain structures (Chellvarajoo, Abdullah, & Samsudin, 2015).

2.9   Summary

Sub-topics of 2.2 and 2.3 are written to clarify the basis of solder in which SnAgCu is one of the popular solder group and Sn3.0Ag0.5Cu composition was selected in this research due to its closest eutectic solder and has lower melting point. Subtopic 2.4 is the main focus in this thesis in which PM method is accounted as new solder alloy fabrication and can be the most suitable technique to generate a higher homogeneity distribution for Sn3.0Ag0.5Cu solder alloy. According to listed literatures, there were researches conducted different elements other than solder alloy which succeeded to be well-incorporated but parameters on speed and time duration while the milling process needs to be controlled.

Some researchers also found that having short milling duration might lead to lower homogeneity issue as well as other solder alloy characterisations including wettability. Therefore, this research is conducted to bring an uplift to PM method on the better parameters in terms of duration to prepare the homogenous distribution on

33

Sn3.0Ag0.5Cu solder alloy. Nonetheless, there were minimum significant discussion on compaction process in PM method other than remarks on the values and machines usage. Therefore, further research has to be conducted to study the effect of compacting onto the microstructure of the milled solder alloy pre-mixture.

Sub-topics 2.5, 2.6 and 2.7 are the added values of literatures to solder alloy properties fabricated by PM method which are crucial in determining the performances of solder alloy characterisations in which reflow soldering, wettability and IMC respectively. It is recommended by solder researchers to use 250℃ as the temperature for reflow soldering on Sn3.0Ag0.5Cu solder alloy as the constituents inside alloy may not be damaged and well-suited to melt down the solder alloy pre-mixture. As the melting going smooth, it can create a well distributions of solder liquid droplets and spreads on its substrate to have an optimum contact angle which can lead to better electrical interconnections. Therefore, having an optimum solder alloy wetting can further achieving the optimum IMC profile.
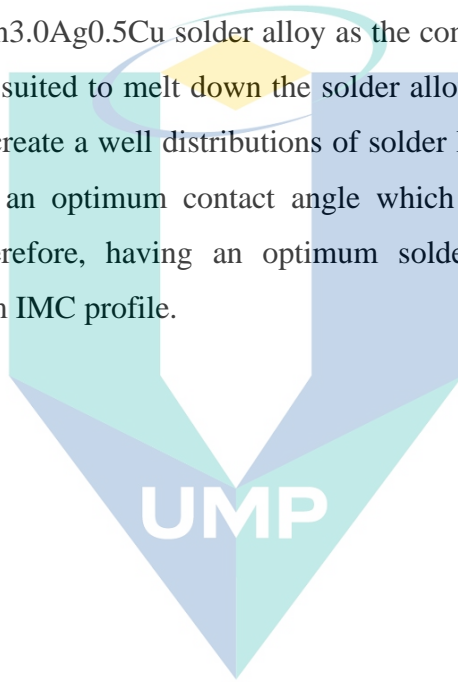
CHAPTER 3

METHODOLOGY

3.1   Introduction

This chapter presents the details of experimental works and methods that have been done to reach the objectives in this research. These includes the research flowchart, selection of raw materials, calculations, samples preparation, experimental setup for PM method, reflow testing setup, microstructure analysis setup and mechanical testing setup. The samples preparation followed the ASTM E3-11 for Metallographic Specimens and was divided into two methods which were Method A and B. Method A was the setup for microhardness, cross section and top microstructure which did not have to go through reflow process whereas Method B was for reflowed samples such as wettability, IMC formation and IMC thickness analyses.

3.2   Research Frameworks

In this research, Sn3.0Ag0.5Cu solder alloy is developed by using PM method. The methods included were milling and compacting processes which different than the conventional casting method. Throughout the process, there were few variables that have been selected for milling and compacting in order to study the effects and the abilities of both methods to practically fabricate the solder alloy. The solid solder alloy was then being tested with numbers of analyses to check the properties whether it can be an alternative to conventional casted solder alloy or it is not an option to do so. Figure 3.1 shows the flow chart for this research.
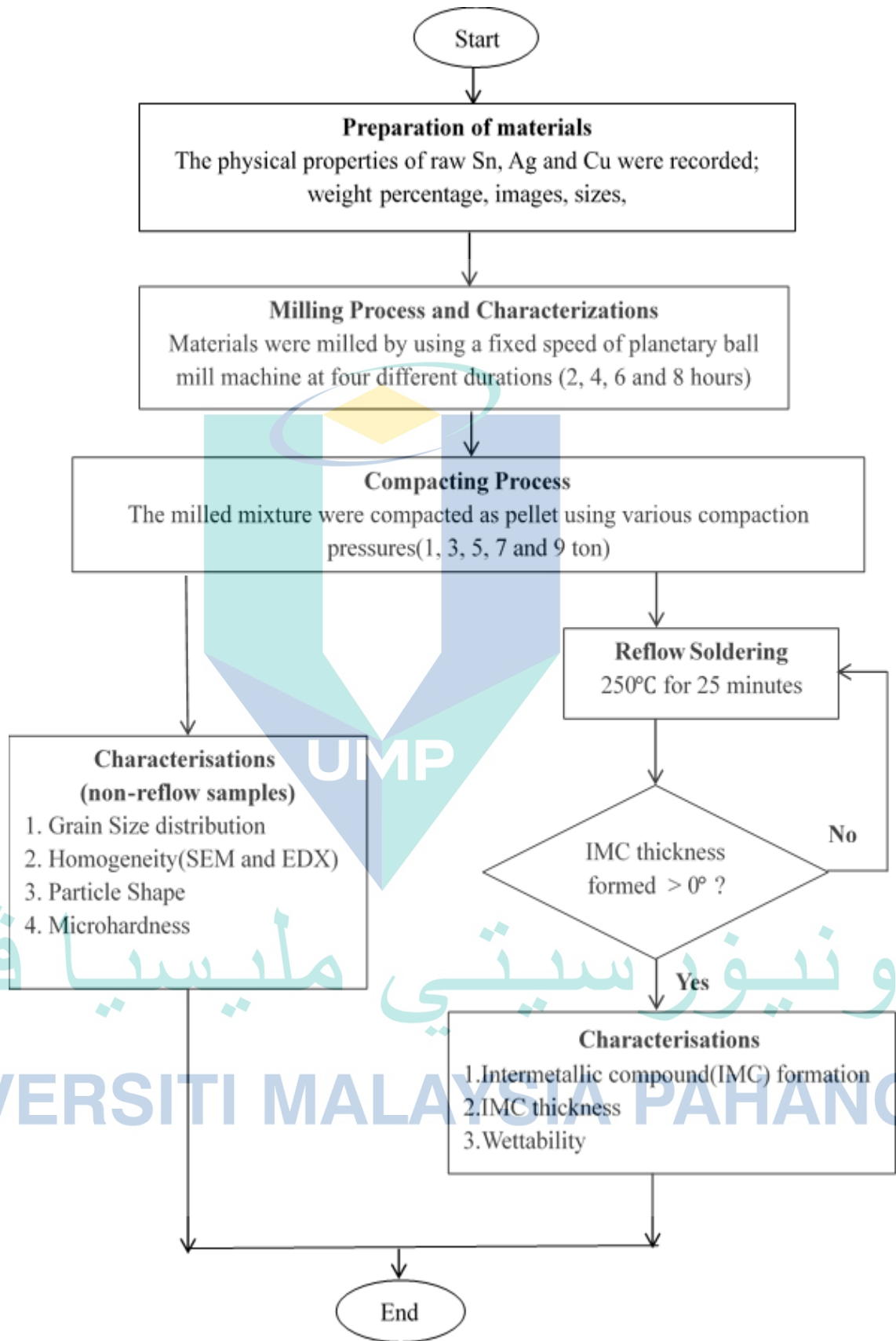
Figure 3.1   Flowchart of the research

3.3   Raw Materials

Each raw material used to fabricate Sn-3.0Ag-0.5Cu solder alloy in this research was prepared using 99.9% of pure element. The granulated Sn and Cu powder with the sizes between 108 to 750μm whereas the sizes of 4 - 7μm of Ag fine powder were used. They were then pre-weighted according to the wettability percent and preceded throughout the stages of PM routes. Figure 3.2 are the SEM images for the raw materials.
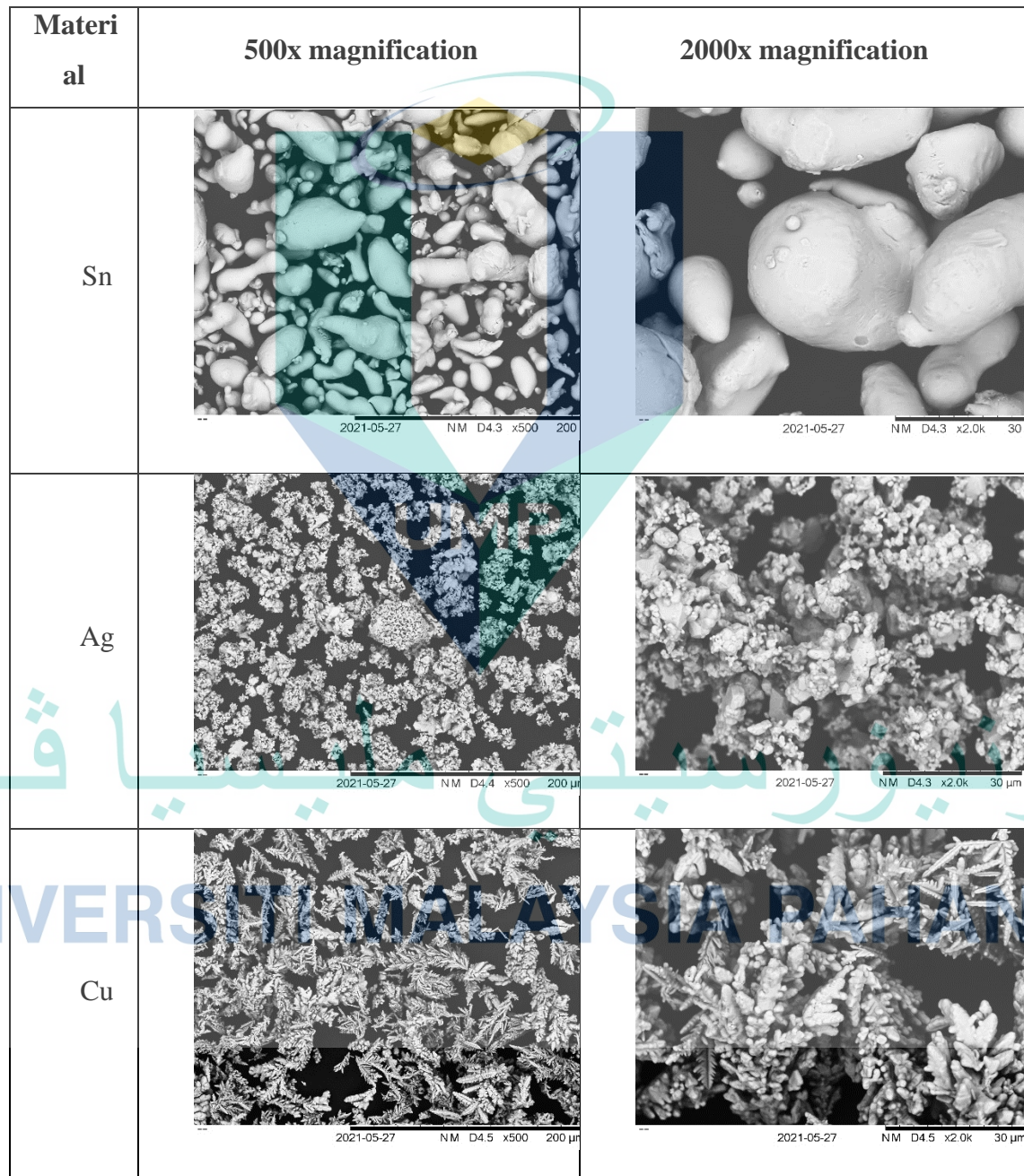
Material	500x magnification	2000x magnification
Sn		
Ag		
Cu		

Figure 3.2   Images of raw materials captured by SEM Sn, Ag, Cu

Table 3.1   Properties of tin(Sn), copper(Cu) and silver(Ag)

Properties	Tin(Sn)	Silver(Ag)	Copper(Cu)
Particle Size	108 - 510μm	4 - 7μm	34 - 750μm
Form/Shape	Irregular, flake	Fine powder	Powdery, agglomerated
Composition	≥99.9%	99.9% metal basis	99.999% metal trace

Source: Sigma Aldrich Merck and Alfa Aesar, (2018)

3.3.1 Particle Size Distribution of As-Received Powder

Figure 3.3 shows the graphs of the particle size distribution for the as-received powder for Sn, Ag and Cu respectively. Sn powder particle presents the highest distribution for the smallest particle followed by Ag and Cu. Thus, this analysis ensured the properties gained from the production company of the materials. The mean values for each powder were also calculated and the value were 3592.4 μm, 3909.8 μm and 2785.6 μm. The skewness of distribution are positively skewed and getting longer to the right showed that those as-received powder particles range to bigger particle sizes.
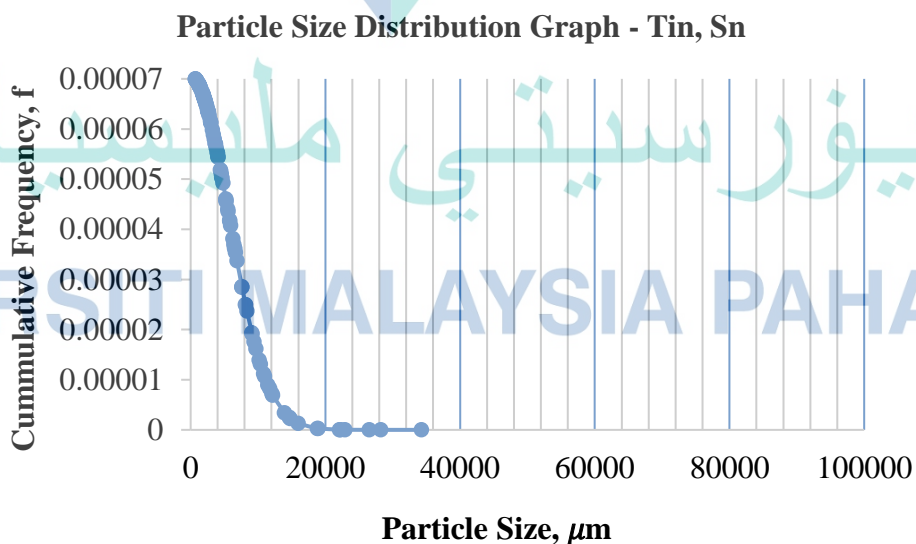

Figure 3.3   The graphs of particle size distribution for the as-received powder; Sn, Ag and Cu
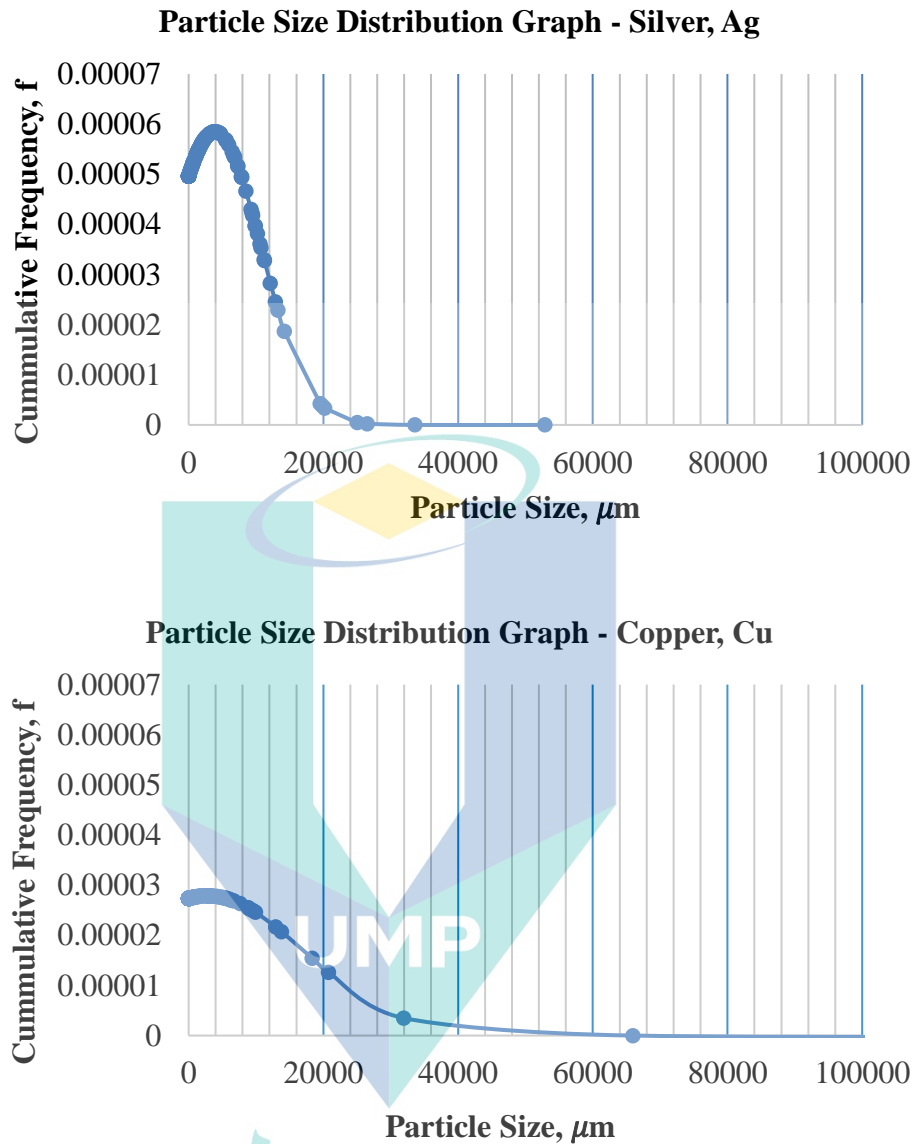
Particle Size Distribution Graph - Silver, Ag

Particle Size Distribution Graph - Copper, Cu

Figure 3.3   Continued

3.4   Calculation to Obtain a Sample

In order to obtain a solid compressed solder alloy pellet, 1.7 gram of mixed raw powder is first calculated but a net weight of 1.5 gram was used to produce a unit of solder alloy in pellet form. In this research, four milling duration were used and each duration proceeded with five different compressing pressures. Therefore, each of duration had a total of five samples to be used in every test conducted onwards. Note that the calculation below was for a single milling duration and a precision laboratory weighing scale was utilized.

No. of sample: 5 units of compacted solder alloy for 1 milling duration

Each sample required 1.7 g x 5 units = 8.5 g

$$Cu = \frac{0.5}{100} \text{ x } 8.5 = 0.0425 \text{ g}$$

$$Ag = \frac{3.0}{100} \text{ x } 8.5 = 0.2550 \text{ g}$$

$$Sn = \frac{96.5}{100} \text{ x } 8.5 = 8.2025 \text{ g}$$

Total = 8.5 g for 1 milling duration x 4 milling durations = 34.0 g

Thus, to obtain all samples for four milling durations, a quantity of 34.0 g of Sn3.0Ag0.5Cu pre-mixture is needed throughout this study.

3.5 Powder Metallurgy Methods

In this research, only two basic processes in PM method were used to fabricate the solder alloy which were milling and compressing process. Both of these methods involve electrical and manual handling respectively.

3.5.1 Milling

As the first step in processing the raw materials by using a mixing technique or also known as milling in PM process, it is crucial to really understand what exactly happened upon the changes on physical properties of raw materials become at the end of the milling process. The milling process took four different durations. Thus, milling duration was a parameter to consider in achieving the optimum properties of solder alloy using the PM method.

The material of milling jar, rotation speed, and milling duration are the considerations for milling process, whereas physical properties of materials such as the size, form, and colours should be concerned at the beginning of the process. This is because, while the machine was working, all these parameters were the main factors of changing the different physical properties of different materials into new mixtured properties.

In this work, 1400 rotation per minute (rpm) of speed rotation by a planetary ball mill machine was used throughout the milling process together with a solid ceramic milling jar as the container to fill up the pre-mixed raw materials. The rotation speed was so high causing the materials hitting the inside layer of the jar wall with the high impact of the collision and creating shear forces(Nandiyanto, Zaen, & Oktiani, 2018; Weerasekara, Liu, & Powell, 2016) . This situation has made each of the raw materials crushed and shrank into smaller size while mixed them homogenously together by the physical assembling during the rotation. Figure 4.2 illustrates this situation.

Using a planetary ball-mill machine (FM-2 Model) as in Figure 3.2, all 102.0 g of pre-mixture of Sn3.0Ag0.5Cu solder alloys were milled for 2, 4, 6 and 8 hours to achieve a uniform distribution and to get similar size of ending pre-mixtures. 25.5 g from the pre-mixture was then taken out at every completed of milling duration as to re-weight it into 1.5 g in each plastic container for further process.
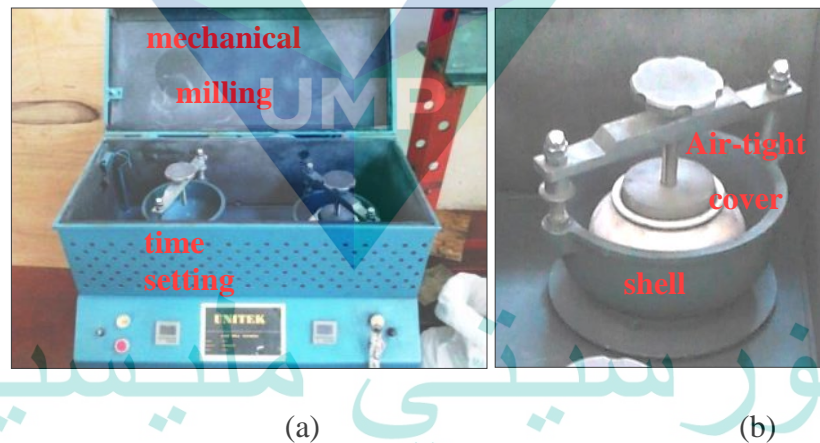

(a)   (b)

Figure 3.4   Image (a) shows the planetary ball mill machine used to mill the pre-mixture of Sn3.0Ag0.5Cu and Figure (b) the inner part

As the shell rotated horizontally, ball mill machine continuously working to grind and blend the mixture at a constant speed of 1400 rpm and this has caused the mixture to move around. By doing so for hours, the solid particles in the mixtures have reduced in size by impact as well as changed its shape and colours. The air tight cover comes with the ceramic bowl to ensure minimum oxidation. Further discussion on oxidation is explained in Chapter 4. Figure 3.5 shows the Sn3.0Ag0.5Cu as before and

after the milling process according to a normal capture of camera. Images by SEM can be found in Chapter 4.

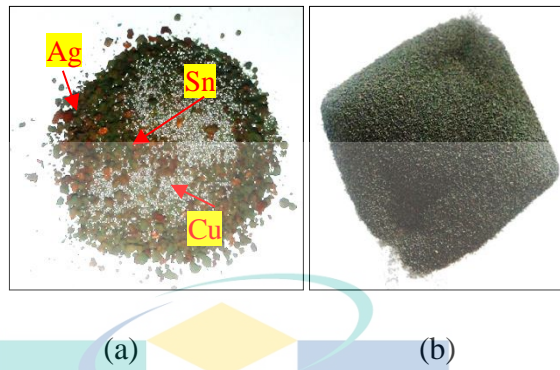(a)　　　　　　　　　　　(b)

Figure 3.5　　　Image (a) and (b) show the mixture of Sn3.0Ag0.5Cu before and after the milling process
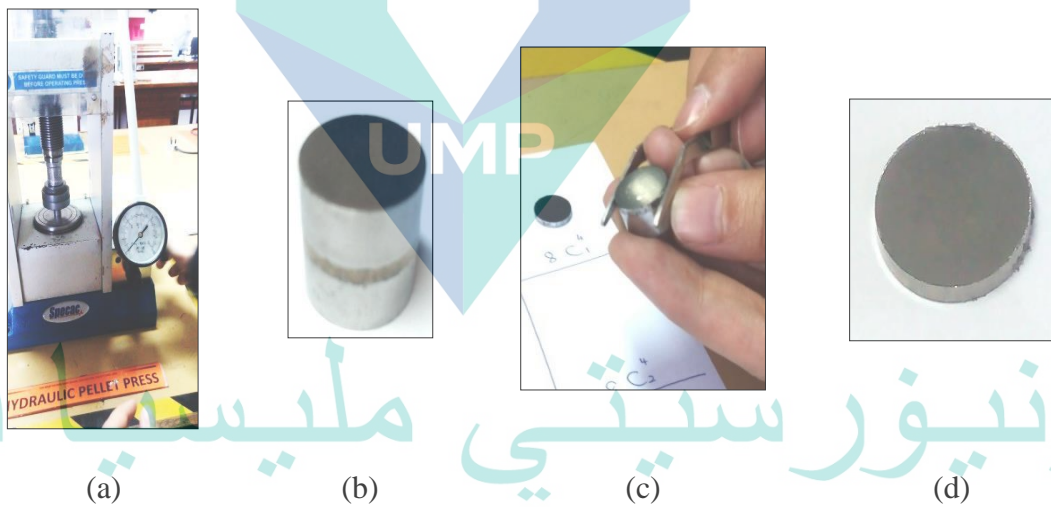

(a)　　　　　(b)　　　　　(c)　　　　　(d)

Figure 3.6　　　Image (a) until (d) displays the procedure to produce a solid, smooth and symmetrical solder pellet from 1.5 g of Sn3.0Ag0.5Cu mixture

3.6　Sample Preparation

Samples were prepared for microstructure characterization. The works were divided into two methods which are sample preparation with and without reflow soldering. Method A was for the samples that did not go through the reflow soldering and

they were used for microstructural imaging for top area and cross section area as well as microhardness. Method B on contrary requires samples to be melted on its substrate to run on few of solder alloy characterisations.

3.6.1   Method A

Samples without going through reflow process required a solid, smooth and symmetrical of solder alloy pellet. Using the cold mounting as the medium is the best way to provide a safe and ergonomic way to hold the sample. The liquid resin and hardener which were mixed and stirred slowly in a paper cup by 5:1 ratio enough to fill up the mounting cups just after swiping them with releasing agent. They were then allowed to harden for at least 2 hours below the sunlight before getting ready for the next testing.

For Figure 3.7(a) and (b), both of these two figures illustrate the position of solder alloy pellet in harden liquid resin. The (a) was for top and microhardness whereas position in figure (b) was for cross section microstructure imaging. The top surface as labelled in figures were the surface to face on the sandpaper in grinding and polishing step.

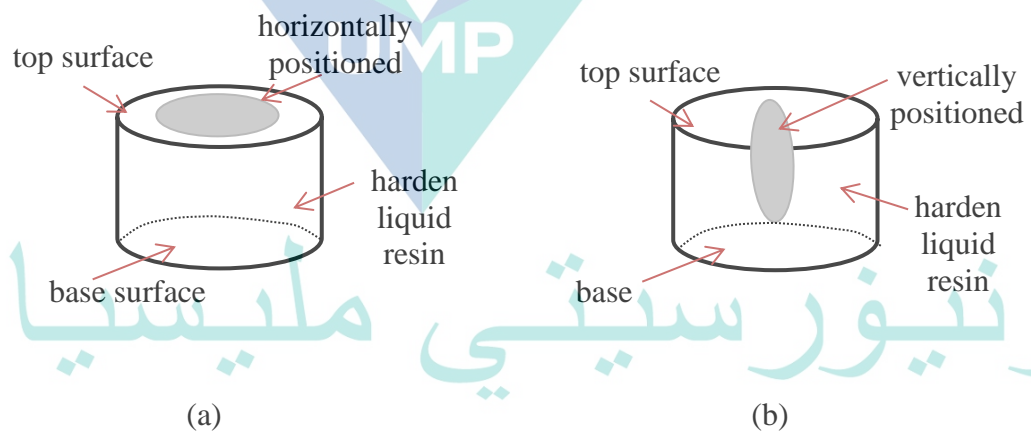(a)   (b)

Figure 3.7   Figure (a) and (b) are the illustrations to position the solder alloy pellet according to their characterization test

The actual microstructure of the samples can only be revealed after passing through grinding and polishing steps. Using a rotating grinding and polishing machine, these were done by alternating the sandpapers starting with the coarse until the finest grit successively before the polishing step. Alumina suspension of 0.05 micron was used to provide a scratch-free mirror finished on the sample.

To have a clearer image shall be obtained with etching process. This technique would be able to remove unwanted parts of a metal by corroding the outer surface of metal and leaving off much clearer microstructure for imaging purpose. The ratio used for the etching liquid was 1:9 for hydrochloric acid, HCl and ethanol.

The images of samples were then captured by using optical microscope of at 10x magnifications for top view microstructure analysis which then being analysed by ImageJ software. SEM, EDX and grain size analyses were running on the samples. The same sample was used for hardness test by utilizing the Vickers Hardness machine and the ASTM standard of B933-09 was followed. 15 straight lines of indentations were attained on the samples like shown in Figure 3.8.
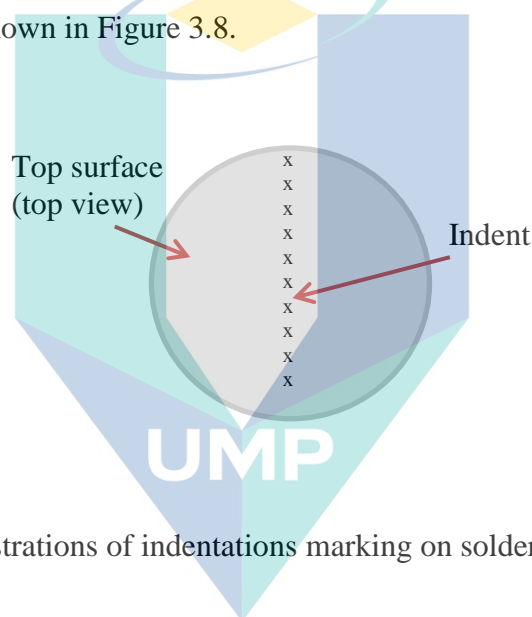

Figure 3.8   Illustrations of indentations marking on solder alloy pellet for microhardness test

3.6.2   Method B

This method was done for the samples that needed to go through the reflow soldering process. After compaction, the solid and round form of solder alloy pellet entailed to be cut into smaller size which approximately 1/8 portion. The cut-out work has been done with a sharp knife and a hammer. They were then placed on the 1cm by 1cm of Cu board as the substrate. An illustration of the cut-out work shows as in Figure 3.9.
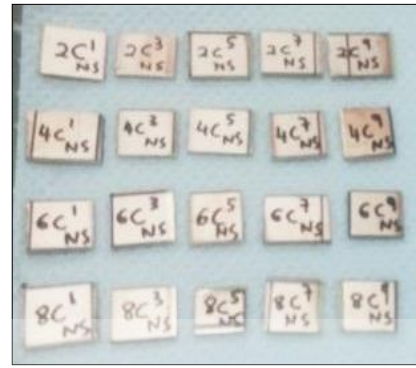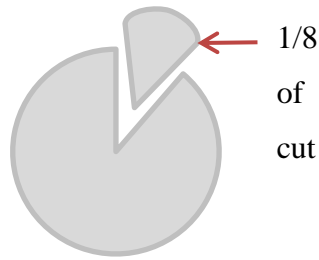
| (a) | (b) |

Figure 3.9   The cut-out solder alloy pellet is illustrated as in (a) and Cu board(b)

   The 1/8 of cut out solder alloy pellet were then attached with the labelled Cu board by using no clean flux as an aid to block oxidation at the surface of solder alloy with the substrate during the reflow soldering. Figure 3.10(a) was to illustrate the way of placing the flux. All samples were inserted into the furnace in a room temperature setting at the beginning before it was set to 250 °C for 25 minutes with an addition of 1 minute holding time to allow reflow soldering process to take place. The samples remained in the furnace for 12 hour to allow the slow cooling process in the furnace.
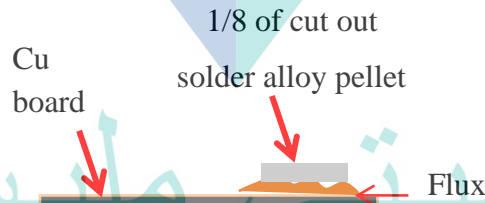
(a)

Figure 3.10   Image (a) is an illustration of assembling the 1/8 of cut out solder alloy pellet, image (b) is the table-top furnace and image (c) is the enlarge display screen
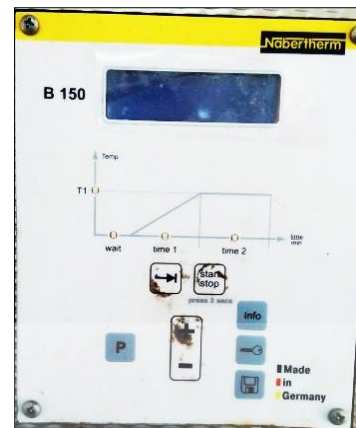
(b)   (c)

Figure 3.10   Continued

After all samples achieved the room temperature, they were then subjected to method B but the samples need to stand inside a mounting cup for the hardening purpose. Using sample holder is essential for this part so that the sample would not move and slanted. This was a crucial technique for the images of cross section of the samples could be captured nicely especially for wettability, formation and thickness of the IMC. The condition in the cup is illustrated in Figure 3.11.
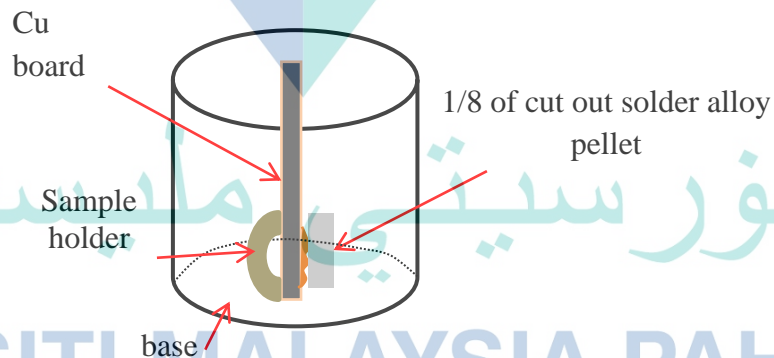

Figure 3.11   Illustration of how to position the method B sample

Figure 3.12 shows the different between small and large wetting angle and how it was measured. When a small wetting angle is measured, this indicated that the molten solder was spread over on the large area of Cu substrate whereas large wetting angle

means that the molten solder is beaded on the surface. In specific, a small wetting angle is sought out in order to perform the optimum wettability. For this reason, it is best to explicate the wettability result according to each of the milling durations. This is much simpler to study and interpret the wettability data so that a comprehensive study of it can be drawn to the maximum.
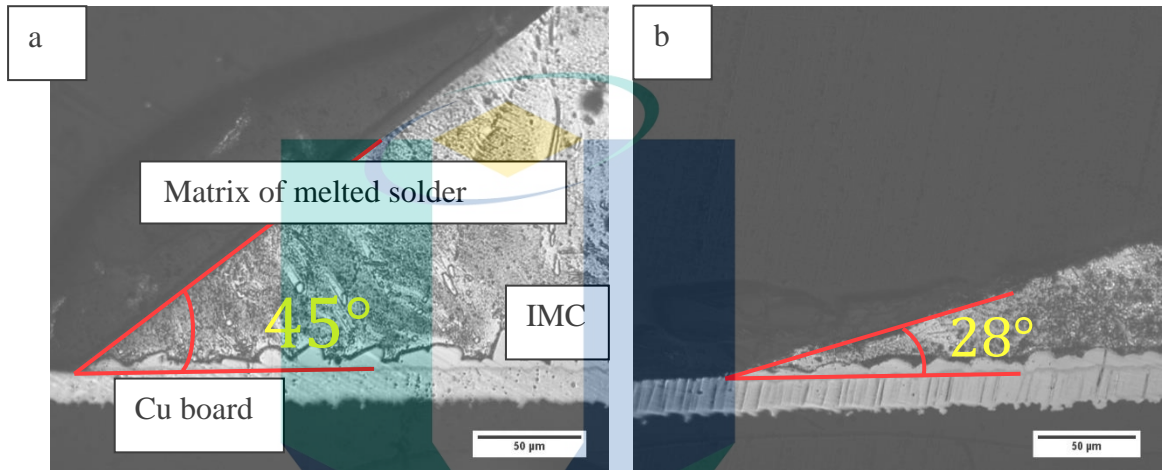

Figure 3.12   The different between;(a)large and (b)small wetting angle and the way of the angle is taken for each sample.

3.7   Calculation using weight percentage(wt. %)

3.7.1   Identification of IMC based on EDX Results

Intermetallic formed between the solder joint can be determined by using simple calculation based on EDX results. For example, the most common intermetallic found in Cu and Sn is Cu_6Sn_5 which is a combination of six copper atom and five tin atoms. The atomic weight of Cu and Sn are 63.54g/mole and 118.69g/mole respectively, based on periodic table. An example of calculation by using weight percentage for Cu_6Sn_5 was shown in Figure 3.12. Table 3.2 shows calculated weight percentage of predicted IMCs formed.
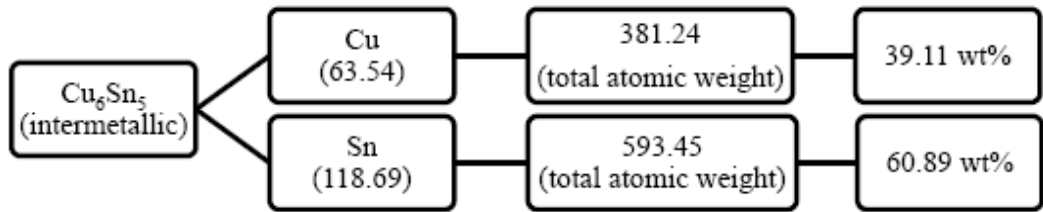
47

Figure 3.13   Calculation of IMC using weight percentage

Source: Zetty & Kahar, (2017)

Table 3.2   Calculated weight percentage of predicted IMCs

Intermetallic compound	Weight percentage, wt.%	
	Cu	Sn
Cu_6Sn_5	39.11	60.89

CHAPTER 4

RESULTS AND DISCUSSION

4.1   Introduction

In this chapter, the findings and results from solder alloy fabrication by PM method were being discussed thoroughly. With this new approach, there would be new outcomes from particular steps. Hence, as well as the solder characterisation, it is considered as the pivotal report in this research on how each raw material reacted towards each step in PM so that an in-depth study and recommendations could be addressed in further research.

4.2   Powder Metallurgy (PM) method

4.2.1   Characterisation of Powder

It was a crucial action to know the physical properties of each raw materials used in this research because the end-products relied on the first step especially the selection of size and form of the raw materials. Sn was the highest percentage of composition to make the Sn3.0Ag0.5Cu solder alloy in this research. It was about 96.5 percent of the solder alloy made from this material followed by 3.0 and 0.5 percent of Ag and Cu, respectively. It was purposely to use the irregular granular-flake form in order to allow particle size deformation and material's incorporation as well as allowing the compacted powder of solder alloy to be melted on its substrate.

Within the thesis scope, the mixed SnAgCu had different properties outcome compared to the pure powder in which differed in homogeneity distribution, particle size, sphericity and the roundness. The milling durations were 2, 4, 6, and 8 hours in which the impaction and collisions between materials has changed the original properties of each element. Colour changes on milled metal was possibly due to the heat energy created by collision (Jwad, Walker, & Dimov, 2018). Generally, the temperature of the powders during milling can be high due to two different reasons. Firstly, it is due to the kinetic

energy of the grinding medium. Secondly, it is possible that exothermic processes occurring during the milling process generate heat(Khajepour, 2011).

4.2.1.1   Morphology of Milled Powder

Figure 4.1 shows the images of SEM analyses of the four-milling duration on the milled powder of Sn3.0Ag0.5Cu materials by the low and high magnification taken by random shot. At a glimpse, the SEM results shown a similar shapes and sizes presented by the 100x magnification. Comparing with the as-received powder of Sn, Ag and Cu, the milling process with certain duration has caused a new formation of powder mixture due to the effect of stress and strain orientation as the factors of deformation(Zeng, Lai, Gan, & Schuh, 2016). By the literature, there are few shapes that can be identified from this research such as hollow, elongated, nearly symmetrical and asymmetrical round shape of milled powder.

All of these features also presented in other researchers works such as Attar (2015) gained the nearly spherical and irregular shape of milled powder as processed by 2 and 4 hours of milling duration and suggested no further duration required which can impact the density and porosity level. The results of elongated shaped are similar to the findings obtained by the previous studies Ulusoy (2015) tested on the talc materials by using ball and rod mill machine in which produced rounder shape of milled product than elongated one. The hollow nanostructures of nickel-based superalloy powders also found in solder research by Simiti (2011) used as filler and engaging density and porosity.

The 5000x magnification images on the milled powder picked the interest that revealed the nature of powder surface is recognized as a key factor that affect interfacial bonding during compaction process (Zheng, 2013). This is subjected to highly irregular surface of the milled powder. Generally, the surface features can be related to differences in the microstructure of the powder, amorphous in the case of a smooth surface and crystalline in the case of an irregular surface. The surface morphology in combination with the XRD results explained in next section.
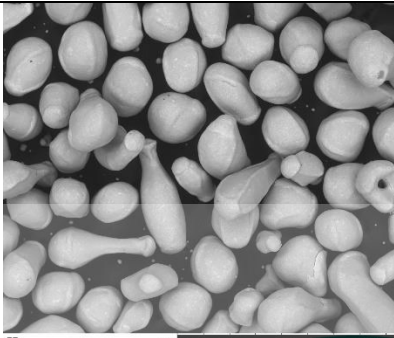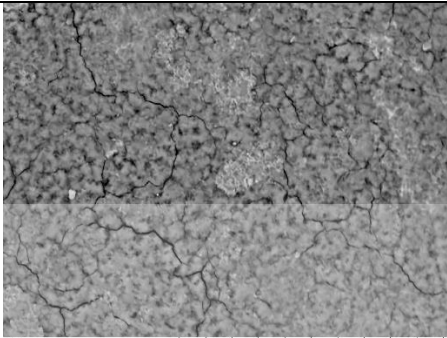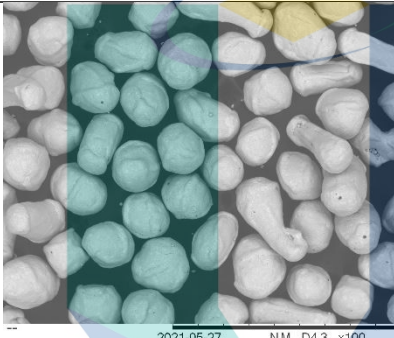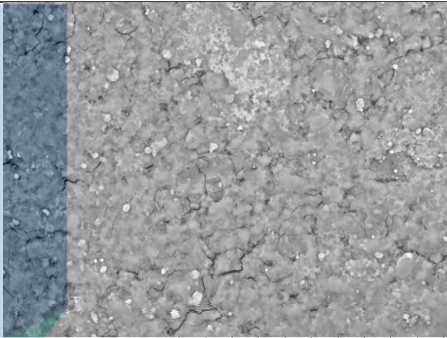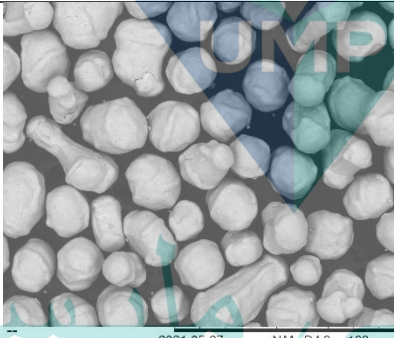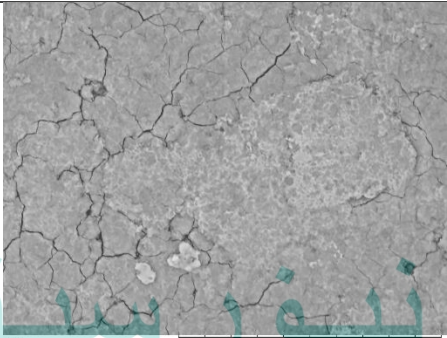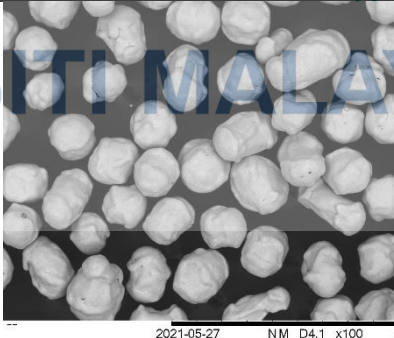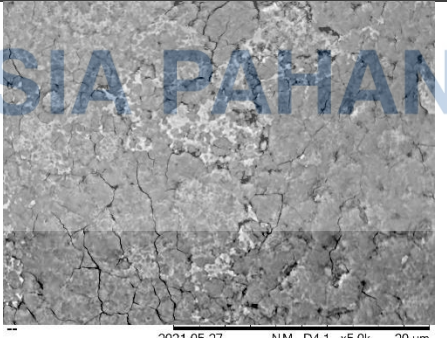
Milling Duration	100x magnification	5000x magnification
2 hour		
4 hour		
6 hour		
8 hour		

Figure 4.1   The images of low and high magnification of the milled powder of Sn3.0Ag0.5Cu by respective milling duration

4.2.2 Homogeneity Distribution

The extensive deformation of milled powder showed that the operation of the milling process has done its job to create a homogeneous mixture in the solder alloy. To ensure the homogeneity distribution of the mixture, microstructure analyses of SEM and EDX had been carried out and Figure 4.2 show the weight percentage of area on milled powder as analysed by SEM and EDX according to milling hour. As can be seen, the EDX results below the image display the value of weight percentage for Sn, Ag, and Cu element, where Sn and Ag were the most contaminated on the surface layer of those milled materials followed by Cu. These milled powders were then being compacted and the surface area which mostly covered by SnAg would soon turn to be the grain boundaries of each particular compacted sample.
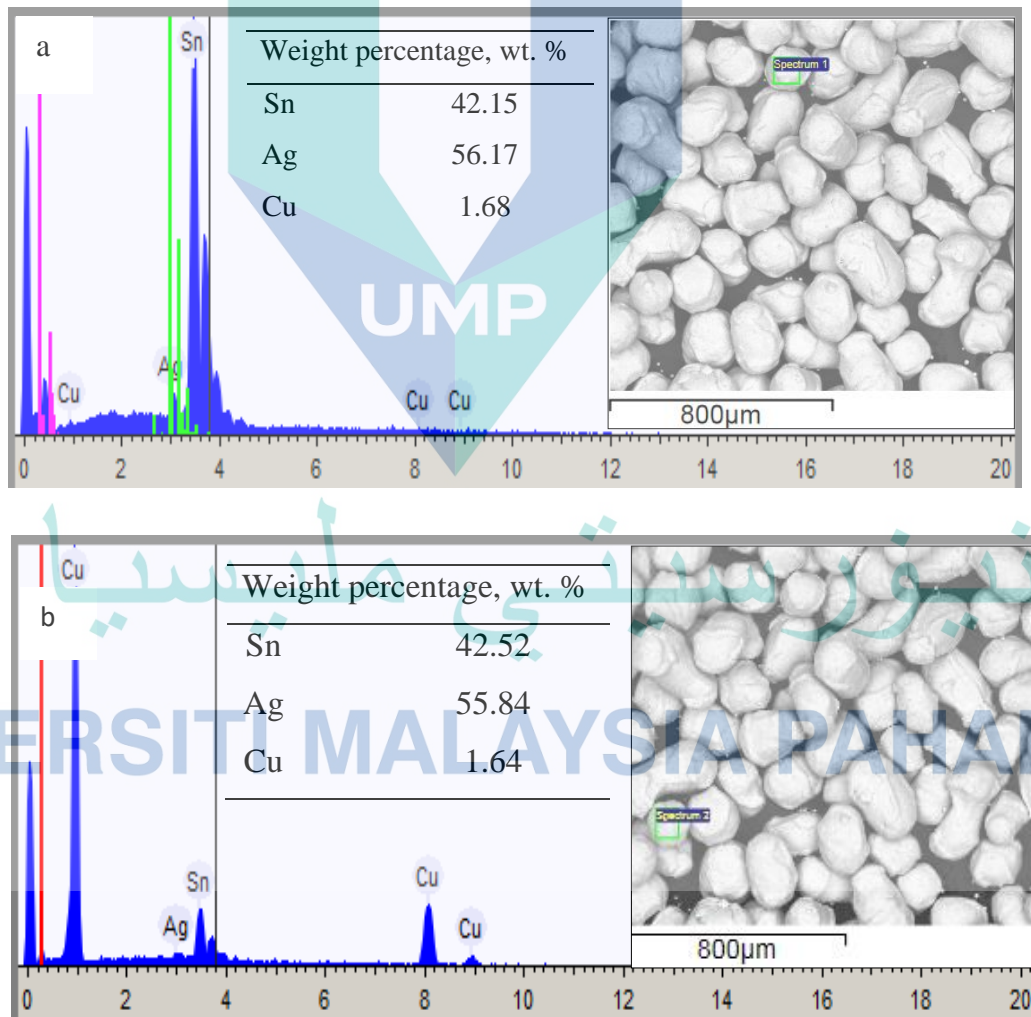

Figure 4.2   Images of (a), (b), (c) and (d) show the weight percentage of area on milled powder as analysed by SEM and EDX according to milling hour
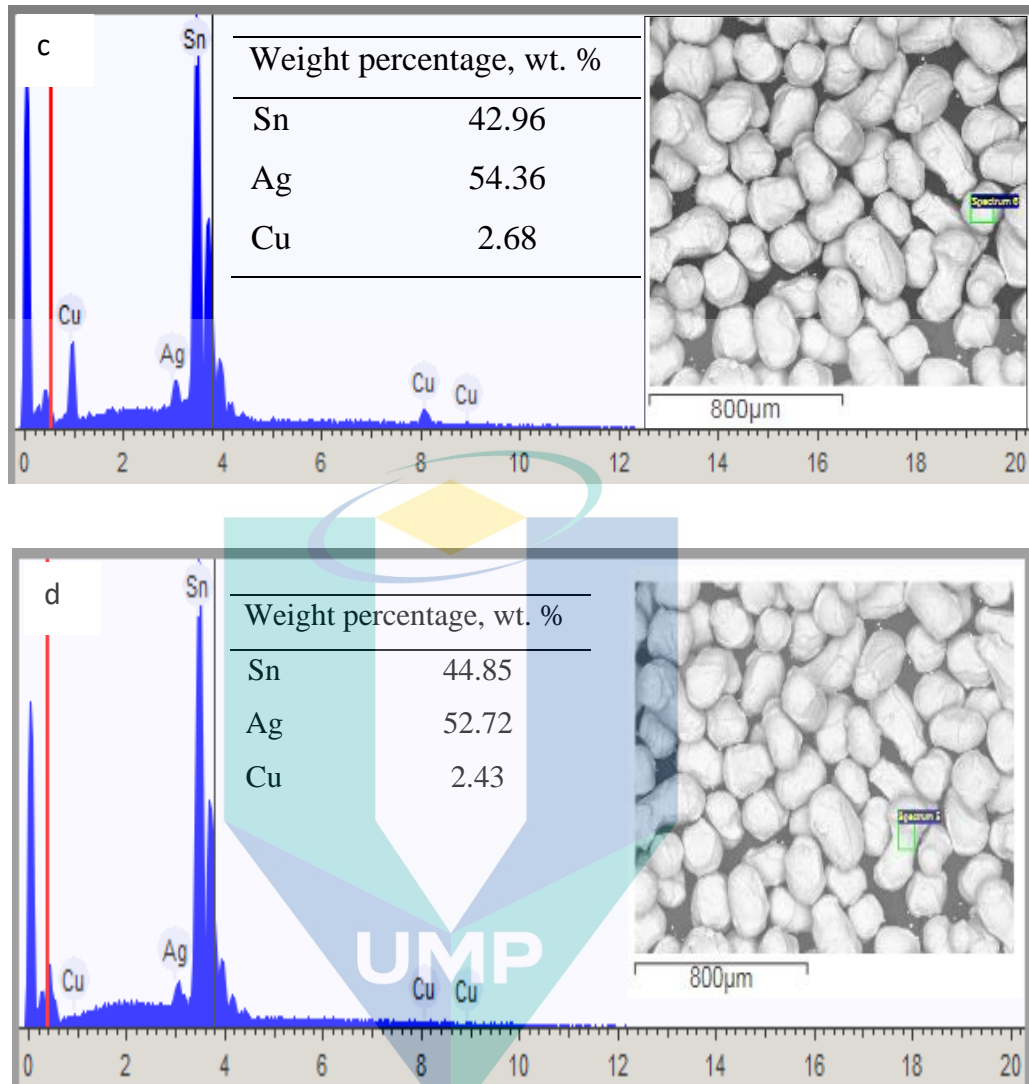
Weight percentage, wt. %	
Sn	42.96
Ag	54.36
Cu	2.68

Weight percentage, wt. %	
Sn	44.85
Ag	52.72
Cu	2.43

Figure 4.2   Continued

4.2.3   Particle Size Distribution

Milling process is the foremost factor to have a homogeneous distribution of elements due to its ability to provide a new phase of grain structures and led to a grain refinement to each granule(Almotairy, Alharthi, Alharbi, & Abdo, 2020). Therefore, in order to study the refinement of SnAgCu by the milling process, analysis on microstructural by particle size distribution was done on milled powder for every milling duration. Figure 4.3 show the graphs of particle size distribution analyses for the Sn3.0Ag0.5Cu solder alloy according to milling duration. According to the graphs, highest distributions of powder size were in the range between 20000μm to 40000μm with positive skewness which indicated that the milled powder size were clustered more

around the left tail of the distribution while the right tail of the distribution is longer. Thus, as calculated by average, the mean value for each milling duration were 28070.7 μm, 26859.2 μm, 27315.4 μm and 36210.1 μm in the same image magnification of 200 μm.

According to the mean values, it can be said that the milled powder sizes were similar and had minimum different values. The mean value of particle distribution size for 2 hour, 4 hour and 6 hours of milling duration depicted similar values while the 8 hour shown a bigger slightly reading. According to Toozanjehdani (2017), when the milled powder mixture reached a steady state, the particles' morphology stabilizes and particles were in an equiaxed shape and certain size, which are randomly oriented as shown in Figure 4.1. It is anticipated that in the steady state, the milling time is sufficient that no considerable change in the morphology of the powders is observable. It can be inferred that the steady state can be achieved with the attainment of a full homogeneity.
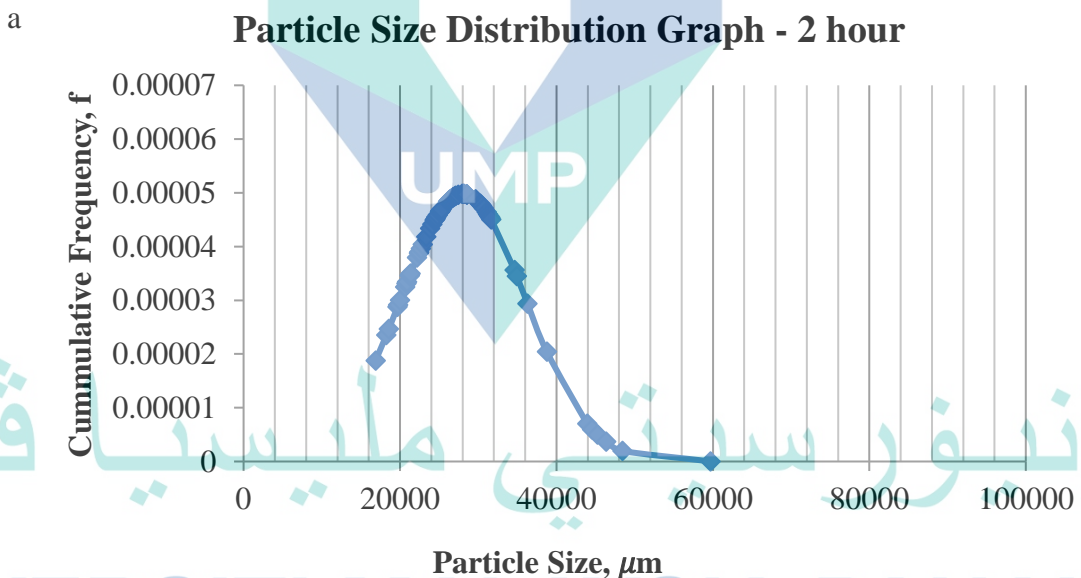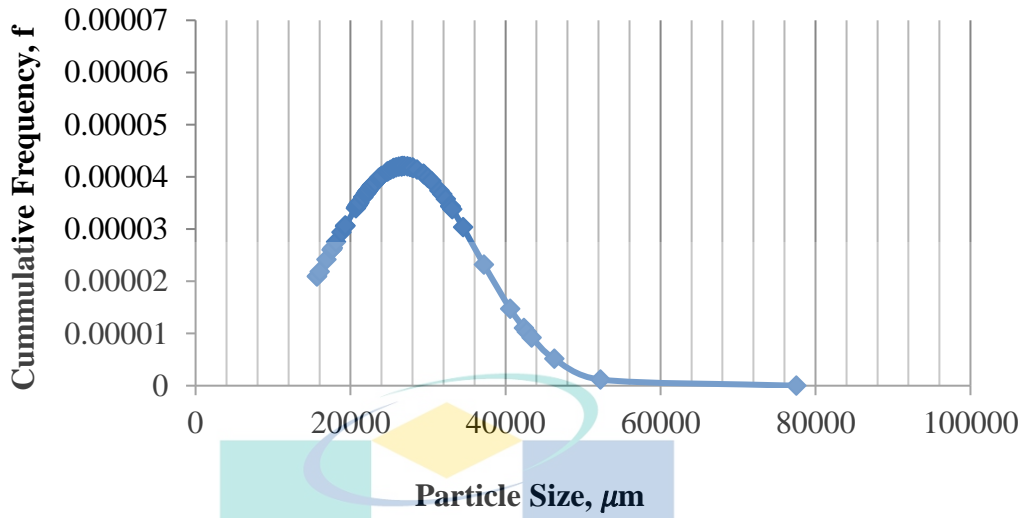
Figure 4.3 Graphs of particle size distribution analyses for the Sn3.0Ag0.5Cu milled powder according to their milling duration; (a)2 hour, (b)4 hour, (c)6 hour and (d)8 hour

54

b

Particle Size Distribution Graph - 4 hour
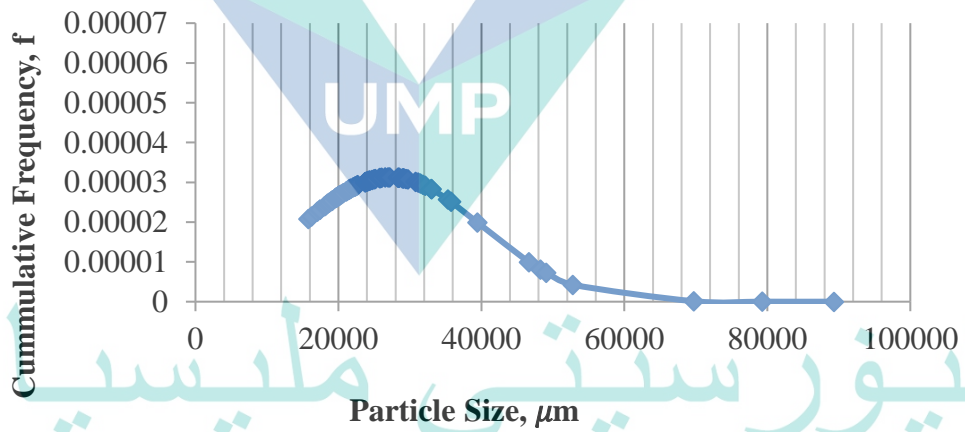

c

Particle Size Distribution Graph - 6 hour

Figure 4.3   Continued

55

d

Particle Size Distribution Graph - 8 hour

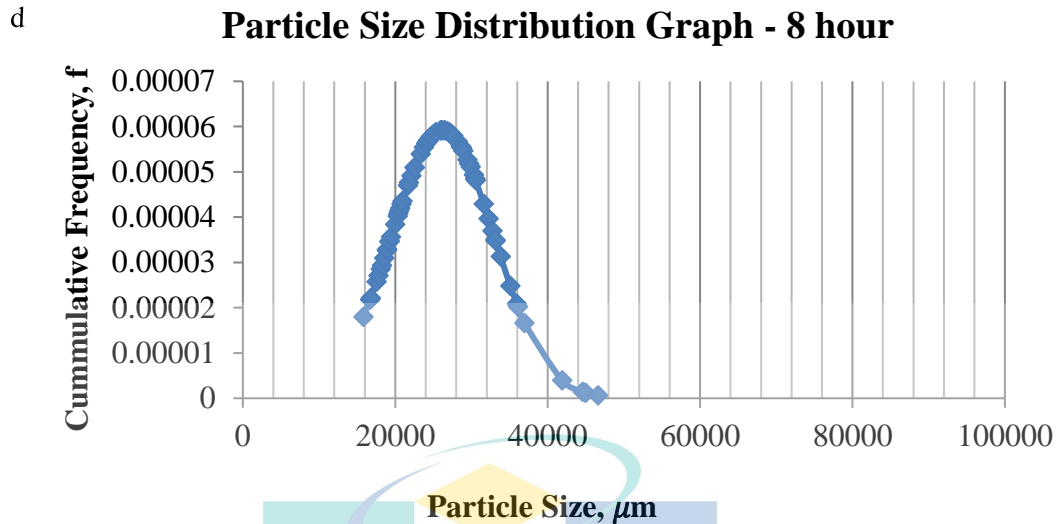
Figure 4.3   Continued

4.2.4 Sphericity and Roundness

Figure 4.4 (a) to (d) show the images of the Sn3.0Ag0.5Cu milled powder that have been examined by ImageJ software. Image provided in the figure was just an example to five images that have been analysed. They were labelled in numbers and reading of average sphericity and roundness were recorded as well. According to Krumbein-Sloss chart, the superior shape should be the closest to degree of 1. Generally, the values reading was almost the same range for all powder and milling hour which was 0.7 with 0.00001 decimal place. Thus, this shown that milling duration from the research scope produced similar shape result of milled pre-alloy granules. In addition, there were also some powders that achieved the sphericity and roundness of solid 1.0. However, it might be due to low counting numbers of this shape made the average as mentioned. In order to obtain the average value of sphericity and roundness, five random captured images of milled powder have been selected according to milling duration. These samples were reliable to conduct the microstructural images by using ImageJ software to process and made the calculation individually powder by powder.

To clarify, the study of sphericity and roundness is required due to the melting issue of compacted solder alloy during reflow in this research. Details of the issue are going to be elucidated in next sub-topic, but in short, the whole compacted solder alloy was not fully melted during reflow on its substrate. They were below than 50 percent of

56

the size that successfully fulfilled the reflow procedure. Thus, this issue has led into a deeper analysis on the compacted solder alloy itself, which induced the study of particle grain.

Table 4.1 summarised the findings of milling analysis. The variation in the morphology of Sn particles, which varies from large flake-shaped particles at early stages of milling to more or less quasi-spherical particles having small particle sizes for SnAgCu milled powder. As-received material was the original raw materials that came straight from manufacturer while as-milled pre-mixture was the finished milling of SnAgCu according to scope of milling duration. The Sn3.0Ag0.5Cu milled powder existed as elongated, angular, hollow, and rounded in shape and had approximately the same average of size. Thus, this has shown that the physical properties of these three elements were totally deformed and the new one was created.

Table 4.1   Summary of the physical properties of Sn3.0Ag0.5Cu pre-alloy after completely milled according to their respective duration

	SnAgCu milled powder compact (duration, hours)			
	2h	**4h**	**6h**	**8h**
Mean Particle size, μm By 10x magnification	28070.7	26859.2	27315.4	36210.1
Particle shape	Elongated, Angular, sphere and Rounded			

57
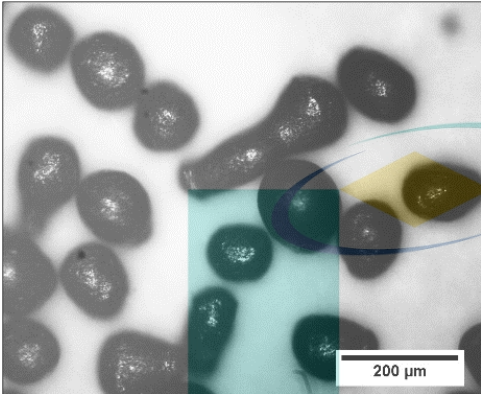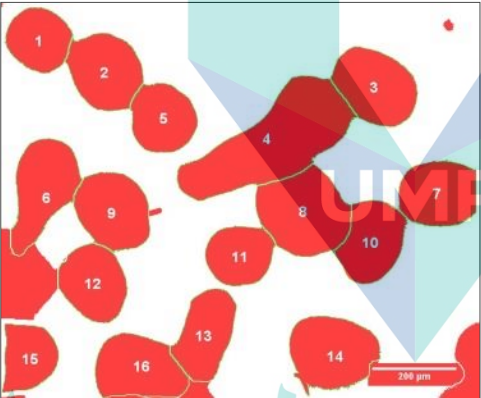
Image of milled powder and the processed image (a)	Average value of Degree/Aspect	
	Sphericity, SKS	Roundness, RKS
	0.70438	0.70378
	Mean particle size, μm	
	28070.7	

Figure 4.4   Average mean value for sphericity, roundness and particle size for (a)2, (b)4, (c) 6, (d)8 hour milled powder sample
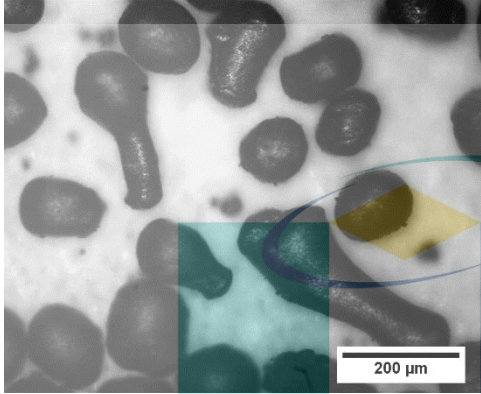
Image of milled powder and the processed image (b)	Average value of Degree/Aspect	
	Sphericity, S^{KS}	Roundness, R^{KS}
	0.705332	0.709792
	Mean particle size, μm	
	26859.2	

Figure 4.4   Continued
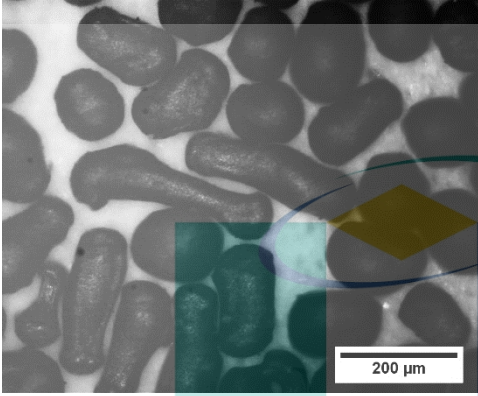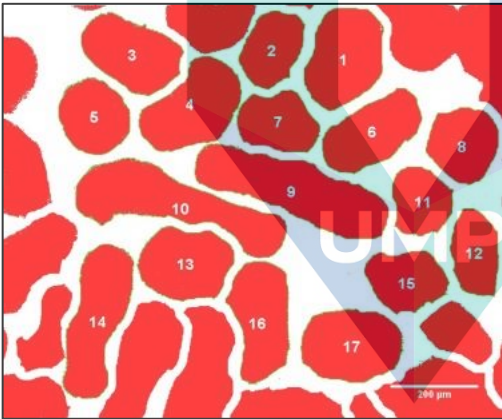
Image of milled powder and the processed image (c)	Average value of Degree/Aspect	
	Sphericity, S^{KS}	Roundness, R^{KS}
	0.715551	0.693486
	Mean particle size, μm	
	27315.4	

Figure 4.4   Continued
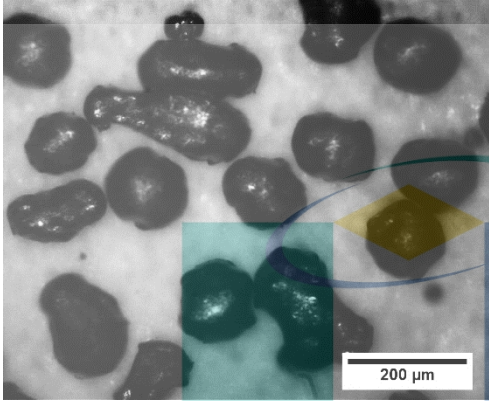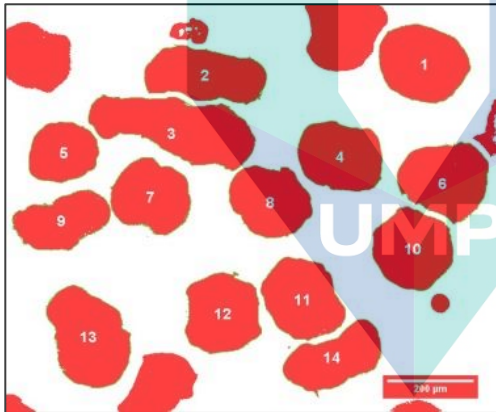
Image of milled powder and the processed image (d)	Average value of Degree/Aspect	
	Sphericity, S^{KS}	Roundness, R^{KS}

| | 0.702124 | 0.7292 |

Mean particle size, μm
36210.1

Figure 4.4　　　Continued

4.2.5　Phase Confirmation using XRD on the milled powder

To confirm the crystalline phases and existence of amorphous material presents in the milled powder of Sn3.0Ag0.5Cu solder alloy, the X-Ray Diffraction(XRD) analysis was carried out. Data was taken for the 2θ range of 10 to 80 degrees with a step of 0.02 degree. Indexing for powder diffraction pattern was done and Miller Indices (h k l) to each peak was assigned in the first step. Each

61

diffraction peak shows a plane in lattice of that material. Heights of a plane show how much x-ray get diffracted from a particular lattice plane and that show dominance of that plane in that material.

By the samples of milled powder of Sn3.0Ag0.5Cu solder alloy, 10 intense peaks appeared in the XRD spectrum of the milled powder at the diffraction angles of $2\theta =$ 30.63, 32.03, 38.10, 43.38, 43.85, 44.89, 55.44, 62.35, 63.68, 64.52 degree can be readily indexed to expected unit cell of solid crystallographic planes of (200), (220), (101) for Sn, (211), (112), (400) for Sn-syn, (111), (301), (200), (220) for face centre cubic of Ag. Meanwhile, the rest of XRD results indicated there were amorphous alloys with 24 diffractions patterns that have low intensities and broad humps identified as Copper Tin, CuSn compounds all at diffraction angles of $2\theta =$ 38.10, 43.38, 50.34, 62.35, 63.68, 64.52, 72.16 and 79.23 degrees for unit cell listed as (642), (820), (844), (12 0 0), (11 5 1), (12 2 2), (12 6 2), (14 4 2) which indicated the amorphous phase in the milled powder. To note, there were no information on the XRD results of the milled powder that shown the oxidation peaks and traces of metal oxide or the presence of oxygen. The XRD analysis onto the milled powder was carried out on the 6 hour sample only. Additional analyses should be done to address the rest of the milling duration. But the result is optimized as confirm the phase structures of milled powder in this research.
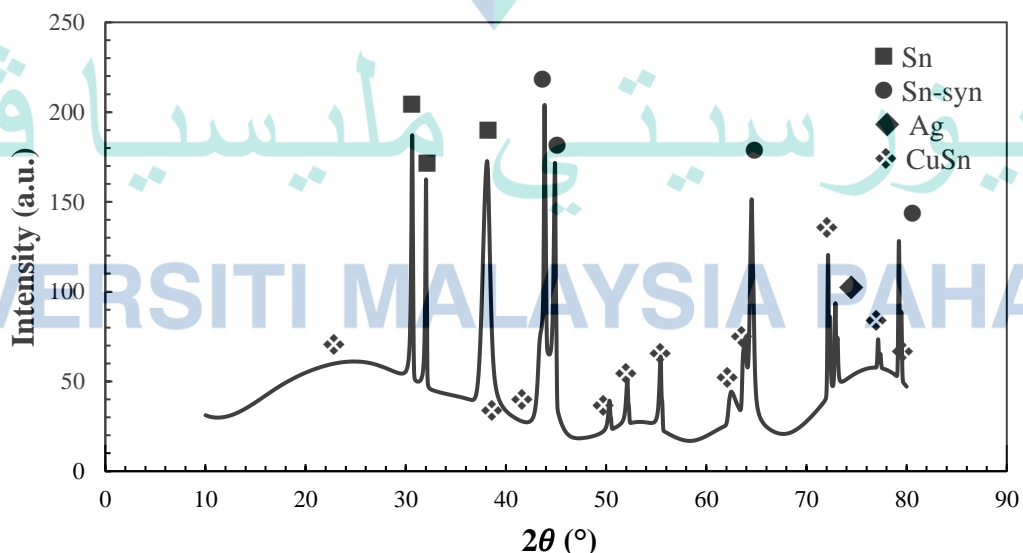

Figure 4.5   XRD analysis on milled powder of Sn3.0Ag0.5Cu solder alloy for 6 hour of milling duration

4.2.6 Powder Compaction

The study on the surface of compacted Sn3.0Ag0.5Cu milled powder solder alloy in this research is essential where three different phases of the sample could be seen and analysed. There are as-received raw materials, as-milled and as-compacted. Those phases had their particular microstructure, which respected to the PM process. This sub-chapter just focussing on diameter size of as-compacted Sn3.0Ag0.5Cu solder alloy. The Sn3.0Ag0.5Cu milled powder by milling method had to deal with the external force called compaction load which came from hydraulic press machine. The aim of work was to create a bulk body for solder alloy. This has made the milled powder to be compressed with equal load as they were pulled inwards, collided with other different shapes and sizes of granules which consequently, end up with heterogeneous structures inside the bulk body of compacted solder alloy. This had also resulted in various shapes and sizes of compacted granules as well as granules or grain boundaries.

Figure 4.6(a) to (d) shows the top view of compacted Sn3.0Ag0.5Cu milled powder solder at the magnification of 200μm, where all the grain boundaries and solder matrix can be seen clearly. A computer software called ImageJ is used to measure the diameter of the compacted milled powder where similar shape and size were selected as to standard the measurement.

Various shapes, sizes, and grain boundaries of Sn3.0Ag0.5Cu pre-alloy granulates have many deals to do with reflow process, primarily. Reflow process is a process where the heat is fully functioned to melt the compacted solder alloy bulk on the substrate board(Feng, Xu, Tian, & Mayer, 2019). Nonetheless, it had a heat flow constraint to supply the heat to all of the compacted granules.

Concerning the compactivity of milled powder, it was impossible for the furnace heat to flow through the compacted structure and melt the bulk body. Thus, the morphology study is required to explain the melting mechanism and the explanation can be found in next sub-chapter.

Figure 4.7 displays the graph of the average diameter of compacted Sn3.0Ag0.5Cu milled powder by according to compaction load with respect to the milling duration respectively. The value ranges from 200μm to 250μm assured that the milled powder has successfully compacted and expanded its diameter (grain size). The line graphs were all fluctuate and seemed to be no pattern at all.

This was being expected at the beginning where the powder size, sphericity, and roundness of each of the milled powder was different from each other. As being compacted, the milled powder had forced to receive tons of compaction loads onto their surface and the grain inside were being pushed. They tend to fill up the unoccupied areas with forces from the compaction loads(M. Li, Zhang, Song, & Germain, 2019).
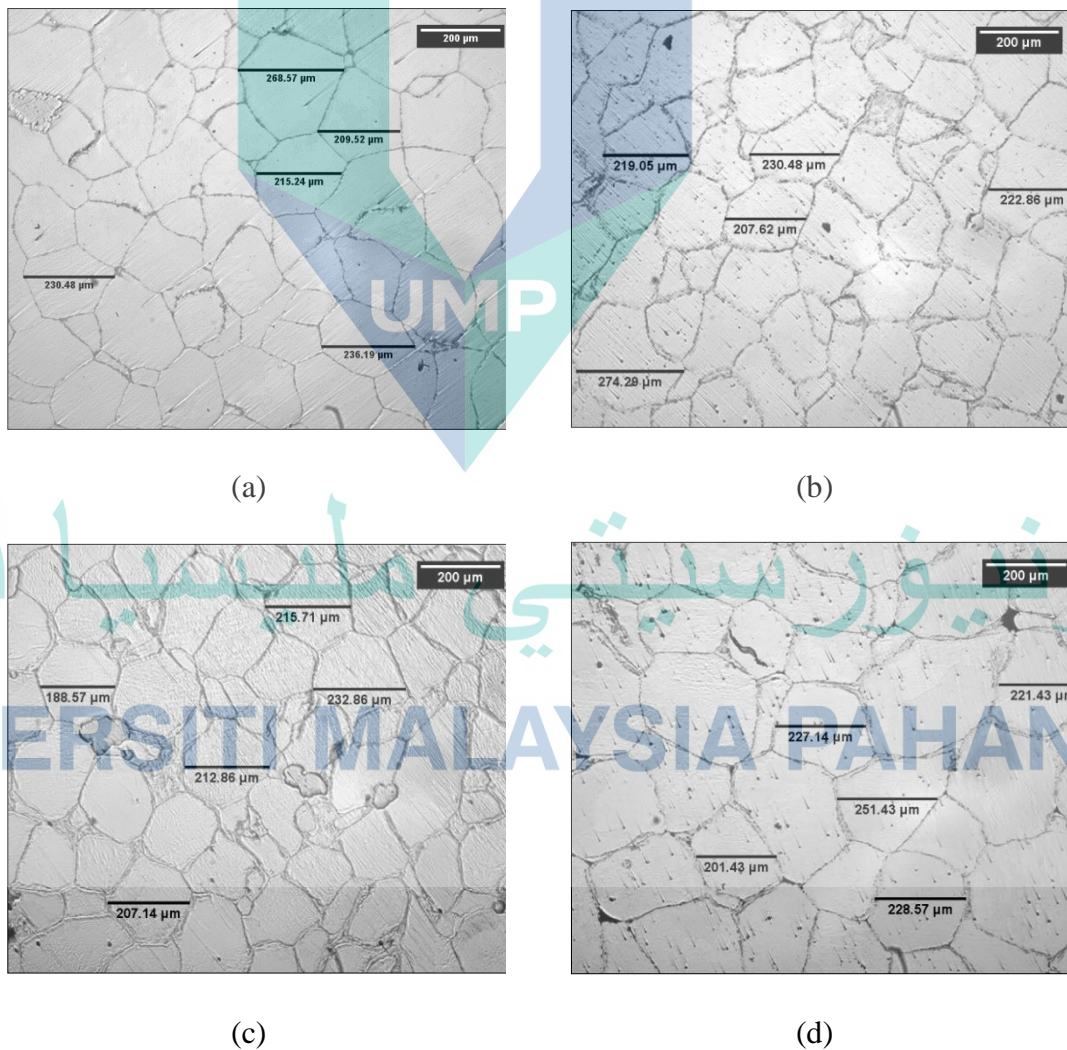

(a) (b)

(c) (d)

Figure 4.6   Images of top view of compacted solder alloy bulk after sample preparation procedure and the method of measuring the diameter of each sample; representing (a)2 hours (b)4 hours (c) 6 hours and (d) 8 hours as each of image is compacted with 5 tons
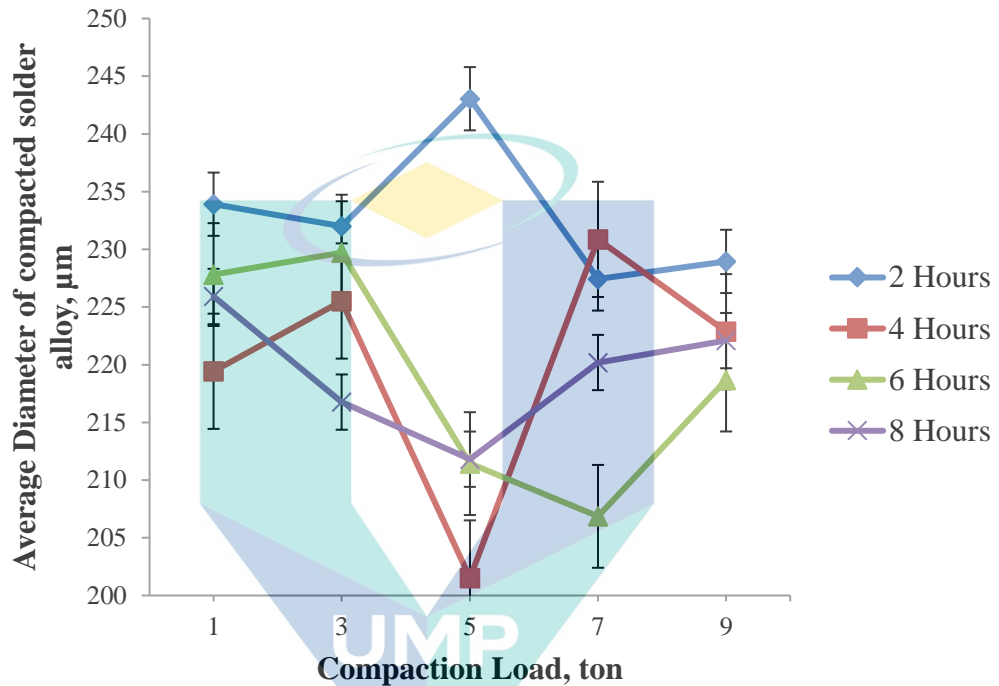

Figure 4.7   Average of compacted solder alloy particle diameter as according to the respective compaction load

4.2.6.1   Homogeneity Distribution of Compacted Powder

Figure 4.8 displays the element mapping images by EDX analysis for compacted granules which shows the distributions of each Sn, Ag, and Cu particles as being milled for 2, 4, 6, and 8 hours and compacted by 5 ton. Note that only one compaction load is required as compaction was a least factor with EDX element mapping analysis. Besides, there was dissimilar image magnification in the figure in order to show different views.
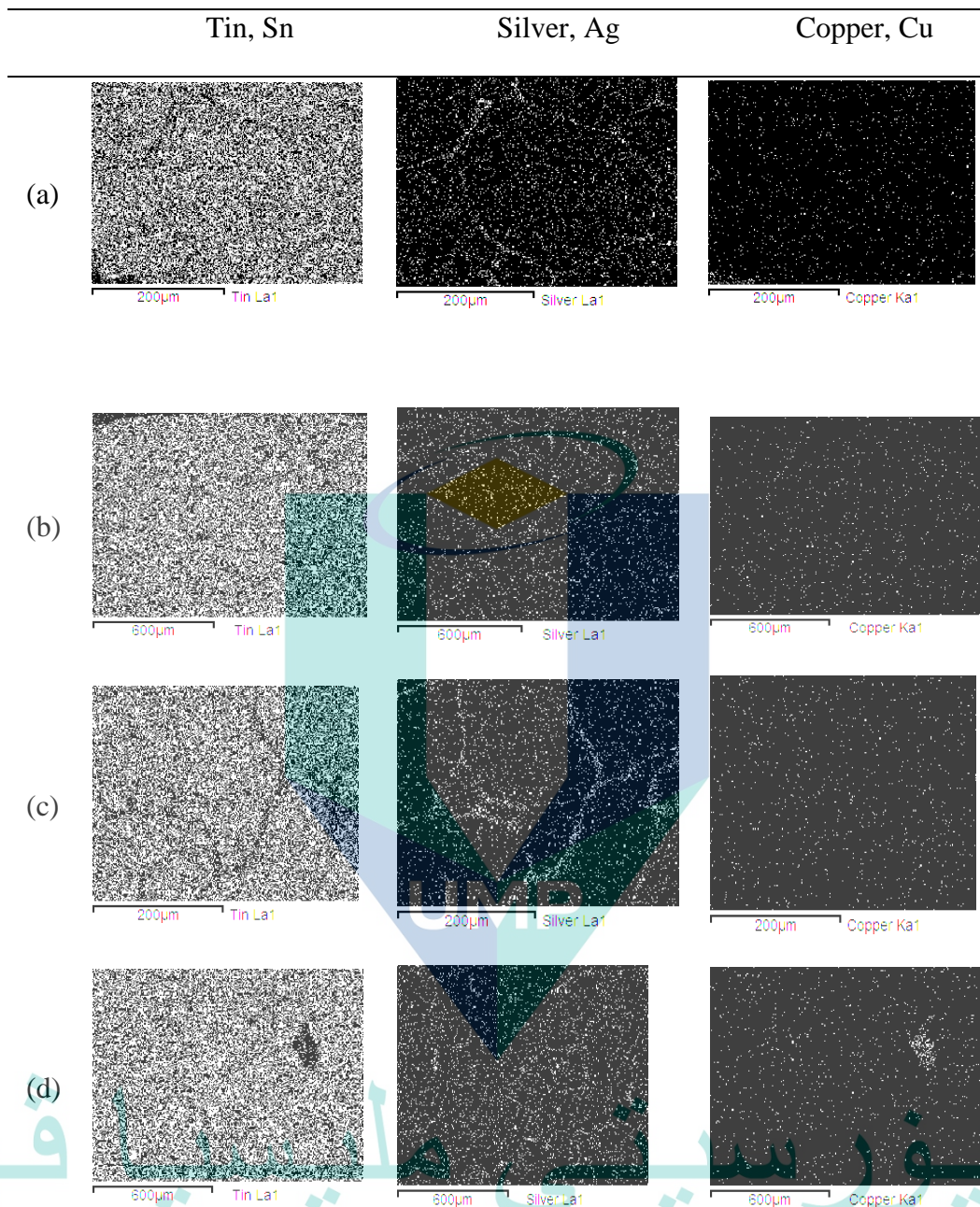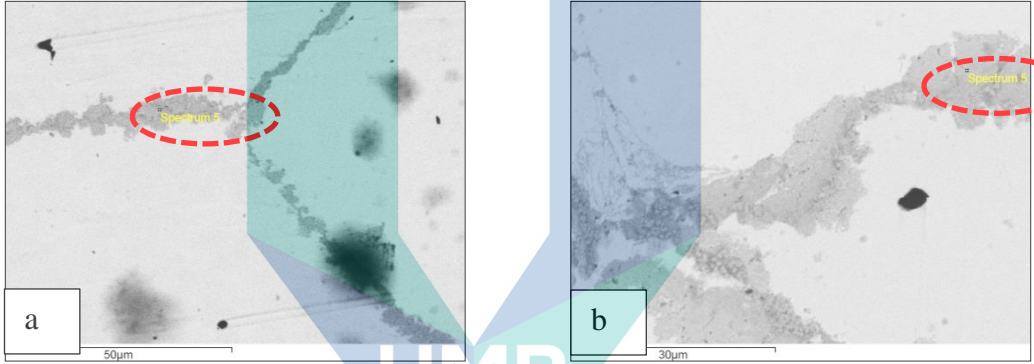
	Tin, Sn	Silver, Ag	Copper, Cu
(a)			

Figure 4.8   Element map images for; (a) 2 hours, (b) 4 hours, (c) 6 hours, (d) 8 hours

Figure 4.8(a) and (c) have magnification of 200μm while Figure 4.8(b) and (d) have 600 μm, respectively. According to all images, the distribution of each element in the Sn3.0Ag0.5Cu milled powder were homogenously mixed. The elements were all over the surface and inside the granules. It is picked an interest to note at Figure 4.8 (a) and (c) where an obvious Sn element line appeared the most at grain boundaries. It also means that Sn covering the surface of compacted milled powder the most too. Thus Ag element

showed it function as the additive element to Sn-Cu solder alloy by reinforcing the grain boundaries and slowing down the dislocation movement of particles(Y. Park, Bang, Oh, Hong, & Kang, 2017). However, an accumulated Cu element was detected on 8 hour milling duration sample. The figures in Table 4.2 show that SEM images focusing a point on the grain boundary. EDX results for both 4 and 8 hours of Sn3.0Ag0.5Cu pre-alloy granulates were tabulated as in Table 4.2. This result also proved that there were homogenous mixtures of SnAgCu at the grain boundaries. The values in table were the weight percentage of each element focused on a spot.

Table 4.2   SEM images with a weight percentage of selected milling durations at grain boundaries for; (a) 4 hours at 50μm and (b) 8 hours at 30μm

Weight Percentage, wt. %		Weight Percentage, wt. %	
Tin, Sn	0.520	Tin, Sn	0.000
Silver, Ag	51.715	Silver, Ag	40.020
Copper, Cu	47.765	Copper, Cu	59.980

4.2.6.2   Porosity

Figure 4.9 shows the porosity spots, the oxygen and non-oxygen weight percentage in that particular area obtained by SEM and EDX analyses. Note that the image magnifications were all different but did not change the fact of oxygen weight percentage at the spot just to show different views of porosity spot size. The 6 hour sample had the largest magnification but porosity spot size was very tiny.
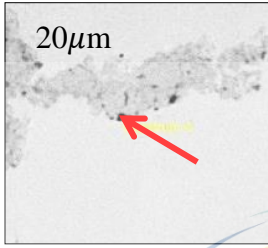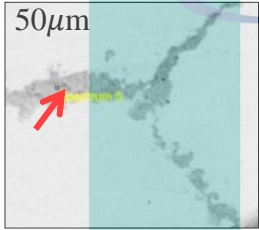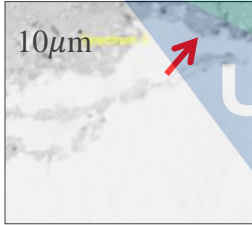
Milling Duration	SEM image	Weight percentage, wt. %	
		Oxygen	Non-Oxygen
2 hours		27.035	72.965
4 hours		26.637	73.363
6 hours		14.397	85.603
8 hours		51.047	48.953

Figure 4.9   Images show the SEM and EDX analyses of random spots for compacted Sn3.0Ag0.5Cu milled powder and the weight percentage

4.3   Microhardness

Figure 4.10 outlines the graph of the average value for all samples according to milling durations. In general, every graph shows a positive trend by the increasing value

of microhardness across the compaction load. This indicated that the compacted Sn3.0Ag0.5Cu milled powder prepared by PM method provided a positive possibility of reinforcement to the solder alloy. It can even reached as high as 11.86 Hv, almost the same as SnAgCu solder alloy that improved with fourth element or Ag replacement to that of SnCu-based solder alloy prepared by casting method(Ali, Sabri, Jauhari, & Sukiman, 2016).

There were three factors identified affecting the trend of graph. First, the solidity of compacted milled powder. As compaction load by compacting method exerted to each milled powder were higher. This had forced the arrangement of milled powder to move closer. Thus, a compacted bulk of Sn3.0Ag0.5Cu milled powder is produced. By the microhardness testing, a closed compacted milled powder had a resistance towards an external force that came from the Vickers diamond indenter(T. Xu, Wang, & Li, 2020). The indenter was tending to break the resistance by hitting the targeted spot with 10N load and a diamond shape of depth was created. Hence, the value of microhardness is obtained. Thus, increasing microhardness value in the graph shows that a harder compacted milled powder were created across increasing compaction load.
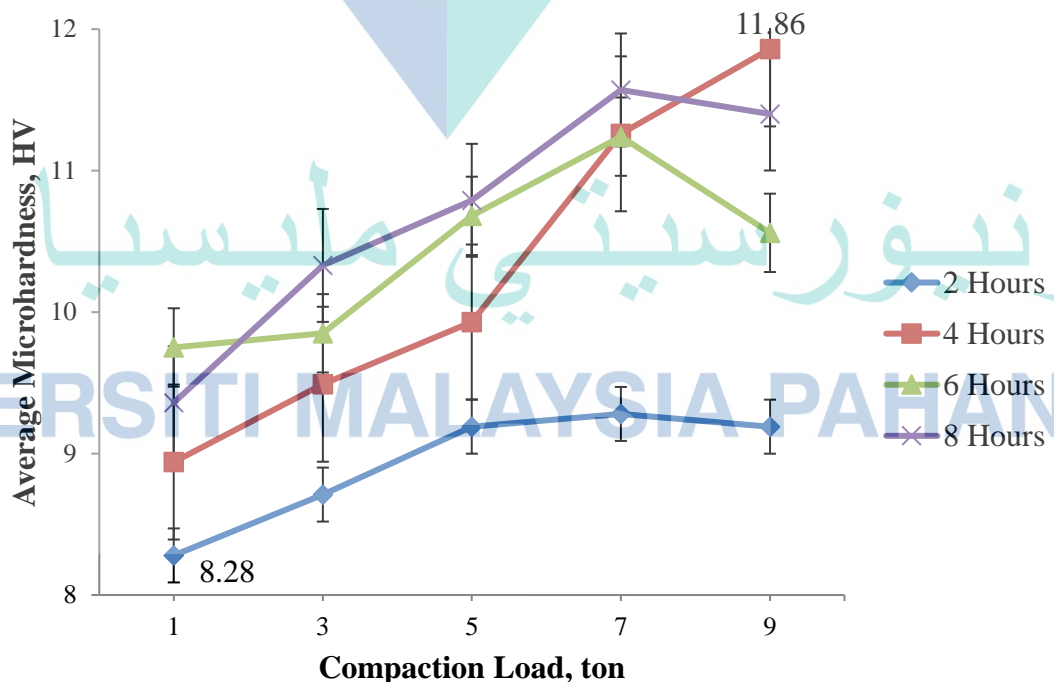

Figure 4.10   Graph of average microhardness values according to compaction load upon the milling durations respectively

Secondly, the compactivity of Ag particles as the reinforced additive in Sn-Cu solder alloy. To note, Ag element has not only acted as an additive to lowering down the melting point of Sn-Cu based solder alloy but it could also nurture the reinforcement of solder matrix and grain boundaries(Chen et al., 2016). Owing to the homogenous distribution of Ag particles indicated by SEM and EDX analyses in previous section, as the arrangement of milled powder became closer, the reinforcement properties of Ag also became higher in the solder matrix and at the grain boundaries. Having the fair dispersion of Ag element also has impeded the dislocation motion of milled powder in the solder matrix. Principally, the higher microhardness value indicated that the diamond tip of indenter had possibly targeting an area of the higher and compacted Ag particles. Thus, it resulted in a low microhardness value at the beginning but increased steadily as compaction loads getting increased.

Lastly, there must be a consideration on dependability of different shapes and sizes of compacted milled powder with the microhardness values. As these milled powders being compacted, they were forced to form up a solid body by filling in the gap and moved closer to one another. Some of them successfully got into the gab perfectly covered their surface layer but there were also some spots that still had some porous especially in between grain boundaries. Thus, the tips of Vickers diamond indenter possibly had targeted this porous spot during indentation and came out with a low microhardness value.

Frankly, microhardness value should be as higher as it can but when it comes into the compacted solder alloy prepared by PM method, it does not have to be. This is because, the higher the microhardness value, the more compact the solder alloy, thus the harder for the compacted solder alloy to melt by reflow process which this is the top priority of having a solder alloy so that it will do its job on Cu substrate. Therefore, the most crucial here is to find the optimum microhardness value of the compacted solder alloy, which can induce those solder to melt.

4.4   Reflow Soldering Results

The reflow process was done to the compacted Sn3.0Ag0.5Cu milled powder as to carry out several solder alloy microstructure analyses such as wettability, the formation of IMC and its thickness. To be cleared, each sample used for all three analyses because

these analyses required the compacted solder to be melted on the Cu board. This process has been conducted at one time to have a standard environment and to save cost and time as well. Thus, this procedure was one of the critical and crucial steps in the solder fabrication, especially by PM method.

Wettability analysis was started by carrying out a pre-test of the sample size used to melt on the Cu board. Figure 4.11 displays the result of this test. From the pre-test, it can be concluded that the smaller the sample, the more amount of melted solder on the Cu board. Thus, all the samples for compacted Sn3.0Ag0.5Cu milled powder were cut into smaller pieces to get the maximum amount of melted solder.
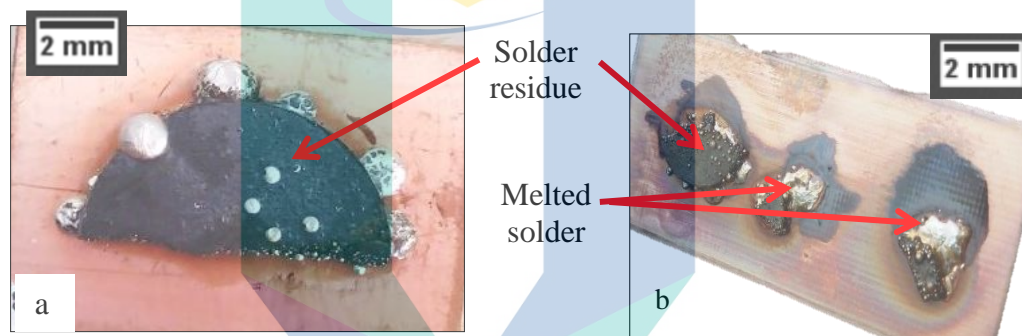

Figure 4.11   The pre-test of the sample size used to melt on the Cu board

The circular-shaped of compacted Sn3.0Ag0.5Cu milled powder was cut into the much smaller piece in order to allow maximum melting of solder sample on the Cu board. This procedure was also performed to see the mechanical bonding strength of compacted inter- particle held to each other during the cutting process(Perez-Gandarillas, 2016).

For the lower value of compaction loads such as 1 and 3 ton, there were some powder dispersed from the tiny arrangement of compacted solder bulk when the hammer and knife used to tap on top of the flat surface of compacted solder. The dispersion was due to strong external force from the two tools. This issue showed that there was a weak bonding between milled powder in the compacted solder and this could reduce the volume of the sample and handling risk thus lead to disruption of analysis. But this situation was getting better when all of those compacted samples were able to cut into smaller pieces with nice sharp edges without dispersion.

71

Therefore, this proved that as the compaction loads increased, the higher the bonding strength of inter-granulates. It was also identified that each compaction loads were just functioned to hold the Sn3.0Ag0.5Cu milled powder into a solid bulk shape and handling purpose. But still, identifying the optimum compaction loads is required.

Figure 4.12 indicates the sample of wettability, formation of IMC and its thickness analysis after the reflow process. They were organized according to milling duration and compaction load as the graphical graph simplified the arrangement. This position was also the same way as they were put inside the tabletop furnace while underwent reflow operation. Concurrently these results of reflow have brought attention to the solder alloy and reflow processing knowledge upon the fabrication of solder alloy by PM method, as these outcomes need to be analysed and reported.
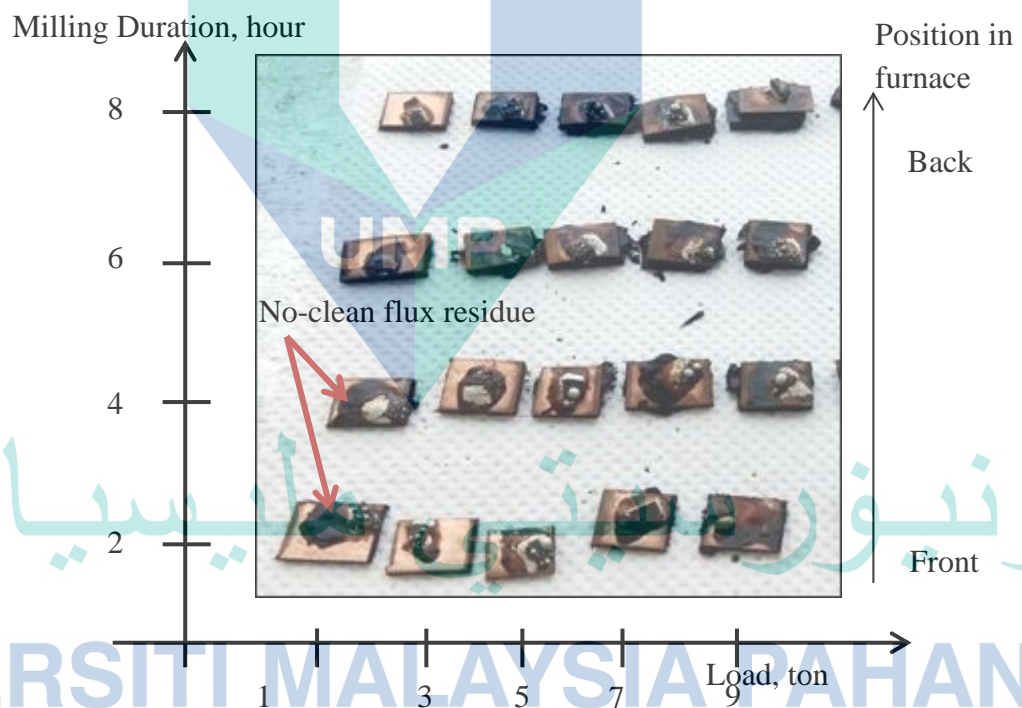

Figure 4.12   The compacted solder bulk after the reflow process for wettability analysis

According to the image in Figure 4.12, the condition of each of the samples here, especially when looking from the forefront to the back (upon the position in the furnace). Therefore, it is a must to clarify what had happened to those samples so that better

procedure and operation could be improved. The first attention should be the state of Cu board for all these samples in the image. It is clearly depicted that the conditional state of Cu board has burned out as going through to the back of the inside of the tabletop furnace. This was happened because no solder mask was applied on the Cu board to withstand extreme reflow temperature(Sperança, Virgilio, Pereira-Filho, & de Aquino, 2018).

A higher amount of heat produced and accumulated as far as going into the furnace. But that was not restricting the cut out compacted solder to melt on the Cu board or even worse, being burned out together. They were still receiving the same amount of heat but not to the layer of Cu board where the layers were made up of FR-4 which has a lower melting point than Cu thin sheet(Wu, Wang, & Jang, 2018). So, messed situation for the Cu board is explained.

Secondly, the no-clean flux on the Cu board. In terms of cleanliness, it is not necessarily to remove the dirt around the melted solder but in terms of long duration, this excessive amount of flux residue could inhibit the electrical connections on the printed circuit board (PCB) owing to the amount of solids-resin, gelling agents and activators it contained. This flux residue could absorb moisture yet removed the oxidation which cause a lower degree of wetting on the Cu board(Piotrowska, Grzelak, & Ambat, 2019). Thus, incomplete adhesion of molten solder could exist during the reflow process. This was also elucidated the fluctuate graphs of wetting angle in the next section.

The last one is the melted solder and flux residue which obviously can be viewed by the same image. It seemed like almost none of the compacted solder were melt but in reality, there was quite enough amount of melted solder to carry out three important solder alloy analyses such as wettability, formation and thickness of IMC.

4.4.1 Heat Distribution through Compacted Powder

A thorough discussion on melting mechanism of compacted milled powder was finely elucidated. But before proceed to the mechanism, it is crucial to know how possible the heat is distributed to the compacted Sn3.0Ag0.5Cu milled powder. Solder alloy is engineered to have a maximum melting whenever heat is conveyed to them. As the pre-alloy granulates being compressed, the pathway of the heat flow through the particles has been minimized intentionally. Figure 4.13 illustrates the flow of heat distribution around

73

the solder bulk during the reflow process. To note, the higher the compaction load, the more compacted pre-alloy granulates is which leads to very low heat flow distribution.

The heat cannot just flow through the compacted grain boundaries to reach for the internal granulates and melt them at once, they absorbed the heat granule by granule(Zhang, Liu, Zhao, Xiao, & Lei, 2019). But because of the sphericity and roundness degree was 70 percent close to 1, the granules can manage some melting behaviour. The sizes and shapes of compacted milled powder were definitely different, and this was related to the specific latent heat of a body. The bigger the size of a solid, the longer time it takes to absorbs the heat as they need to melt on the Cu board.
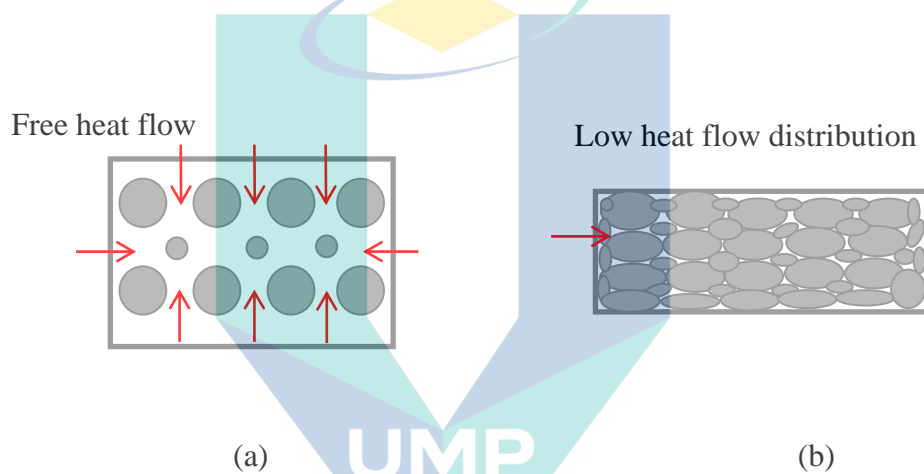
Figure 4.13   Illustration of heat flow distribution of free to compacted milled powder; (a) within zero compaction load, (b) within compaction load

4.4.2   Melting Mechanism of Compacted Powder

Figure 4.14 illustrates the cross section of melted compacted milled powder. It had different sizes and shapes even though when they had been compacted. Thus, one by one of the compacted milled powder absorbed the heat. Based on the amount of unmelted milled powder on top, the activity of heat-absorbing by milled powder had surely taken a long time to reach another neighbouring milled powder as on top which explained the presence of tiny molten solder alloy. Melted solder was covered by the compacted milled powder on top and a little amount just on top, so this could be possibly mean that the process of melting was first started at the interconnection between Cu board and the compacted solder bulk. This was definitely attributed to the fact that the Cu layer has

reached the melting point of Sn3.0Ag0.5Cu solder alloy which is 217℃ and activated flux has triggered the activity of melting at the interconnection.

Elucidating the melting mechanism of compacted milled powder is a must to clearly understand the reflow result. The compacted milled powder underneath gained the 217℃ heat temperature from the Cu layer and changed its solid body into molten solder. The heated molten solder then distributed its heat to another neighbour granulates. Inside the molten solder, each molecule is pulled equally in every direction creating a zero-net force. So they were stationary in the middle(Azani & Hassanpour, 2018).
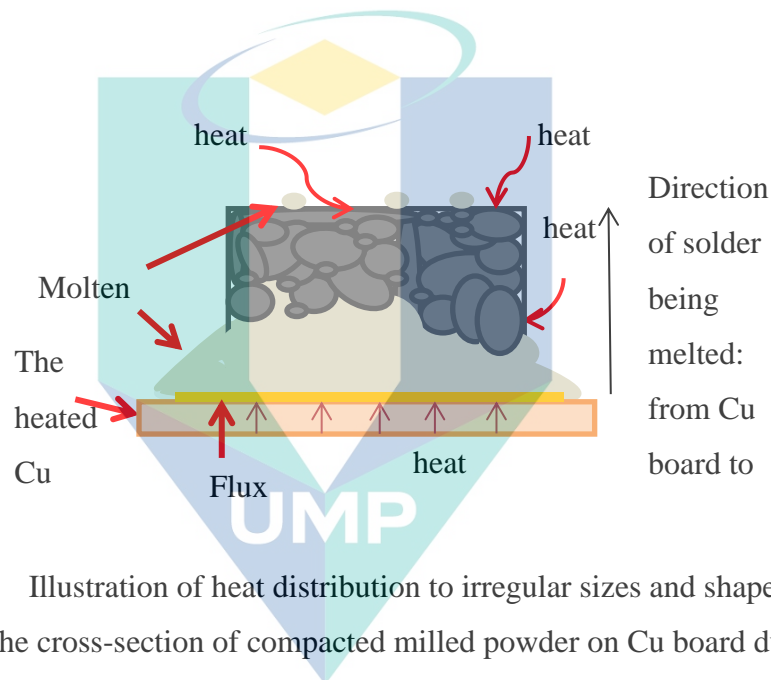
Figure 4.14   Illustration of heat distribution to irregular sizes and shapes of granules upon the cross-section of compacted milled powder on Cu board during the reflow process

4.5   Wettability

Figure 4.15 displays sample that had a little melted solder on top of the unmelted milled powder solder alloy. That small amount of melted solder was due to the size of compacted milled powder with the supplied heat. When the exposed surface of compacted milled powder received 217℃ of heat, smaller milled powder started to absorb heat faster than bigger granule. It tended to execute its chemical reaction which was to melt but the intermolecular forces between the powder were so strong prevented those particles to break the bond. To quantify, only smaller granules succeeded to break the chemical bond and melted away. That explained the little amount of melted solder alloy on top of the compacted milled powder.
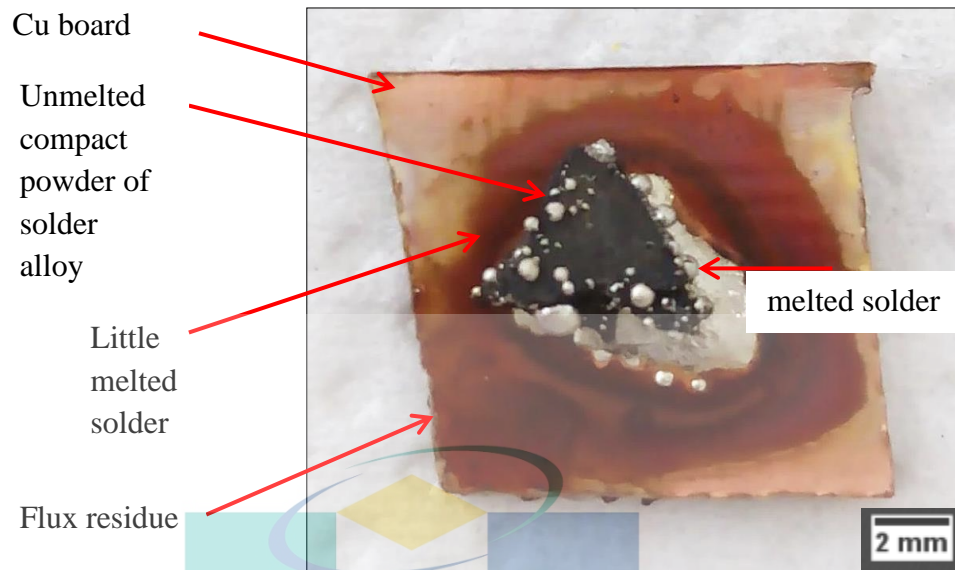
Figure 4.15   The melted solder, the unmelted and the small amount of melted solder on top of unmelted after reflow soldering the Sn3.0Ag0.5Cu milled powder

In addition, by the aid of no-clean flux, the melting process for compacted milled powder solder has been able to spread and achieved better wettability on the Cu board. Flux helped the compacted milled powder to spread over on Cu board by getting rid of the oxidation. The oxidation during reflow process should be avoided as it will form metal oxide which could impede the adhesion between melted solder and Cu board(Kim et al., 2017). If this happened, there would be no metal joining, the solder cannot function well and the devices would not perform that good. Figure 4.16 to Figure 4.19 displays all contact angle of samples in this research.
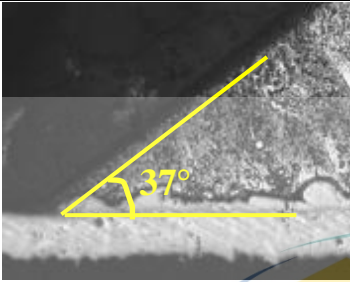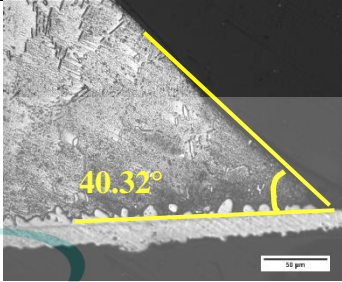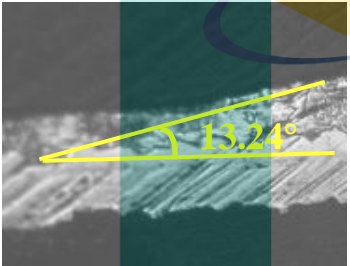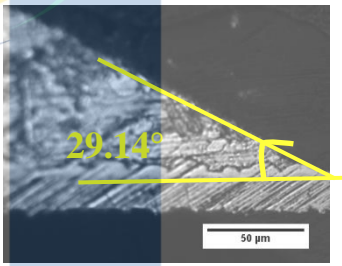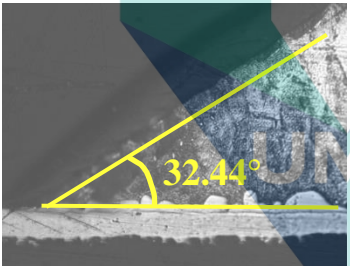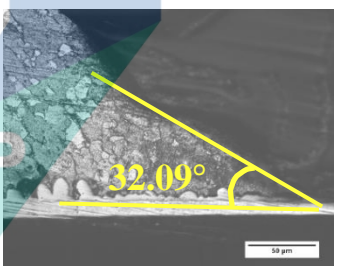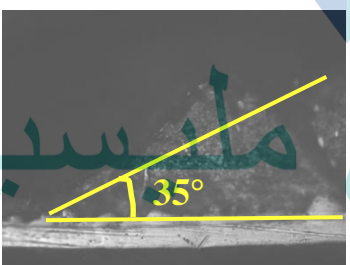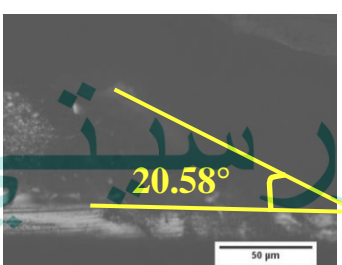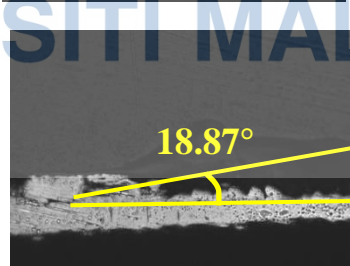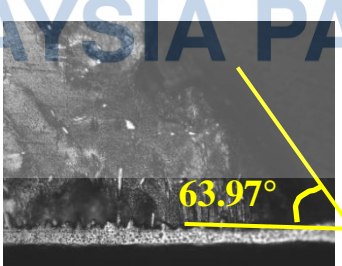
| Pressure, ton | Images of wetting angle, scaled to 50μm per 0.5cm | | Mean value of wetting angle, ° |
	Left	Right	
1	37°	40.32°	38.66
3	13.24°	29.14°	21.19
5	32.44°	32.09°	32.79
7	35°	20.58°	27.79
9	18.87°	63.97°	41.42

Figure 4.16   Images of wetting angle(contact angle) which has been measured accordingly; 2 hour milling duration
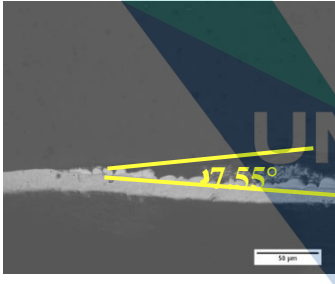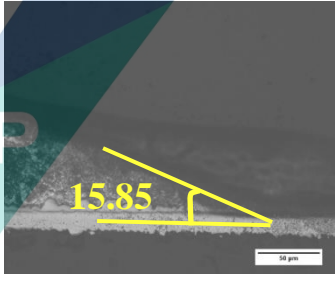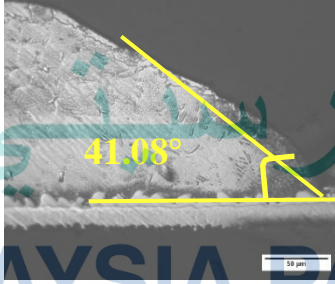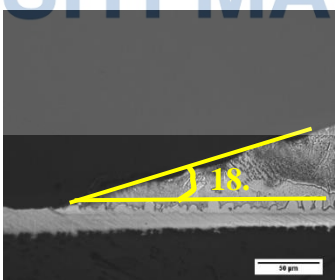
Pressure, ton	Images of wetting angle, scaled to 50μm per 0.5cm		Mean value of wetting angle, °
	Left	Right	
1	15.11°	26.33°	20.72
3	25.18°	13.88	19.53
5	7.55°	15.85	11.7
7	16°	41.08°	28.54
9	18.	23.24	20.72

Figure 4.17   Images of wetting angle(contact angle) which has been measured accordingly; 4 hour milling duration
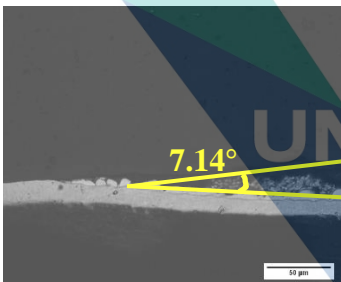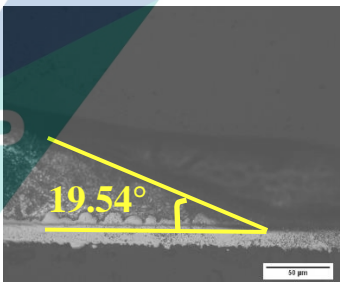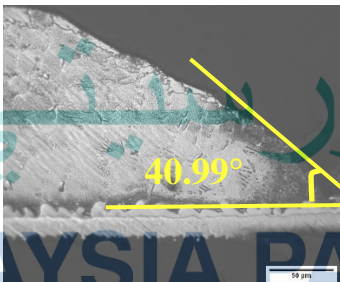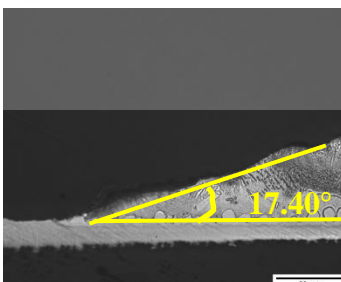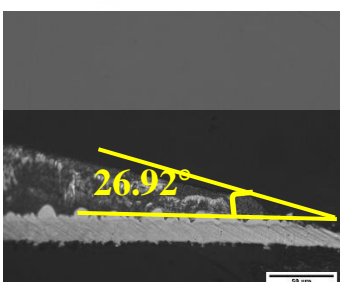
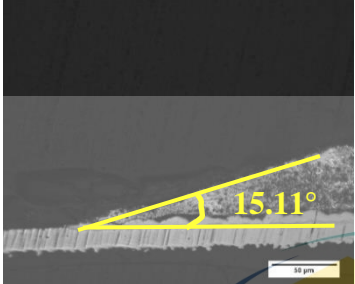| Pressure, ton | Images of wetting angle, scaled to 50μm per 0.5cm | | Mean value of wetting angle, ° |
	Left	Right	
1	19.53°	22.07°	20.8
3	14.92°	25.54°	20.23
5	7.14°	19.54°	13.34
7	16.83°	40.99°	28.91
9	17.40°	26.92°	22.16

Figure 4.18 Images of wetting angle(contact angle) which has been measured accordingly; 6 hour milling duration
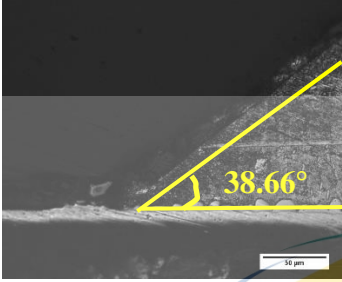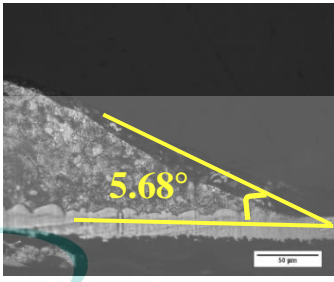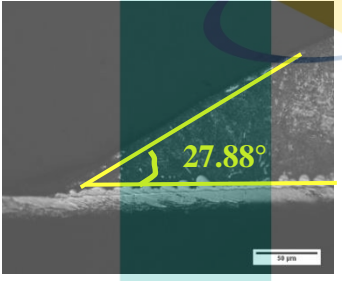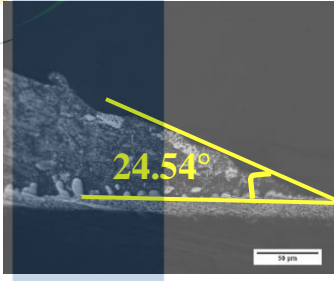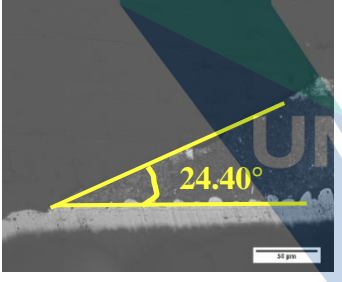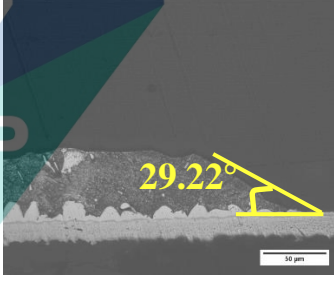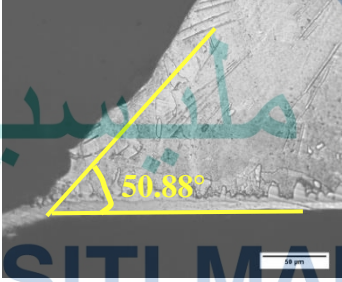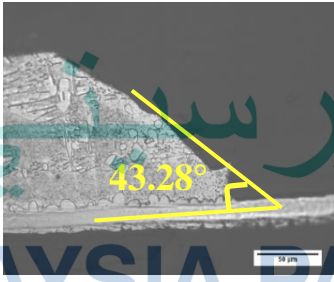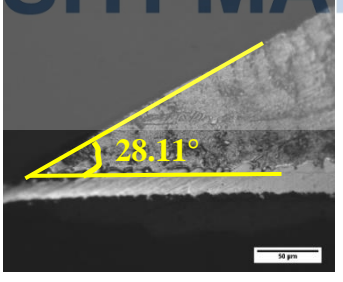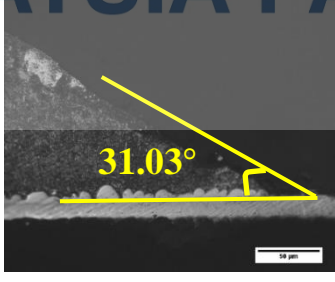
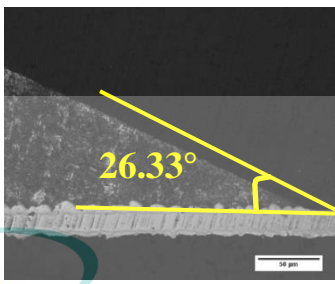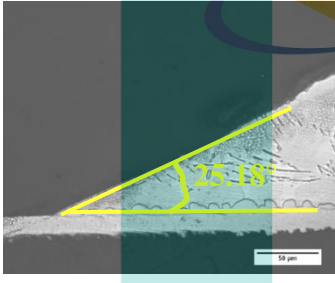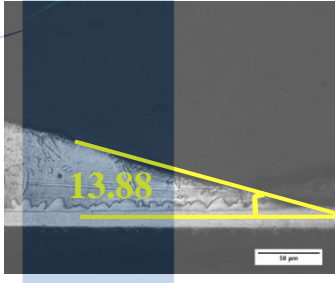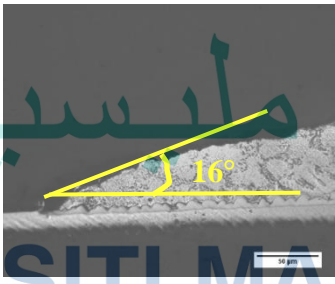| Pressure, ton	Images of wetting angle, scaled to 50μm per 0.5cm		Mean value of wetting angle, °
	Left	Right	
1	38.66°	5.68°	22.17
3	27.88°	24.54°	26.21
5	24.40°	29.22°	26.81
7	50.88°	43.28°	47.08
9	28.11°	31.03°	29.57

Figure 4.19   Images of wetting angle(contact angle) which has been measured accordingly; 8 hour milling duration

For this reason, it is best to explicate the wettability result according to each of the milling durations. This is much simpler to study and interpret the wettability data so that a comprehensive study of it can be drawn to the maximum. Table 4.3 shows the table of wetting contact angle of every sample according to the milling hour over increasing compaction load respectively. Noted that, each value is the average reading over f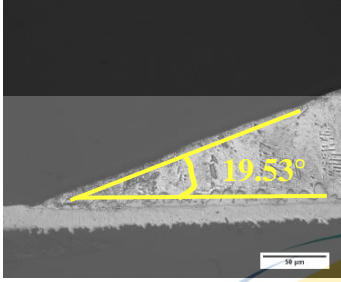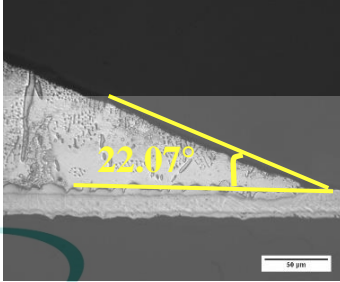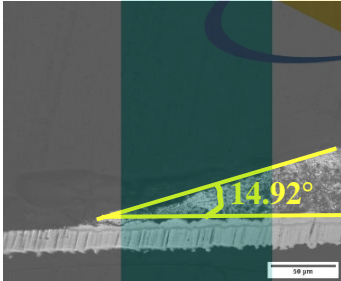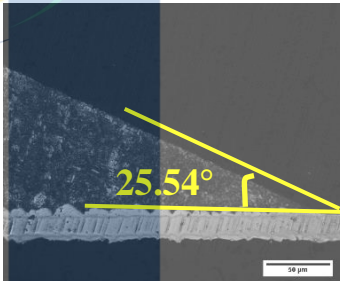ive same parameters of sample. To read and understand Table 4.3, Table 4.4 is prepared to show indicator of wettability degree. Generally, according to the result, all samples passed the acceptance to be a perform solder alloy. Plus, by percentage, 80 percent of sample showed a very good wetting angle. This depicted that the Sn3.0Ag0.5Cu compact powder solder alloy prepared by PM method could be the next green technology choice of fabricating solder alloy. Another two 10 percent were good and acceptable wetting angle.

Table 4.3   The average value of the wetting contact angle according to milling duration and compaction load

	Wetting angle, θ			
	2 hour	4 hour	6 hour	8 hour
1 ton	38.66	20.72	20.8	22.17
3 ton	21.19	19.53	20.23	26.21
5 ton	32.79	11.7	13.34	26.81
7 ton	27.79	28.54	28.91	47.08
9 ton	41.42	19.57	22.16	29.57

Indicator

🟩	very good wetting if $0° < \theta < 30°$	🟦	poor wetting if $55° < \theta < 70°$,
🟧	good wetting if $30° < \theta < 40°$	🟨	very poor wetting if $\theta > 70°$
🟥	acceptable wetting if $40° < \theta < 55°$		
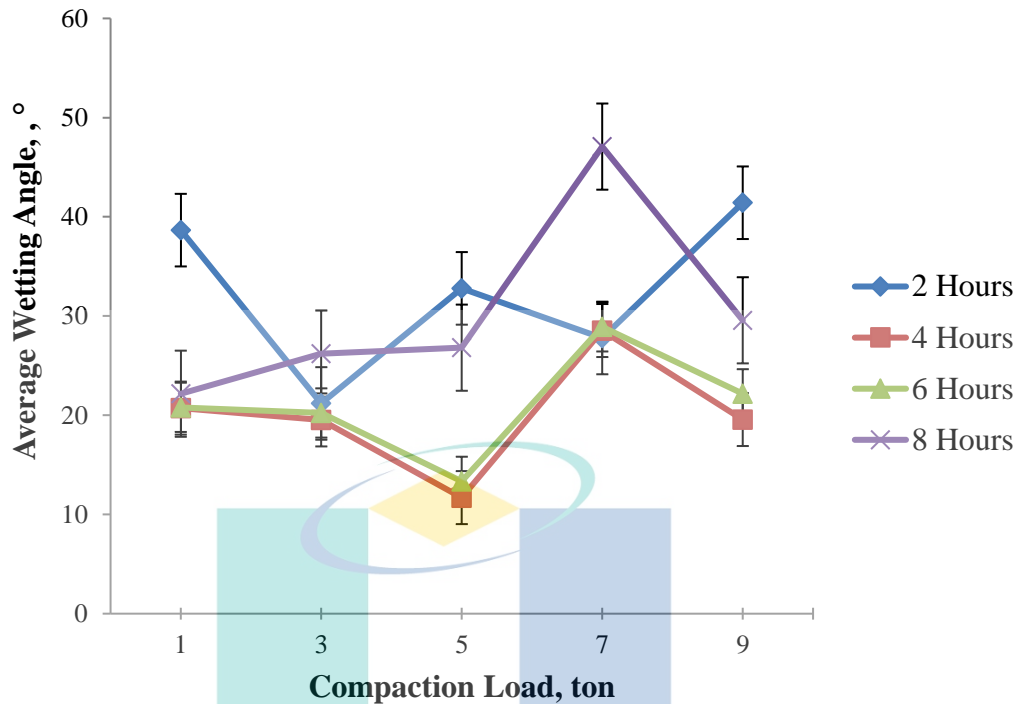
Figure 4.20   Graph of average wetting angle based on compaction loads upon milling durations

Result in Table 4.3 was graphically display into a graph in Figure 4.20. After the samples were taken out from the reflow furnace, those fluctuate graphs were indeed expected at first place because of the occurrence of melted solder droplets on the Cu board seemed irregular in shape. Thus, to understand these phenomena, analyses and discussions have been reported in this section. This fluctuate graph of wetting angles in this section were mainly due to the shape of solder droplet on its substrate. As have been elucidated, the activity of melting was first started at the interconnection of compacted solder bulk and the Cu board. All samples experienced this melting activity as they were in the same furnace which also received the same heat. But the varieties of solder droplet shapes were dissimilar to each other as their acceptance of heat was different due to their dissimilar size and shape of individual milled powder. As the molten molecules pulled each other downwards and spread out on Cu board, this mechanism has been responsible for the shape of molten solder droplets thus created different edges of molten solder droplets. Hence, explicating the variation of wetting angles. In short, different shape of solder droplet led to different values of wetting angle.

4.6   Formation of Intermetallic Compound (IMC)

This sub-chapter presents the findings from the compacted Sn3.0Ag0.5Cu milled powder solder and its substrate. Discussions on the cross-section morphology in terms of formation of the intermetallic compound at the solder joint and solder matrix have been made purposely for this research. The study of IMC with respects to its formation is a must to achieve an in-depth understanding of the structural integrity of interfaces along the solder joint.

4.6.1   Phase Confirmation using XRD on the formed IMC

The specimen for XRD analysis was prepared by mechanically removed the solder part and the impurities from the surface using etching procedures. Figure 4.21 shows the XRD result for the formed IMC at the solder joint for the sample 6 hours. It is calculated by Molecular Dynamic method that the formed IMC were all from the Cu_6Sn_5 type of IMC and this has been confirmed by the XRD outcomes. Result shown that there were two types of the Cu_6Sn_5 IMC phases, crystalline and amorphous alloy at the solder joint. This information was crucial that supported the melted and unmelted solder alloy by the reflow soldering process and the additional data to the configure the compacted milled powder.
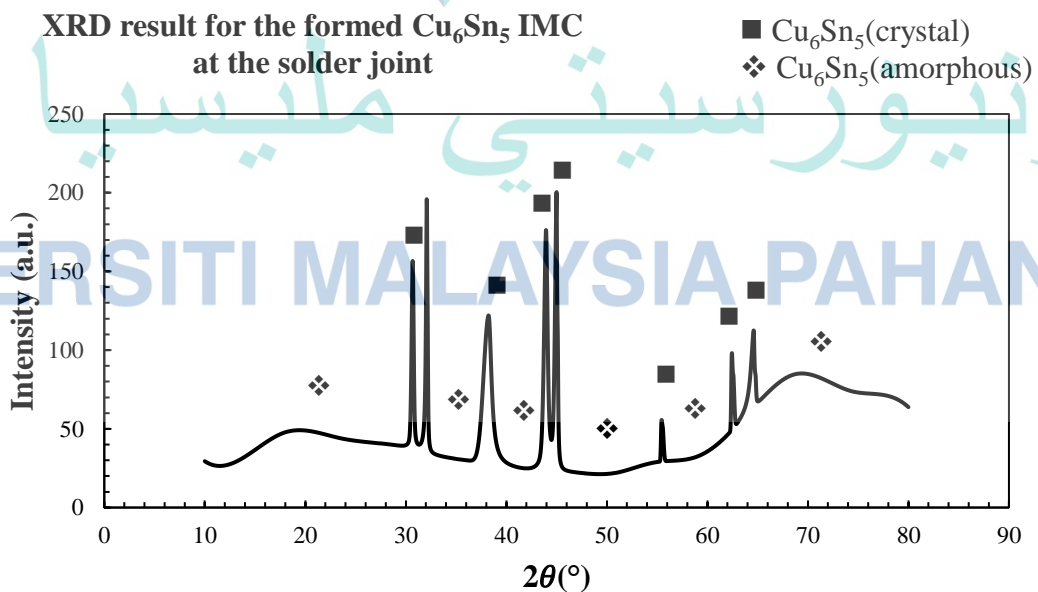
Figure 4.21   The XRD result on the formed IMC at the solder joint

4.6.2 Morphology at the Solder Joint/IMC-Cu Substrate Interface

IMC at the solder joint shall be discussed based on the morphological evolution. The explanation also will be explicated by the compaction loads upon the milling durations. Besides, to make it easier to comprehend the behaviours along the solder joint, clarification on the significant behaviour is essential. With this together, Figure 4.22 depicts the illustration of the IMC structure where it will get a clearer description of how is the next analyses are written up. The figure also describes the theory of IMC-solid substrate interface. Noted that the grey-ish colour of bumpy structures on the Cu substrate were the IMC. The IMC size and shape are varying with one another showing that they have different growth stages. Thus, shows the differences of IMC distribution on the Cu substrate.
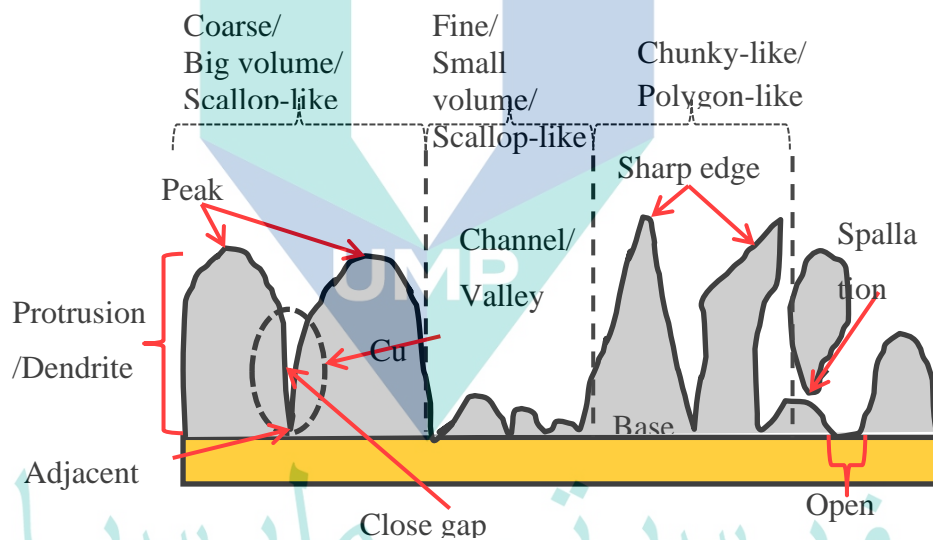
Figure 4.22   The illustration of IMC structures and the interface of IMC-solid substrate

There are quite resemblances between the structure in Figure 4.23 with the IMC samples that have been recorded in Figure 4.23 to Figure 4.26. Each of the structure has its own significance. The discussion on the IMC-Cu substrate interfacial layer will be based on a few terms. These include shape, spallation, neighbouring IMC scallop and the adjacent between the scallops. The scallop shape is a result of ripening mechanism from the sharp edge IMC.

Figure 4.24 to Figure 4.27 show the cross-section micrographs of the interfaces between Sn3.0Ag0.5Cu solder alloy and Cu substrate according to their compaction loads upon their respective milling duration. Noted that all IMC sample in this research has gone through the similar reflow process where the setting of furnace even the sample preparations were all exactly identical. By all means, a temperature of 250℃ for 25 minutes with 1 minute of holding time was all it took to complete the reflow process.

For the 2 hours of milling duration, in terms of shape; rounded scallop-like and the sharp edge of IMC peaks were seen to appear on the interfacial of IMC and Cu substrate for 1,3,5,7 ton of compaction loads sample. While sample from 9 ton appeared to have a similar projection but was in a very small volume fraction compared to others. The effect of having long dendritic IMC, spallation was happening to all compaction loads but 1 ton. The neighbouring IMC scallops for the 1-ton sample were far from each other but there was quite closed gap for the rest of compaction loads samples. This indicated that IMC growths were well distributed on the Cu substrate. Overall, the adjacent between the scallops was joining and grow either into deep channels or away from the longitudinal intersection. To define, the deep channel is when the adjacent base of IMC touches the Cu substrate which would be a sign of slow diffusion and vice versa before it turns into layer type of IMC.

What is the interesting matter to note by the above elucidation is that, the explanation is applicable for the rest samples of the 4, 6 and 8 hours of milling durations in this research but it must be relevant with the actual morphology. This is due to identical appearances and structures projected by each sample. To make a better clarification on this idea, the summarization of result is tabulated Table 4.4.
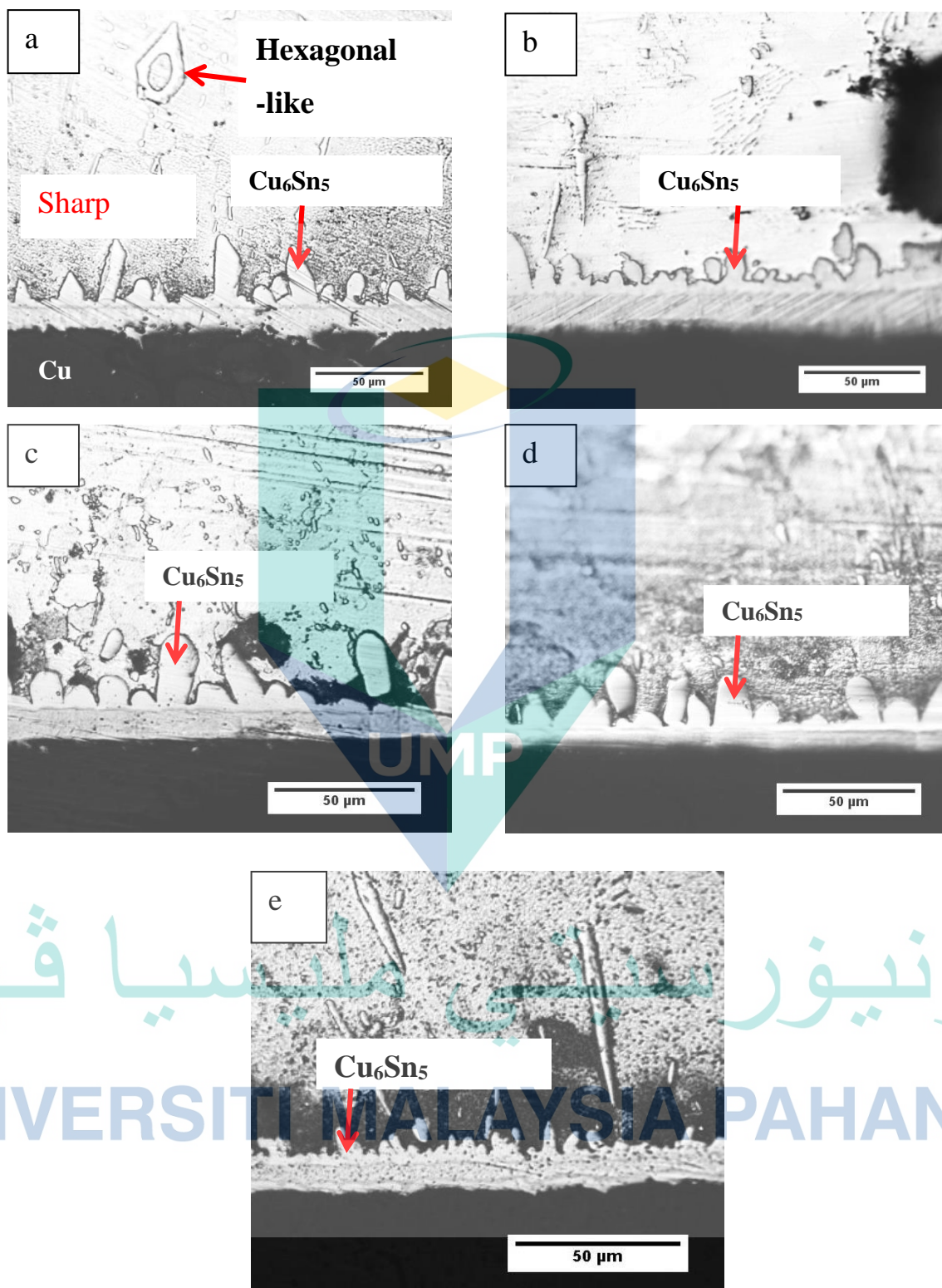
Figure 4.23   Cross-section of Sn3.0Ag0.5Cu solder alloy by 2 hours of milling durations; (a)1, (b) 3, (c)5, (d)7 and (e)9 ton of compaction loads
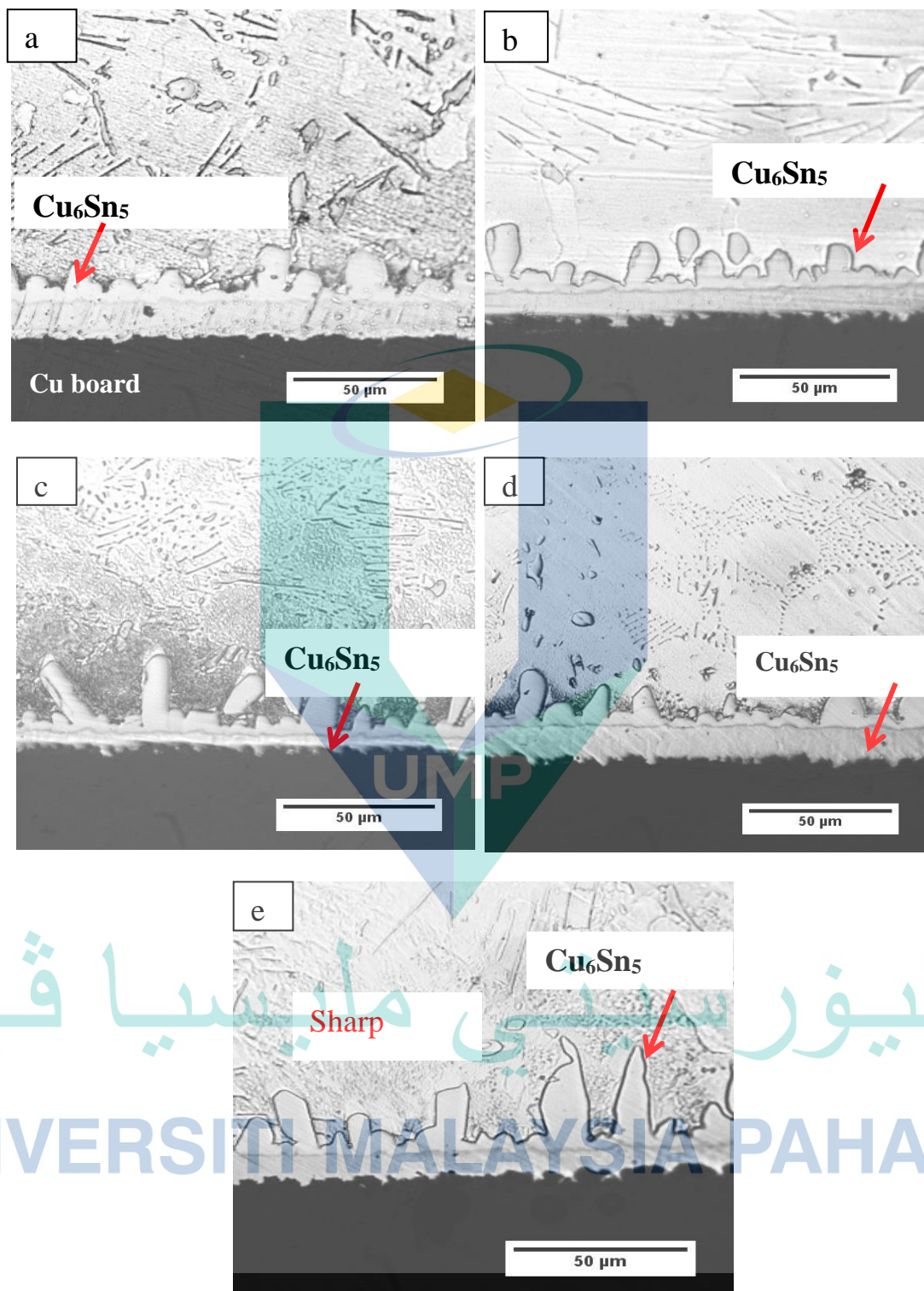
Figure 4.24   Cross-section of Sn3.0Ag0.5Cu solder alloy by 4 hours of milling durations; (a)1, (b) 3, (c)5, (d)7 and (e)9 ton of compaction loads
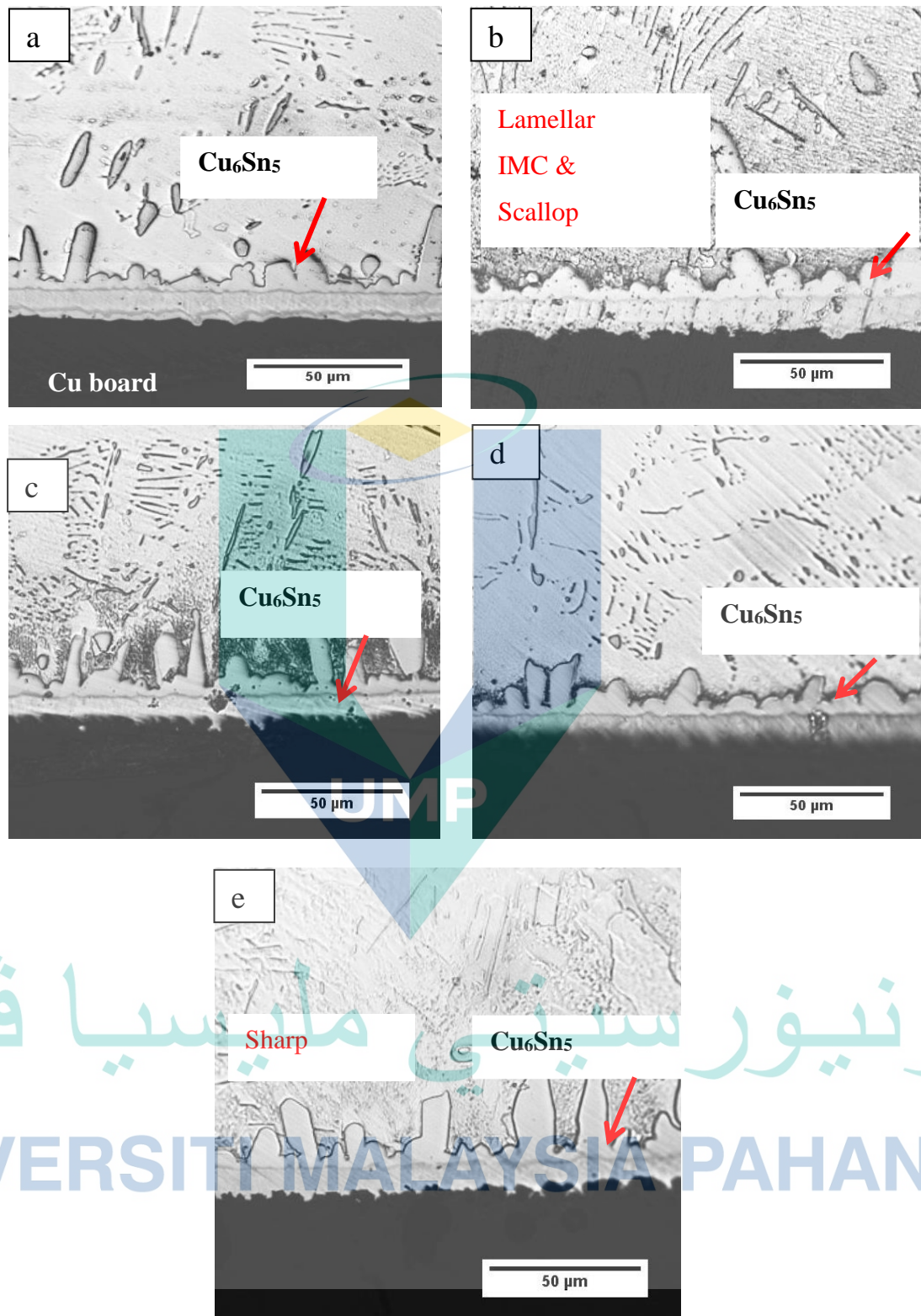
Figure 4.25   Cross-section of Sn3.0Ag0.5Cu solder alloy by 6 hours of milling durations; (a)1, (b) 3, (c)5, (d)7 and (e)9 ton of compaction loads
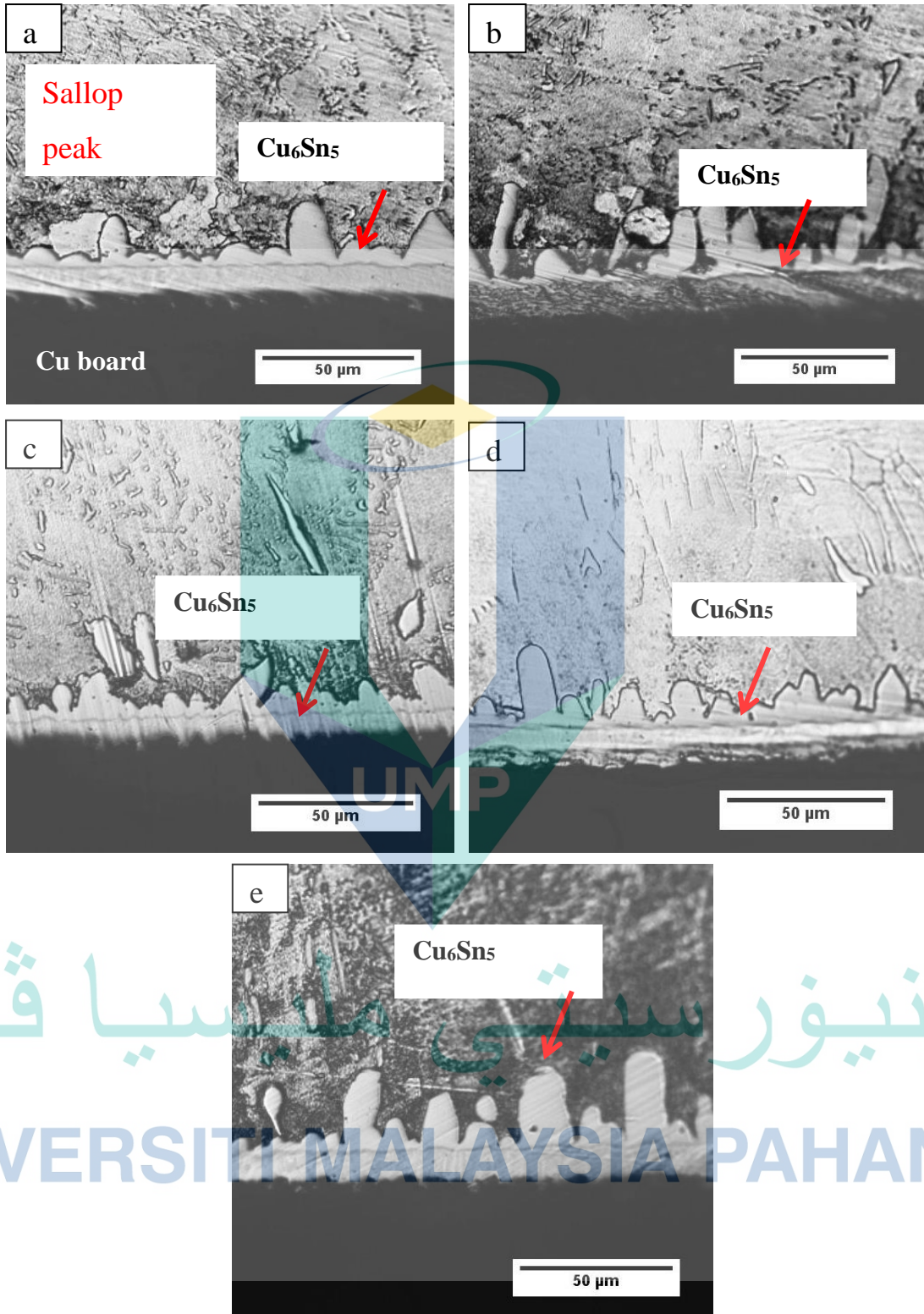
Figure 4.26   Cross-section of Sn3.0Ag0.5Cu solder alloy by 8 hours of milling durations; (a)1, (b) 3, (c)5, (d)7 and (e)9 ton of compaction loads

Table 4.4   Morphology analyses on the interfacial IMC-Cu substrate/solder joint for all samples according to their compaction loads upon their milling duration respectively; initial CL represents compaction load and both represent scallop and sharp edge

CL*	Aspects	Milling Duration(Hours)			
		2	4	6	8
1	Peak shape	Sharp edge	Scallop	Both	Both
	Spallation	None	None	Available	None
	Neighbouring	Far	Far	Far	Close
	Channel	Away	Away	Deep	Deep
3	Peak shape	Scallop	Scallop	Scallop	Both
	Spallation	Available	Available	None	Available
	Neighbouring	Close	Close	Close	Far
	Channel	Away	Deep	Away	Deep
5	Peak shape	Scallop	Scallop	Sharp edge	Both
	Spallation	Available	Available	Available	Available
	Neighbouring	Close	Close	Close	Close
	Channel	Deep	Away	Deep	Away
7	Peak shape	Scallop	Scallop	Sharp edge	Both
	Spallation	Available	Available	None	None
	Neighbouring	Close	Far	Close	Close
	Channel	Away	Deep	Deep	Away
9	Peak shape	Scallop	Sharp edge	Sharp edge	Both
	Spallation	Available	None	None	Available
	Neighbouring	Close	Close	Close	Close
	Channel	Away	Away	Deep	Deep

4.6.3 Morphology in the IMC-Solder matrix Bulk

Figure 4.27 shows the illustration of IMC-solder bulk interface and can also be referred to Figure 4.23 to Figure 4.26. The atomic migration between the atom from the substrate and the atom from the molten solder alloy at the interfaces during the reflow process has formed the IMC. The forming site will follow the concentration gradient of the atom by the diffusion-controlled mechanism(Baheti, Kashyap, Kumar, Chattopadhyay, & Paul, 2017). Based on the cross-sectional images disclose with EDX, it is found that Sn and Cu have precipitated in the solder matrix as Cu_6Sn_5. No trace of Cu_3Sn was ever detected in response to zero-hour ageing but slow cooling may have a few affections to the solder.
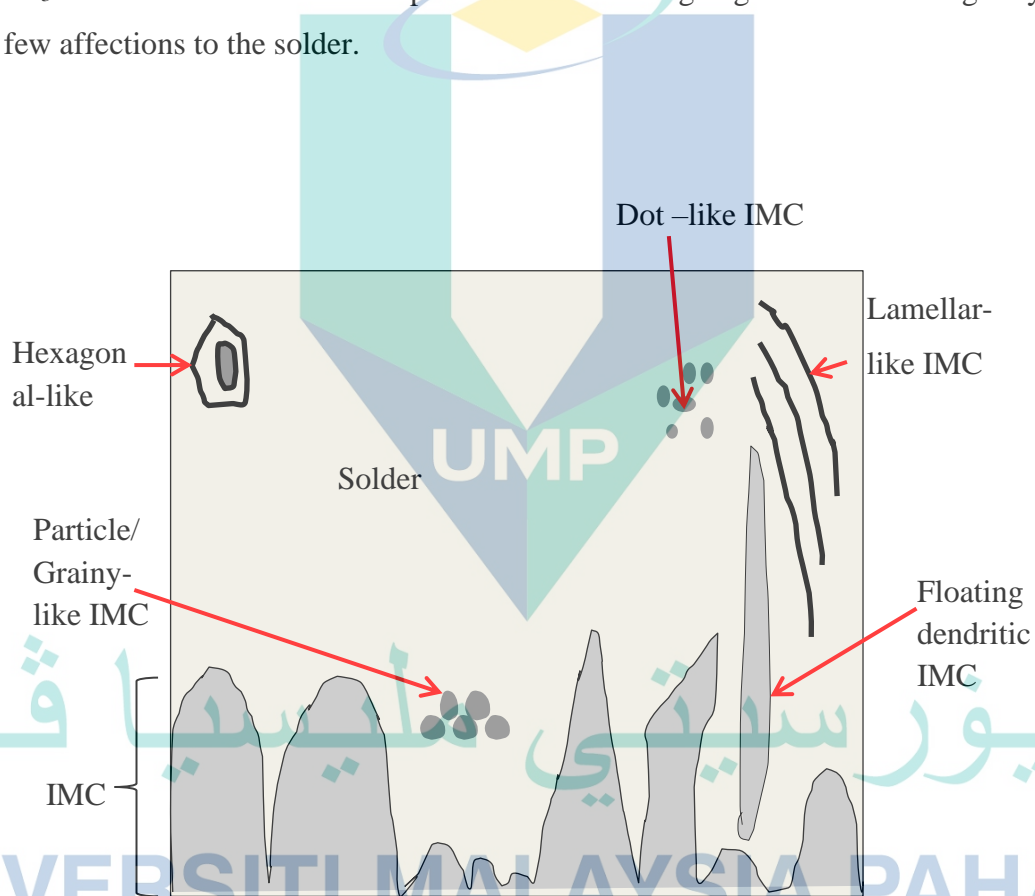
Figure 4.27   The illustration of IMC-solder matrix bulk interface

There were lots of similarities found in the solder matrix for all samples in this research. Probably because of the identical reflow settings in the beginning. For example, there were grainy/particle-type, fine/dot-type, floating plate-type, floating dendritic-type, lamellar-type and hexagonal-type of IMC that have been traced out in the interfacial of

IMC-solder bulk. The lamellar structure corresponds to the state where the molten solder reaches its eutectic point and phasing the solidification and decomposition level(Kenel & Leinenbach, 2015).

Besides, there were some patterns of IMC inside the solder matrix that seems to be in a nice coordinate order where there were IMC types that accumulated on the same spots. This phenomenon can also strengthen the facts that there was a well-distribution of particles inside each milled powder. The molecule was just close to each other and combined up to be in cordially pattern. As they followed the solid-state reaction, they went through the pinning mechanism and stayed floated in the solder matrix(P. Zhang, 2019). Large dendrites, particles, dot, and thin elongated IMC were the Cu_6Sn_5 IMC that had something to do with the activation energy, crystal orientation, diffusivity, local distribution and so on which not covered by this research.

The floated Cu_6Sn_5 IMC inside the solder matrix were appeared because of the Sn, Ag and Cu atoms were being close to each other as the sign of well-distribution of those particles inside the milled powder which was achieved by milling method. According to the chemical formula of Cu_6Sn_5, it needs five molecules of Sn and six molecules of Cu to become the solid Cu_6Sn_5 molecule compound in which corresponds to the five and six molecules happened to be close to each other inside the granule. Thus, when they reached out their melting point, they became a molten solder and started to coalesce which ultimately end up to be the IMC.

At the beginning of the solder-substrate interfacial reaction, Cu atom from substrate diffuse into solder matrix bulk and triggered the scallop layer of Cu_6Sn_5(Tang, Luo, Wang, & Li, 2016). Between the scallops, Cu atom has interstitially diffused into the SnAgCu molten solder bulk due to driving force that insisted the transferring. There are two sources of Cu atom supply, the SnAgCu solder bulk, and the Cu substrate. Thus, there can be two transferring mechanisms in which Sn comes from the solder matrix bulk which is the only source and yet it is found both at the solder joint and solder matrix. This indicates that Sn atom also migrated and deposited on Cu substrate to induce the IMC.

The grooving channel either vertically closed or away from the substrate was affecting the diffusion of the Cu atom to get into the solder matrix. Deeper grooving means fast Cu atom diffusion into the solder matrix. As it away and scallop-like IMC yet became a flatten layer of IMC, the diffusion stopped right away(H. Li, An, Wang, Tian,

& Jiang, 2015). No consumption of Cu atom from the substrate would ever take place into solder matrix anymore. Otherwise, the Cu atom still diffuse but in a timely manner and under heat controlled.

Cu_6Sn_5 corresponds to be coarser grain inside the solder matrix due to high temperature, crystal orientation and went through the solid-state reaction via the cooling effect. Due to concentration gradient, Cu atom from substrate diffuses into the molten solder. Cu atom diffuses into molten solder bulk interstitially while Sn atom diffuses to Cu site substantially(Tu & Liu, 2019). By the time, Cu atom from the substrate has gained enough interfacial energy and initiated the migration. The atom then diffused interstitially upwards, paired up with the closest Sn atom and deposited on the solder joint. Yet, those bigger granules could also be melted the same way but they might require a longer time. Therefore, this leads to different growth stages and distributions of IMC at the solder joint which ultimately resulted in dissimilar sizes and shapes of IMC.

Due to different growth stages and crystal orientation that compacted Sn3.0Ag0.5Cu solder alloy had at the moment, there were different nucleation site that led to non-uniform IMC distributions on the Cu substrate. Plus, this was also the reason why the volume sizes and shapes of IMC were all contrasting. Hence, it can be theoretically said that the distributions and growth kinetics of IMC at the solder joint could be controlled by regulating the shapes and sizes of compacted solder alloy granule which fully-utilized by the PM method.

4.7   Thickness of the Intermetallic Compound (IMC)

The average thicknesses of the grown Cu_6Sn_5 layer have been studied for all samples in Figure 4.23 to Figure 4.26 and results shown in Figure 4.28. All graphs depict fluctuate trends which starting from 6.58μm to 11.64μm. Those values were definitely quite high for IMC thickness but noted that all these samples had gone through slow cooling by the furnace. They were also having the same set of reflow, sample preparations and were in the furnace all at once.

Those fluctuate graphs of average thicknesses below were the consequences from the non-identical shapes and sizes of compacted Sn3.0Ag0.5Cu milled powder solder alloy which drawn directly from the milling method in this research. The

compacted milled powder had a bit of difficulty when they tend to become molten as reaching their liquid-state melting temperature. It was when the 217℃ heat was all over, each of the compacted granules absorbed that heat differently due to limiting factors of shapes and sizes that they had. The bigger individual milled powder would have a longer reaction time to absorb the heat and become molten as per smaller one was in opposite situation which approachable the specific latent heat concept. Thus, they were complicated to melt equally at once and resulted in non-homogenous of IMC distributions on Cu board where ultimately affecting the IMC thickness as well.
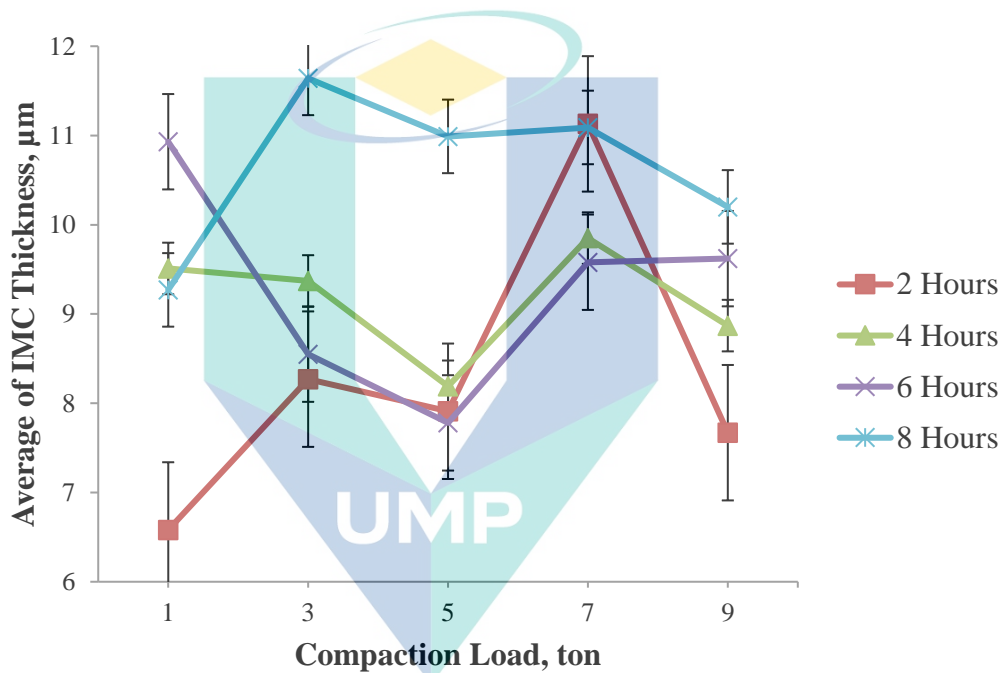
Figure 4.28   The average of IMC thickness values by according to milling durations upon compaction loads respectively

The same technique to analyse wetting angle is done to report thickness of IMC, quantitatively. Table 4.5 shows the table of IMC thickness for every sample according to the milling hour over increasing compaction load respectively. Generally, a low thickness of IMC is sought after in solder alloy characterisation. However, unlike wetting angle, there is still no official degree measurement of IMC thickness to determine the value. Therefore, the IMC thickness values were categorised. Sample of 2 hour of milling duration with 1 ton compaction whereas sample of 8 hour of milling duration with 3 ton compaction were the lowest and highest IMC thickness, respectively.

Table 4.5 The average of IMC thickness value according to milling duration and compaction load for every sample

	IMC thickness, μm			
	2 hour	**4 hour**	**6 hour**	**8 hour**
1 ton	6.58	9.51	10.93	9.27
3 ton	8.27	9.37	8.55	11.64
5 ton	7.91	8.19	7.78	10.99
7 ton	11.13	9.85	9.58	11.09
9 ton	7.67	8.87	9.62	10.2

Indicator

[green box] Lowest IMC thickness   [red box] Highest IMC thickness

4.7.1 Area Fraction of IMC

The thickness and SEM results of formed IMCs were not sufficient for validated data as the thicknesses, morphology and shapes of the IMCs were differs significantly in every sample. Hence, to address the quantity of IMCs formed along the solder joint, calculation on the size of formed IMCs were done to support the IMCs' thicknesses conclusively. This was done by calculating the area fraction of IMCs area on the Cu substrate. Table 4.6 shows the thresholded images as of morphology and of the mean area fractions of the IMCs at the solder joint.

Compaction Load (Ton)	Thresholded Images of The Formed IMC at Solder Joint (a)	Mean Area Fraction (%)
1	200 µm	35.97
3	200 µm	33.37
5	200 µm	26.47
7	200 µm	33.99
9	200 µm	32.81

Table 4.6   The thresholded images as of morphology and of the mean area fractions of the IMCs at the solder joint for (a)2, (b)4, (c)6 and (d)8 hour milling duration

96

Compaction Load(Ton)	Thresholded Images of The Formed IMC at Solder Joint(b)	Mean Area Fraction(%)
1		37.47
3		29.04
5		25.76
7		37.24
9		27.49

Table 4.6   Continued

Compaction Load(Ton)	Thresholded Images of The Formed IMC at Solder Joint (c)	Mean Area Fraction(%)
1	200 µm	35.37
3	200 µm	39.61
5	200 µm	34.89
7	200 µm	24.53
9	200 µm	32.94

Table 4.6   Continued

98

Compaction Load(Ton)	Thresholded Images of The Formed IMC at Solder Joint (d)	Mean Area Fraction(%)
1	200 μm	26.44
3	200 μm	32.67
5	200 μm	32.54
7	200 μm	37.51
9	200 μm	35.25

Table 4.6   Continued

Figure 4.29 displays the scatterplot for mean area fraction values for every sample subjected to milling durations and compaction loads in this research. The data is included to validate the formation of IMC and the thickness along the solder joint. By right, the fluctuate graph of mean area fraction is expected in accordance to the dissimilar thicknesses and size area of the closed region in the formed IMCs at the solder joint. The shown values in the graph were the highest and lowest mean area fraction value that subjected to the sample 6 hour both for 3 and 7 compaction loads.

By the solder-substrate interfacial reaction, Cu atom from substrate diffuses into solder matrix bulk and combine with Cu atom in the solder matrix. Due to different interfacial energy and driving forces, this has triggered the development of Cu_6Sn_5 with volume and area(Tang, Luo, Wang, & Li, 2016). Thus, supporting the IMC thickness data with area fraction is conclusive to validate the development formation of IMCs at the solder joint rather than presenting the thickness only.
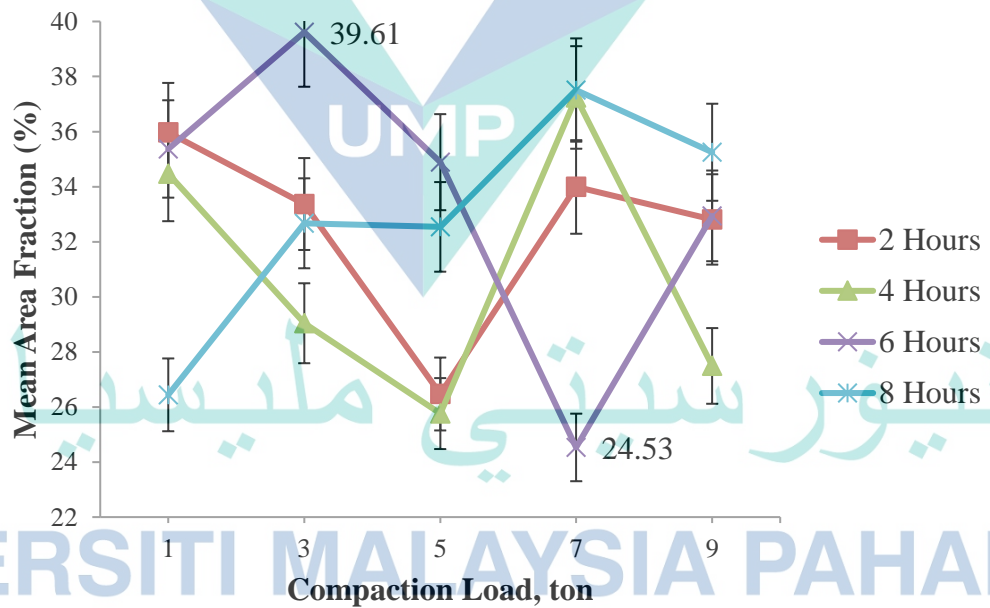
Figure 4.29   The mean area fraction values by according to milling durations upon compaction loads respectively

CHAPTER 5

CONCLUSION

5.1   Introduction

This research work has been conducted to study the properties of Sn3.0Ag0.5Cu solder alloy upon the fabrication of PM method. The important of outcomes out of this research were listed down in this Chapter 5. This section will also present the recommendations for a better study in future.

5.2   Conclusion

Besides sustaining the human and environments, PM can be found as a smart move to support the Green Technology call for a better production of solder alloy. Here are the concluded versions of every result drawn by this research:

i.   IMCs have formed and grown along the solder joint interfaces which shown that PM method parameters such as milling had a high potential to create a homogeneous distribution of Sn, Ag and Cu particles in solder alloy.

ii.   All of wetting angles measured between 0° to 55° signified a very good to accepted wettability degree in which better solder joint interfaces were highly performed.

iii. Scallop and sharp peak structures of crystalline and amorphous phase of Cu_6Sn_5 grown along the solder joint interfaces with up to 11.64 μm in thickness which incompatible with slow cooling.

5.3 Recommendations for Future Works

Recommendations should be addressed based on limited and insight worked in this research. The recommendations are listed as follows:

i. Conduct sieve work after milling to obtain higher degree of powder characterisation in terms of sphericity and roundness in which may induce better reflow for solder alloy performances.

ii. Performs the powder density study on both individual and compacted milled powder to define porosity for factors of volume fraction.

iii. Increase the reflow soldering duration to allow better heat dissipation and absorption by the milled powder to spread more on its substrate for better wettability
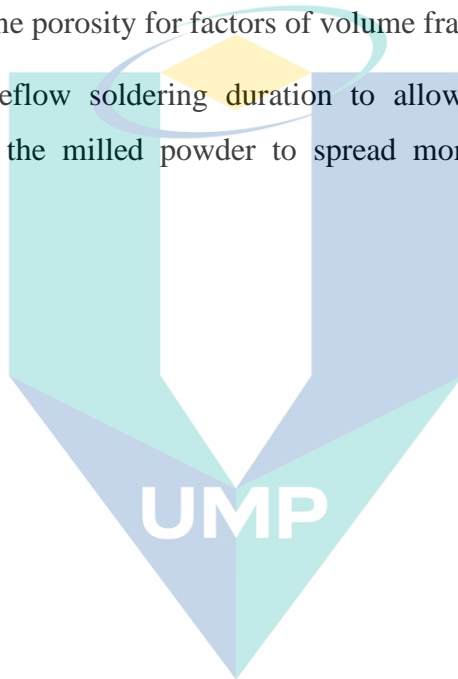
REFERENCES

Akhtar, Z., & Malek, A. (2017). Effect of nickel doping into solder alloy and its strength between SnCu-Ni/immersion gold joint. Universiti Malaysia Pahang.

An, T., & Qin, F. (2014). Effects of the intermetallic compound microstructure on the tensile behavior of Sn3. 0Ag0. 5Cu/Cu solder joint under various strain rates. Microelectronics Reliability, 54(5), 932–938.

Azreen, A. R., Sutjipto, A. G. E., & Adesta, E. Y. T. (2011). Fabrication of CuSiC Composite by Powder Metallurgy Route. In Advanced Materials Research (Vol. 264, pp. 748–753). Trans Tech Publ.

Attar, H., Prashanth, K. G., Zhang, L. C., Calin, M., Okulov, I. V., Scudino, S., ... & Eckert, J. (2015). Effect of powder particle shape on the properties of in situ Ti–TiB composite materials produced by selective laser melting. Journal of Materials Science & Technology, 31(10), 1001-1005.

Bobal, T. (2018). What Are The Best Materials For High-Temperature Soldering. Retrieved May 1, 2018, from https://www.ametek-ecp.com/resources/blog/2018/may/what-are-the-best-materials-for-high-temperature-soldering

Boostani, A. F., Tahamtan, S., Jiang, Z. Y., Wei, D., Yazdani, S., Khosroshahi, R. A., … Gong, D. (2015). Enhanced tensile properties of aluminium matrix composites reinforced with graphene encapsulated SiC nanoparticles. Composites Part A: Applied Science and Manufacturing, 68, 155–163.

Cagala, M., Břuska, M., Lichý, P., & Beňo, J. (2013). Influence of aluminium-alloy remelting on the structure and mechanical properties.

Akhtar, Z., & Malek, A. (2017). Effect of nickel doping into solder alloy and its strength between SnCu-Ni/immersion gold joint. Universiti Malaysia Pahang.

An, T., & Qin, F. (2014). Effects of the intermetallic compound microstructure on the tensile behavior of Sn3. 0Ag0. 5Cu/Cu solder joint under various strain rates. Microelectronics Reliability, 54(5), 932–938.

Azreen, A. R., Sutjipto, A. G. E., & Adesta, E. Y. T. (2011). Fabrication of CuSiC Composite by Powder Metallurgy Route. In Advanced Materials Research (Vol. 264, pp. 748–753). Trans Tech Publ.

Bobal, T. (2018). What Are The Best Materials For High-Temperature Soldering. Retrieved May 1, 2018, from https://www.ametek-ecp.com/resources/blog/2018/may/what-are-the-best-materials-for-high-temperature-soldering

Boostani, A. F., Tahamtan, S., Jiang, Z. Y., Wei, D., Yazdani, S., Khosroshahi, R. A., … Gong, D. (2015). Enhanced tensile properties of aluminium matrix

composites reinforced with graphene encapsulated SiC nanoparticles. Composites Part A: Applied Science and Manufacturing, 68, 155–163.

Cagala, M., Břuska, M., Lichý, P., & Beňo, J. (2013). Influence of aluminium-alloy remelting on the structure and mechanical properties.

Chaudhry, A. (2014). Metal Casting processes including pattern making and mold making,Patterns,Casting Defects. Retrieved from https://www.slideshare.net/azlanchaudhry/casting-processes

Chellvarajoo, S., Abdullah, M. Z., & Samsudin, Z. (2015). Effects of Fe2NiO4 nanoparticles addition into lead free Sn–3.0 Ag–0.5 Cu solder pastes on microstructure and mechanical properties after reflow soldering process. Materials & Design, 67, 197–208.

Chennu, V. R. (2017). Casting Process: Advantages and Limitations. Retrieved December 11, 2018, from https://me-mechanicalengineering.com/casting-process-advantages-and-limitations/

El-Kady, O., Yehia, H. M., & Nouh, F. (2018). Preparation and characterization of Cu/(WC-TiC-Co)/graphene nano-composites as a suitable material for heat sink by powder metallurgy method. International Journal of Refractory Metals and Hard Materials.

Ghasali, E., Alizadeh, M., Niazmand, M., & Ebadzadeh, T. (2017). Fabrication of magnesium-boron carbide metal matrix composite by powder metallurgy route: comparison between microwave and spark plasma sintering. Journal of Alloys and Compounds, 697, 200–207.

Gong, J., Liu, C., Conway, P. P., & Silberschmidt, V. V. (2008). Evolution of CuSn intermetallics between molten SnAgCu solder and Cu substrate. Acta Materialia, 56(16), 4291–4297.

Hassan, N. A. (2009). Study of Interfacial Reation During Reflow Soldering of Sn-Ag-Cu Lead-Free Solders on Bare Copper and Immersion Silver Surface Finishes. Universiti Teknologi Malaysia.

Hu, X., Xu, T., Keer, L. M., Li, Y., & Jiang, X. (2017). Shear strength and fracture behavior of reflowed Sn3. 0Ag0. 5Cu/Cu solder joints under various strain rates. Journal of Alloys and Compounds, 690, 720–729.

KAHAR, H. B. (2017). Effect of electroless nickel-boron (EN-B) surface finish on solderability of SAC305 and solder joint strength. Universiti Malaysia Pahang.

Karlsson, J., Norell, M., Ackelid, U., Engqvist, H., & Lausmaa, J. (2015). Surface oxidation behavior of Ti–6Al–4V manufactured by Electron Beam Melting (EBM®). Journal of Manufacturing Processes, 17, 120–126. http://doi.org/https://doi.org/10.1016/j.jmapro.2014.08.005

Kim, Y., Suh, H. S., & Yun, T. S. (2019). Reliability and applicability of the

Krumbein-Sloss chart for estimating geomechanical properties in sands. Engineering Geology, 248, 117–123. http://doi.org/https://doi.org/10.1016/j.enggeo.2018.11.001

Kotadia, H. R., Howes, P. D., & Mannan, S. H. (2014). A review: on the development of low melting temperature Pb-free solders. Microelectronics Reliability, 54(6–7), 1253–1273.

Kunwar, A., Ma, H., Ma, H., Guo, B., Meng, Z., Zhao, N., & Huang, M. (2016). On the thickness of Cu6Sn5 compound at the anode of Cu/liquid Sn/Cu joints undergoing electromigration. Journal of Materials Science: Materials in Electronics, 27(7), 7699–7706.

Lee, L. M., & Mohamad, A. A. (2013). Interfacial reaction of Sn-Ag-Cu lead-free solder alloy on Cu: a review. Advances in Materials Science and Engineering, 2013.

Lee, W. W., Nguyen, L. T., & Selvaduray, G. S. (2000). Solder joint fatigue models: review and applicability to chip scale packages. Microelectronics Reliability, 40(2), 231–244.

Li, H., An, R., Wang, C., & Jiang, Z. (2015). In situ quantitative study of microstructural evolution at the interface of Sn3. 0Ag0. 5Cu/Cu solder joint during solid state aging. Journal of Alloys and Compounds, 634, 94–98.

Li, Y., & Chan, Y. C. (2015). Effect of silver (Ag) nanoparticle size on the microstructure and mechanical properties of Sn58Bi–Ag composite solders. Journal of Alloys and Compounds, 645, 566–576.

Liashenko, O. Y., & Hodaj, F. (2015). Differences in the interfacial reaction between Cu substrate and metastable supercooled liquid Sn–Cu solder or solid Sn–Cu solder at 222°C: Experimental results versus theoretical model calculations. Acta Materialia, 99, 106–118. http://doi.org/https://doi.org/10.1016/j.actamat.2015.07.066

Liashenko, O. Y., Lay, S., & Hodaj, F. (2016). On the initial stages of phase formation at the solid Cu/liquid Sn-based solder interface. Acta Materialia, 117, 216–227.

Ma, H. R., Li, S., Yao, M. J., Wang, Y. P., Chen, J., Zhao, N., & Ma, H. T. (2017). The effect of cooling rate on growth kinetics of interfacial IMCs during multiple reflows. In Electronic Packaging Technology (ICEPT), 2017 18th International Conference on (pp. 1323–1326). IEEE.

Microsemi Corporation. (2008). Standard Reflow Profile for Standard and Lead-Free Packages. Retrieved December 3, 2018, from https://www.microsemi.com/document-portal/doc_view/131105-solder-reflow-leadfree

Najib, S. I., Salleh, M., Anuar, M. A., & Norainiza, S. (2013). Effect of Aging Time Towards Intermetallic Compound (IMC) Growth Kinetics Formation for

Sn-0.7 Cu-Si3N4 Composite Solder on Copper Substrate. In Advanced Materials Research (Vol. 795, pp. 505–508). Trans Tech Publ.

Pal, M. K., Gergely, G., Horváth, D. K., & Gácsi, Z. (2018). Microstructural investigations and mechanical properties of pure lead-free (Sn–3.0 Ag–0.5 Cu and Sn–4.0 Ag–0.5 Cu) solder alloy. Metallurgical and Materials Engineering, 24(1), 27–36.

Pawełkiewicz, M., Danielewski, M., & Janczak-Rusch, J. (2015). Intermetallic Layer Growth Kinetics in Sn-Ag-Cu System using Diffusion Multiple and Reflow Techniques. Advanced Engineering Materials, 17(4), 512–522.

Qin, L., Majumder, A., Fan, J. A., Kopechek, D., & Fan, L.-S. (2014). Evolution of nanoscale morphology in single and binary metal oxide microparticles during reduction and oxidation processes. Journal of Materials Chemistry A, 2(41), 17511–17520. http://doi.org/10.1039/C4TA04338C

Razak, N. R. A., Salleh, M., Anuar, M. A., Saud, N., Said, R. M., & Ramli, M. I. I. (2018). Influence of Bismuth in Sn-Based Lead-Free Solder–A Short Review. In Solid State Phenomena (Vol. 273, pp. 40–45). Trans Tech Publ.

Reeve, K. N., Anderson, I. E., & Handwerker, C. A. (2015). Nucleation and growth of Cu-Al intermetallics in Al-modified Sn-Cu and Sn-Ag-Cu lead-free solder alloys. Journal of Electronic Materials, 44(3), 842–866.

Salleh, M. A. A. M., McDonald, S. D., & Nogita, K. (2017). Effects of Ni and TiO2 additions in as-reflowed and annealed Sn0. 7Cu solders on Cu substrates. Journal of Materials Processing Technology, 242, 235–245.

Salleh, M., Anuar, M. A., Hazizi, M. H., Ahmad, Z. A., Hussin, K., & Ahmad, K. R. (2011). Wettability, electrical and mechanical properties of 99.3 Sn-0.7 Cu/Si3N4 novel lead-free nanocomposite solder. In Advanced Materials Research (Vol. 277, pp. 106–111). Trans Tech Publ.

Shah, L. H., Mohamad, U. K., Yaakob, K. I., Razali, A. R., & Ishak, M. (2016). Lap joint dissimilar welding of aluminium AA6061 and galvanized iron using TIG welding. Journal of Mechanical Engineering and Sciences, 10, 1817–1826.

Somidin, F., Salleh, M., Anuar, M. A., & Khairel, R. A. (2013). Intermetallic compound formation on solder alloy/Cu-substrate interface using lead-free Sn-0.7 Cu/recycled-Aluminum composite solder. In Advanced Materials Research (Vol. 620, pp. 105–111). Trans Tech Publ.

Sona, M., & Prabhu, K. N. (2013). Review on microstructure evolution in Sn–Ag–Cu solders and its effect on mechanical integrity of solder joints. Journal of Materials Science: Materials in Electronics, 24(9), 3149–3169.

Tan, A. T., Tan, A. W., & Yusof, F. (2015). Influence of nanoparticle addition on the formation and growth of intermetallic compounds (IMCs) in Cu/Sn–Ag–Cu/Cu solder joint during different thermal conditions. Science and

Technology of Advanced Materials, 16(3), 33505.

Tang, Y., Luo, S. M., Li, Z. H., Hou, C. J., & Li, G. Y. (2018). Morphological Evolution and Growth Kinetics of Interfacial Cu 6 Sn 5 and Cu 3 Sn Layers in Low-Ag Sn-0.3 Ag-0.7 Cu-xMn/Cu Solder Joints During Isothermal Ageing. Journal of Electronic Materials, 47(10), 5913–5929.

Tao, Q. B., Benabou, L., Vivet, L., Le, V. N., & Ouezdou, F. B. (2016). Effect of Ni and Sb additions and testing conditions on the mechanical properties and microstructures of lead-free solder joints. Materials Science and Engineering: A, 669, 403–416.

Tian, Y., Zhang, R., Hang, C., Niu, L., & Wang, C. (2014). Relationship between morphologies and orientations of Cu6Sn5 grains in Sn3. 0Ag0. 5Cu solder joints on different Cu pads. Materials Characterization, 88, 58–68.

Transparency Market Research. (2018). Lead-Free Solder Balls Market - Global Industry Analysis, Size, Share, Growth, Trends, and Forecast 2017 - 2025. India. Retrieved from https://www.transparencymarketresearch.com/lead-free-solder-balls-market.html

Tsao, L. C., & Chang, S. Y. (2010). Effects of nano-TiO2 additions on thermal analysis, microstructure and tensile properties of Sn3. 5Ag0. 25Cu solder. Materials & Design, 31(2), 990–993.

Tu, K. N., & Liu, Y. (2019). Recent advances on kinetic analysis of solder joint reactions in 3D IC packaging technology. Materials Science and Engineering: R: Reports, 136, 1–12.

Wang, C., Li, M., Chiu, C., & Chang, T. (2018). Kinetic study of solid-state interfacial reactions of p-type (Bi, Sb) 2Te3 thermoelectric materials with Sn and Sn–Ag–Cu solders. Journal of Alloys and Compounds, 767, 1133–1140.

Wang, Q., Johnson, W., Ma, H., Gale, W. F., & Lindahl, D. (2005). Properties of lead free solder alloys as a function of composition variation. In 10 th Electronic Circuit and World Convention Conference (ECWC 10).

Xiong, G., Nie, Y., Ji, D., Li, J., Li, C., Li, W., … Wan, Y. (2016). Characterization of biomedical hydroxyapatite/magnesium composites prepared by powder metallurgy assisted with microwave sintering. Current Applied Physics, 16(8), 830–836.

Xiong, M., & Zhang, L. (2019). Interface reaction and intermetallic compound growth behavior of Sn-Ag-Cu lead-free solder joints on different substrates in electronic packaging. Journal of Materials Science, 54(2), 1741–1768.

Yahya, I., Ghani, A., Asikin, N., Abiddin, N. N. Z., Abd Hamid, H., & Mayappan, R. (2013). Intermetallic evolution of Sn-3.5 Ag-1.0 Cu-0.1 Zn/Cu interface under thermal aging. In Advanced Materials Research (Vol. 620, pp. 142–146). Trans Tech Publ.

Yu, H., & Shangguan, D. (2013). Solidification and reliability of lead-free solder interconnection. Soldering & Surface Mount Technology, 25(1), 31–38.

Zeng, G., Xue, S., Zhang, L., & Gao, L. (2011). Recent advances on Sn–Cu solders with alloying elements. Journal of Materials Science: Materials in Electronics, 22(6), 565–578.

Zhang, Q. K., Long, W. M., Yu, X. Q., Pei, Y. Y., & Qiao, P. X. (2015). Effects of Ga addition on microstructure and properties of Sn–Ag–Cu/Cu solder joints. Journal of Alloys and Compounds, 622, 973–978.

Ahmed, M., Fouzder, T., Sharif, A., Gain, A. K., & Chan, Y. C. (2010). Influence of Ag micro-particle additions on the microstructure, hardness and tensile properties of Sn–9Zn binary eutectic solder alloy. Microelectronics Reliability, 50(8), 1134-1141.

Hashim, J., Looney, L., & Hashmi, M. (1999). Metal matrix composites: production by the stir casting method. Journal of materials processing technology, 92, 1-7.

Kumar, U. K. A. V. (2017). Method of stir casting of aluminum metal matrix composites: a review. Materials Today: Proceedings, 4(2), 1140-1146.

Nadia, A., & Haseeb, A. (2012). Fabrication and properties of Sn-3.5 Ag-XCu solder by ball milling and paste Mixing. Paper presented at the Defect and Diffusion Forum.

Salleh, M., Anuar, M. A., Somidin, F., Al Bakri Abdullah, M. M., Noriman, N., Mayappan, R., & Alui, N. F. M. (2013). Effects of Recycled-Aluminum Additions on the Mechanical Properties of Sn-0.7 Cu/Cu-Substrate Lead-Free Solder Joints. Paper presented at the Advanced Materials Research.

Soltani, S., Khosroshahi, R. A., Mousavian, R. T., Jiang, Z.-Y., Boostani, A. F., & Brabazon, D. (2017). Stir casting process for manufacture of Al–SiC composites. Rare Metals, 36(7), 581-590.

Abdelhadi, O. M., & Ladani, L. (2012). IMC growth of Sn-3.5 Ag/Cu system: Combined chemical reaction and diffusion mechanisms. Journal of Alloys and Compounds, 537, 87-99.

Ali, B., Sabri, M. F. M., Jauhari, I., & Sukiman, N. L. (2016). Impact toughness, hardness and shear strength of Fe and Bi added Sn-1Ag-0.5 Cu lead-free solders. Microelectronics Reliability, 63, 224-230.

Almotairy, S. M., Alharthi, N. H., Alharbi, H. F., & Abdo, H. S. (2020). Superior Mechanical performance of inductively Sintered Al/Sic nanocomposites processed by novel Milling Route. Scientific Reports, 10(1), 1-13.

Azani, M. R., & Hassanpour, A. (2018). Silver nanorings: New generation of transparent conductive films. Chemistry–A European Journal, 24(72), 19195-19199.

Baheti, V. A., Kashyap, S., Kumar, P., Chattopadhyay, K., & Paul, A. (2017). Solid–state diffusion–controlled growth of the intermediate phases from room temperature to an elevated temperature in the Cu–Sn and the Ni–Sn systems. Journal of Alloys and Compounds, 727, 832-840.

Bokstein, B., Klinger, L. M., & Apikhtina, I. (1995). Liquid grooving at grain boundaries. Materials Science and Engineering: A, 203(1-2), 373-376.

Cabeza, M., Feijoo, I., Merino, P., Pena, G., Pérez, M., Cruz, S., & Rey, P. (2017). Effect of high energy ball milling on the morphology, microstructure and properties of nano-sized TiC particle-reinforced 6005A aluminium alloy matrix composite. Powder Technology, 321, 31-43.

Chen, G., Peng, H., Silberschmidt, V. V., Chan, Y., Liu, C., & Wu, F. (2016). Performance of Sn–3.0 Ag–0.5 Cu composite solder with TiC reinforcement: physical properties, solderability and microstructural evolution under isothermal ageing. Journal of Alloys and Compounds, 685, 680-689.

Cox, B. N., & Landis, C. M. (2018). Solitary waves in morphogenesis: Determination fronts as strain-cued strain transformations among automatous cells. Journal of the Mechanics and Physics of Solids, 111, 239-276.

Feng, J., Xu, D. E., Tian, Y., & Mayer, M. (2019). Sac305 solder reflow: Identification of melting and solidification using in-process resistance monitoring. IEEE Transactions on Components, Packaging and Manufacturing Technology, 9(8), 1623-1631.

Ghosh, S., Haseeb, A., & Afifi, A. (2013). Effects of metallic nanoparticle doped flux on interfacial intermetallic compounds between Sn-3.0 Ag-0.5 Cu and copper substrate. Paper presented at the 2013 IEEE 15th Electronics Packaging Technology Conference (EPTC 2013).

Goh, H. P., Heng, P. W. S., & Liew, C. V. (2018). Comparative evaluation of powder flow parameters with reference to particle size and shape. International journal of pharmaceutics, 547(1-2), 133-141.

Ju, W., Jiang, B., Qin, Y., Wu, C., Wang, G., Qu, Z., & Li, M. (2019). The present-day in-situ stress field within coalbed methane reservoirs, Yuwang Block, Laochang Basin, south China. Marine and Petroleum Geology, 102, 61-73.

Jwad, T., Walker, M., & Dimov, S. (2018). Erasing and rewriting of titanium oxide colour marks using laser-induced reduction/oxidation. Applied Surface Science, 458, 849-854.

Kenel, C., & Leinenbach, C. (2015). Influence of cooling rate on microstructure formation during rapid solidification of binary TiAl alloys. Journal of Alloys and Compounds, 637, 242-247.

Kim, S. H., Yang, D.-Y., Kim, Y.-J., Min, T., Choi, J., Yun, J., . . . Do Kim, Y.

(2017). Thermo-mechanical evolution of ternary Bi–Sn–In solder micropowders and nanoparticles reflowed on a flexible PET substrate. Applied Surface Science, 415, 28-34.

Li, H., An, R., Wang, C., Tian, Y., & Jiang, Z. (2015). Effect of Cu grain size on the voiding propensity at the interface of SnAgCu/Cu solder joints. Materials Letters, 144, 97-99.

Li, M., Zhang, J., Song, W., & Germain, D. M. (2019). Recycling of crushed waste rock as backfilling material in coal mine: effects of particle size on compaction behaviours. Environmental Science and Pollution Research, 26(9), 8789-8797.

Nandiyanto, A. B. D., Zaen, R., & Oktiani, R. (2018). Working volume in high-energy ball-milling process on breakage characteristics and adsorption performance of rice straw ash. Arabian Journal for Science and Engineering, 43(11), 6057-6066.

Park, M., & Arróyave, R. (2012). Concurrent nucleation, formation and growth of two intermetallic compounds (Cu6Sn5 and Cu3Sn) during the early stages of lead-free soldering. Acta Materialia, 60(3), 923-934.

Park, Y., Bang, J.-H., Oh, C. M., Hong, W. S., & Kang, N. (2017). The Effect of Eutectic Structure on the Creep Properties of Sn-3.0 Ag-0.5 Cu and Sn-8.0 Sb-3.0 Ag Solders. Metals, 7(12), 540.

Perez-Gandarillas, L., Perez-Gago, A., Mazor, A., Kleinebudde, P., Lecoq, O., & Michrafy, A. (2016). Effect of roll-compaction and milling conditions on granules and tablet properties. European Journal of Pharmaceutics and Biopharmaceutics, 106, 38-49.

Piotrowska, K., Grzelak, M., & Ambat, R. (2019). No-clean solder flux chemistry and temperature effects on humidity-related reliability of electronics. Journal of Electronic Materials, 48(2), 1207-1222.

Sperança, M. A., Virgilio, A., Pereira-Filho, E. R., & de Aquino, F. W. B. (2018). Determination of elemental content in solder mask samples used in printed circuit boards using different spectroanalytical techniques. Applied Spectroscopy, 72(8), 1205-1214.

Tang, Y., Luo, S., Wang, K., & Li, G. (2016). Effect of Nano-TiO2 particles on growth of interfacial Cu6Sn5 and Cu3Sn layers in Sn3. 0Ag0. 5CuxTiO2 solder joints. Journal of Alloys and Compounds, 684, 299-309.

Tu, K.-N., & Liu, Y. (2019). Recent advances on kinetic analysis of solder joint reactions in 3D IC packaging technology. Materials Science and Engineering: R: Reports, 136, 1-12.

Weerasekara, N., Liu, L., & Powell, M. (2016). Estimating energy in grinding using DEM modelling. Minerals Engineering, 85, 23-33.

Wu, I.-C., Wang, M.-H., & Jang, L.-S. (2018). Experimental location of damage in microelectronic solder joints after a board level reliability evaluation. Engineering Failure Analysis, 83, 131-140.

Xu, B., Wu, Y., Zhang, L., Chen, J., & Yuan, Z. (2016). Wettability and spreadability study of molten Sn-3.0 Ag-0.5 Cu wetting on V-shaped substrate. Soldering & Surface Mount Technology.

Xu, T., Wang, M., & Li, J. (2020). Dynamic hardness of rock materials under strong impact loading. International Journal of Impact Engineering, 103555.

Zeng, X. M., Lai, A., Gan, C. L., & Schuh, C. A. (2016). Crystal orientation dependence of the stress-induced martensitic transformation in zirconia-based shape memory ceramics. Acta Materialia, 116, 124-135.

Zhang, P., Xue, S., Wang, J., Xue, P., Zhong, S., & Long, W. (2019). Effect of nanoparticles addition on the microstructure and properties of lead-free solders: a review. Applied Sciences, 9(10), 2044.

Zhang, Z., Liu, Y., Zhao, X., Xiao, Y., & Lei, X. (2019). Mixing and Heat Transfer of Granular Materials in an Externally Heated Rotary Kiln. Chemical Engineering & Technology, 42(5), 987-995.

Zheng, J., & Hryciw, R. D. (2016). Roundness and sphericity of soil particles in assemblies by computational geometry. Journal of Computing in Civil Engineering, 30(6), 04016021.

Abdelhadi, O. M., & Ladani, L. (2012). IMC growth of Sn-3.5 Ag/Cu system: Combined chemical reaction and diffusion mechanisms. Journal of Alloys and Compounds, 537, 87-99.

Ahmed, M., Fouzder, T., Sharif, A., Gain, A. K., & Chan, Y. C. (2010). Influence of Ag micro-particle additions on the microstructure, hardness and tensile properties of Sn–9Zn binary eutectic solder alloy. Microelectronics Reliability, 50(8), 1134-1141.

Ali, B., Sabri, M. F. M., Jauhari, I., & Sukiman, N. L. (2016). Impact toughness, hardness and shear strength of Fe and Bi added Sn-1Ag-0.5 Cu lead-free solders. Microelectronics Reliability, 63, 224-230.

Almotairy, S. M., Alharthi, N. H., Alharbi, H. F., & Abdo, H. S. (2020). Superior Mechanical performance of inductively Sintered Al/Sic nanocomposites processed by novel Milling Route. Scientific Reports, 10(1), 1-13.

Azani, M. R., & Hassanpour, A. (2018). Silver nanorings: New generation of transparent conductive films. Chemistry–A European Journal, 24(72), 19195-19199.

Baheti, V. A., Kashyap, S., Kumar, P., Chattopadhyay, K., & Paul, A. (2017). Solid–state diffusion–controlled growth of the intermediate phases from room temperature to an elevated temperature in the Cu–Sn and the Ni–Sn

systems. Journal of Alloys and Compounds, 727, 832-840.

Bokstein, B., Klinger, L. M., & Apikhtina, I. (1995). Liquid grooving at grain boundaries. Materials Science and Engineering: A, 203(1-2), 373-376.

Cabeza, M., Feijoo, I., Merino, P., Pena, G., Pérez, M., Cruz, S., & Rey, P. (2017). Effect of high energy ball milling on the morphology, microstructure and properties of nano-sized TiC particle-reinforced 6005A aluminium alloy matrix composite. Powder Technology, 321, 31-43.

Chen, G., Peng, H., Silberschmidt, V. V., Chan, Y., Liu, C., & Wu, F. (2016). Performance of Sn–3.0 Ag–0.5 Cu composite solder with TiC reinforcement: physical properties, solderability and microstructural evolution under isothermal ageing. Journal of Alloys and Compounds, 685, 680-689.

Cox, B. N., & Landis, C. M. (2018). Solitary waves in morphogenesis: Determination fronts as strain-cued strain transformations among automatous cells. Journal of the Mechanics and Physics of Solids, 111, 239-276.

Ducros, G. (2012). Fission product release and transport. Nuclear safety in light water reactors: severe accident phenomenology, 1st edn. Elsevier, Oxford, 425-517.

Feng, J., Xu, D. E., Tian, Y., & Mayer, M. (2019). Sac305 solder reflow: Identification of melting and solidification using in-process resistance monitoring. IEEE Transactions on Components, Packaging and Manufacturing Technology, 9(8), 1623-1631.

Ghosh, S., Haseeb, A., & Afifi, A. (2013). Effects of metallic nanoparticle doped flux on interfacial intermetallic compounds between Sn-3.0 Ag-0.5 Cu and copper substrate. Paper presented at the 2013 IEEE 15th Electronics Packaging Technology Conference (EPTC 2013).

Goh, H. P., Heng, P. W. S., & Liew, C. V. (2018). Comparative evaluation of powder flow parameters with reference to particle size and shape. International journal of pharmaceutics, 547(1-2), 133-141.

Inci, G., Arnold, A., Kronenburg, A., & Weeber, R. (2014). Modeling nanoparticle agglomeration using local interactions. Aerosol Science and Technology, 48(8), 842-852.

Jiang, H., Moon, K. S., & Wong, C. P. (2008, May). Tin/silver/copper alloy nanoparticle pastes for low temperature lead-free interconnect applications. In 2008 58th Electronic Components and Technology Conference (pp. 1400-1404). IEEE.

Ju, W., Jiang, B., Qin, Y., Wu, C., Wang, G., Qu, Z., & Li, M. (2019). The present-day in-situ stress field within coalbed methane reservoirs, Yuwang Block, Laochang Basin, south China. Marine and Petroleum Geology, 102, 61-73.

Jwad, T., Walker, M., & Dimov, S. (2018). Erasing and rewriting of titanium oxide colour marks using laser-induced reduction/oxidation. Applied Surface Science, 458, 849-854.

Kenel, C., & Leinenbach, C. (2015). Influence of cooling rate on microstructure formation during rapid solidification of binary TiAl alloys. Journal of Alloys and Compounds, 637, 242-247.

Kim, S. H., Yang, D.-Y., Kim, Y.-J., Min, T., Choi, J., Yun, J., . . . Do Kim, Y. (2017). Thermo-mechanical evolution of ternary Bi–Sn–In solder micropowders and nanoparticles reflowed on a flexible PET substrate. Applied Surface Science, 415, 28-34.

Kumar, U. K. A. V. (2017). Method of stir casting of aluminum metal matrix composites: a review. Materials Today: Proceedings, 4(2), 1140-1146.

Li, H., An, R., Wang, C., Tian, Y., & Jiang, Z. (2015). Effect of Cu grain size on the voiding propensity at the interface of SnAgCu/Cu solder joints. Materials Letters, 144, 97-99.

Li, M., Zhang, J., Song, W., & Germain, D. M. (2019). Recycling of crushed waste rock as backfilling material in coal mine: effects of particle size on compaction behaviours. Environmental Science and Pollution Research, 26(9), 8789-8797.

Luu, T.-T., Duan, A., Aasmundtveit, K. E., & Hoivik, N. (2013). Optimized Cu-Sn wafer-level bonding using intermetallic phase characterization. Journal of Electronic Materials, 42(12), 3582-3592.

Manko, H. H. (2001). Solders and soldering. McGraw-Hill Professional Publishing.

Nadia, A., & Haseeb, A. (2012). Fabrication and properties of Sn-3.5 Ag-XCu solder by ball milling and paste Mixing. Paper presented at the Defect and Diffusion Forum.

Nandiyanto, A. B. D., Zaen, R., & Oktiani, R. (2018). Working volume in high-energy ball-milling process on breakage characteristics and adsorption performance of rice straw ash. Arabian Journal for Science and Engineering, 43(11), 6057-6066.

Njobuenwu, D. O., & Fairweather, M. (2017). Simulation of deterministic energy-balance particle agglomeration in turbulent liquid-solid flows. Physics of Fluids, 29(8), 083301.

Noor, E. E. M., Sharif, N. M., Yew, C. K., Ariga, T., Ismail, A. B., & Hussain, Z. (2010). Wettability and strength of In–Bi–Sn lead-free solder alloy on copper substrate. Journal of Alloys and Compounds, 507(1), 290-296.

Park, M., & Arróyave, R. (2012). Concurrent nucleation, formation and growth of two intermetallic compounds (Cu6Sn5 and Cu3Sn) during the early stages of lead-free soldering. Acta Materialia, 60(3), 923-934.

Park, Y., Bang, J.-H., Oh, C. M., Hong, W. S., & Kang, N. (2017). The Effect of Eutectic Structure on the Creep Properties of Sn-3.0 Ag-0.5 Cu and Sn-8.0 Sb-3.0 Ag Solders. Metals, 7(12), 540.

Perez-Gandarillas, L., Perez-Gago, A., Mazor, A., Kleinebudde, P., Lecoq, O., & Michrafy, A. (2016). Effect of roll-compaction and milling conditions on granules and tablet properties. European Journal of Pharmaceutics and Biopharmaceutics, 106, 38-49.

Piotrowska, K., Grzelak, M., & Ambat, R. (2019). No-clean solder flux chemistry and temperature effects on humidity-related reliability of electronics. Journal of Electronic Materials, 48(2), 1207-1222.

Rajkhowa, R., & Wang, X. (2014). Silk powder for regenerative medicine. In Silk Biomaterials for Tissue Engineering and Regenerative Medicine (pp. 191-216): Elsevier.

Ramli, M., Saud, N., Salleh, M. M., Derman, M. N., & Said, R. M. (2016). Effect of TiO2 additions on Sn-0.7 Cu-0.05 Ni lead-free composite solder. Microelectronics Reliability, 65, 255-264.

Roshanghias, A., Yakymovych, A., Bernardi, J., & Ipser, H. (2015). Synthesis and thermal behavior of tin-based alloy (Sn–Ag–Cu) nanoparticles. Nanoscale, 7(13), 5843-5851.

Salleh, M., Anuar, M. A., Somidin, F., Al Bakri Abdullah, M. M., Noriman, N., Mayappan, R., & Alui, N. F. M. (2013). Effects of Recycled-Aluminum Additions on the Mechanical Properties of Sn-0.7 Cu/Cu-Substrate Lead-Free Solder Joints. Paper presented at the Advanced Materials Research.

Sgrott, O. L., & Sommerfeld, M. (2019). Influence of inter-particle collisions and agglomeration on cyclone performance and collection efficiency. The Canadian Journal of Chemical Engineering, 97(2), 511-522.

Soltani, S., Khosroshahi, R. A., Mousavian, R. T., Jiang, Z.-Y., Boostani, A. F., & Brabazon, D. (2017). Stir casting process for manufacture of Al–SiC composites. Rare Metals, 36(7), 581-590.

Sperança, M. A., Virgilio, A., Pereira-Filho, E. R., & de Aquino, F. W. B. (2018). Determination of elemental content in solder mask samples used in printed circuit boards using different spectroanalytical techniques. Applied Spectroscopy, 72(8), 1205-1214.

Tang, Y., Luo, S., Wang, K., & Li, G. (2016). Effect of Nano-TiO2 particles on growth of interfacial Cu6Sn5 and Cu3Sn layers in Sn3. 0Ag0. 5CuxTiO2 solder joints. Journal of Alloys and Compounds, 684, 299-309.

Tu, K.-N., & Liu, Y. (2019). Recent advances on kinetic analysis of solder joint reactions in 3D IC packaging technology. Materials Science and Engineering: R: Reports, 136, 1-12.

Vianco, P. T. (1999). Soldering handbook. American Welding Society.

Wang, D., & Fan, L.-S. (2013). Particle characterization and behavior relevant to fluidized bed combustion and gasification systems. In Fluidized bed technologies for near-zero emission combustion and gasification (pp. 42-76): Elsevier.

Weerasekara, N., Liu, L., & Powell, M. (2016). Estimating energy in grinding using DEM modelling. Minerals Engineering, 85, 23-33.

Wu, I.-C., Wang, M.-H., & Jang, L.-S. (2018). Experimental location of damage in microelectronic solder joints after a board level reliability evaluation. Engineering Failure Analysis, 83, 131-140.

Xu, B., Wu, Y., Zhang, L., Chen, J., & Yuan, Z. (2016). Wettability and spreadability study of molten Sn-3.0 Ag-0.5 Cu wetting on V-shaped substrate. Soldering & Surface Mount Technology.

Xu, T., Wang, M., & Li, J. (2020). Dynamic hardness of rock materials under strong impact loading. International Journal of Impact Engineering, 103555.

Zeng, X. M., Lai, A., Gan, C. L., & Schuh, C. A. (2016). Crystal orientation dependence of the stress-induced martensitic transformation in zirconia-based shape memory ceramics. Acta Materialia, 116, 124-135.

Zhang, P., Xue, S., Wang, J., Xue, P., Zhong, S., & Long, W. (2019). Effect of nanoparticles addition on the microstructure and properties of lead-free solders: a review. Applied Sciences, 9(10), 2044.

Zhang, Z., Liu, Y., Zhao, X., Xiao, Y., & Lei, X. (2019). Mixing and Heat Transfer of Granular Materials in an Externally Heated Rotary Kiln. Chemical Engineering & Technology, 42(5), 987-995.

Zheng, J., & Hryciw, R. D. (2016). Roundness and sphericity of soil particles in assemblies by computational geometry. Journal of Computing in Civil Engineering, 30(6), 04016021.

Zheng, B., Ashford, D., Zhou, Y., Mathaudhu, S. N., Delplanque, J. P., & Lavernia, E. J. (2013). Influence of mechanically milled powder and high pressure on spark plasma sintering of Mg–Cu–Gd metallic glasses. Acta materialia, 61(12), 4414-4428.

APPENDICES

LIST OF PUBLICATIONS AND AWARDS

List of publications

Murad, N., Aisha, S. R., & Ishak, M. (2017). Effects of cooling rates on microstructure, wettability and strength of Sn3. 8Ag0. 7Cu solder alloy. Procedia engineering, 184, 266-273.

Murad, N., Aisha, S., & Muhammad, M. I. (2016, September). Effects of sintering temperatures on microstructures and mechanical properties of Sn4. 0Ag0. 5Cu1. 0Ni solder alloy. In 2016 IEEE 37th International Electronics Manufacturing Technology (IEMT) & 18th Electronics Materials and Packaging (EMAP) Conference (pp. 1-7). IEEE.

List of awards

Best Paper Awards – First Runner Up in The 37th International Electronic Manufacturing Technology & 18th Electronic Materials and Packaging Conference(IEMT 2016 Pulau Pinang)

For "**Effects of sintering temperatures on microstructures and mechanical properties of Sn4.0Ag0.5Cu-1.0Ni solder alloy**"